(2)

PHOTOREGULATION OF ENGINEERED PROTEINS BY INCORPORATION OF NONNATURAL AMINO ACIDS

TAKEHIKO UEDA

1995

CONTENTS

LIST OF ABBREVIATIONS iii

INTRODUCTION 1

PART I IMPROVEMENT AND PHOTOCONTROL OF PROTEIN ACTIVITY BY INCORPORATION OF NONNATURAL AMINO ACIDS

Chapter 1 Biosynthesis of Mutant β-D-Galactosidases Containing Nonnatural Aromatic Amino Acids by *Esherichia coli* 17

Chapter 2 Semisynthesis of Mutant Cytochromes *c* Replaced by Nonnatural Aromatic Amino Acid at Phe^{82} and Photoregulation of Reduction Reaction with 2-Mercaptoethanol 39

Chapter 3 Destabilization of the Heme Region in Mutant Cytochrome *c* by Replacement of Phe^{82} with 3-(1-Pyrenyl)-L-alanine 65

PART II PHOTOCONTROL OF PROTEIN ACTIVITY THROUGH STRUCTURAL TRANSITION INDUCED BY PHOTOISOMERIZATION OF NONNATURAL AMINO ACIDS

Chapter 4 Photoregulation of Hydrolysis Activity of Semisynthetic Mutant Phospholipases A_2 Replaced by Nonnatural Aromatic Amino Acids 87

Chapter 5 Location of Melittin Fragment Carrying Spiropyran in Phospholipid Bilayer Membrane Determined by Thermal Isomerization..... 111

Chapter 6 Photoresponsive Melittin Having a Spiropyran Residue in the Hydrophobic Region of the Sequence 131

ABSTRACT 153

LIST OF PUBLICATIONS..... 159

ACKNOWLEDGMENT..... 161

LIST OF ABBREVIATIONS

AMPA	N^{ε}-amidinated phospholipase A_2
Amd-	amidinated-
Amd-Cytc	N^{ε}-amidinated cytochrome *c*
antAla	3-(9-anthryl)-DL-alanine
Ant-AMPA	[antAla^3]AMPA
Amp^r	ampicillin resistant
ATR-IR	attenuated total reflection-infrared
AzoF-AMPA	[azoPhe^3]AMPA
azoPhe	*p*-phenylazo-L-phenylalanine
B357	wild-type *E. coli* strain
BamHI	bacterial endonuclease
BAP	bacterial alkaline phosphatase
BNL	Brookhaven National Laboratory
Boc	N^{α}-*tert*-butyloxycarbonyl
BSA	bovine serum albumin
bp	base pair
CD	circular dichroism
[^{14}C]-DPPC	1-palmitoyl-2-[1-^{14}C]palmitoylphosphatidylcholine
CF	5 / 6-carboxyfluorescein
CNBr	cyanogen bromide
CP	chloramphenicol
CpA	carboxypeptidase A
DES3	des[Ala^{1}Leu^{2}Trp^3]AMPA
DH5α	recA deficient *Escherichia coli* strain
DMF	dimethylformamide
DMSO	dimethyl sulfoxide
DPPC	dipalmitoylphosphatidylcholine
DCCD	dicyclohexylcarbodiimide
E. coli	*Escherichia coli*
EcoRV	bacterial endonuclease
EDTA	ethylenediamine-*N,N,N',N'*-tetraacetic acid
GdnHCl	guanidine hydrochloride
hEGF	human epidermal growth factor

Hepes	4-(2-hydroxyethyl)-1-piperazine ethanesulfonic acid
HO-Sp	1-(β-hydroxyethyl)-3,3-dimethyl-6'-nitrospiro[indoline-2,2'-2H-benzopyran]
HOOC-Sp	1-hydroxycarbonylmethyl-3,3-dimethyl-6'-nitrospiro[indoline-2,2'-2H-benzopyran]
HOSu	*N*-hydroxysuccinimide
HOBt	1-hydroxybenzotriazole
HPLC	high performance liquid chromatography
Hse	homoserine
IR	infrared spectroscopy
IRS	interface recognition site
LacZ	structural DNA coding *Escherichia coli* β-D-galactosidase
LB-medium	Luria-Bertani medium
M.W.	molecular weight
MLV	multilamellar vesicles
MSp	[Orn^3(Sp), $\varepsilon^{7,21,23}$-amidinated]melittin
napAla	3-(2-naphthyl)-L-alanine
Nap-AMPA	[$napAla^3$]AMPA
NMR	nuclear magnetic resonance
NOE	nuclear Overhauser effect
O.D.	optical density
ONPG	*o*-nitrophenyl β-D-galactopyranoside
OSu	succinimide ester
PAGE	polyacrylamide gel electrophoresis
PGL-Cytc	[$pheGly^{82}$]cytochrome *c*
pheGly	L-phenylglycine
PITC	phenyl isothiocyanate
PLA_2	phospholipase A_2
pNO_2Phe	*p*-nitro-L-phenylalanine
PTC	phenyl thiocarbamoyl
PTH	phenylthiohydantoin
pMC1871	bacterial plasmid carrying *LacZ*
pUC19	bacterial expression vector plasmid
pUC19Z	newly synthesized bacterial plasmid
pyrAla	3-(1-pyrenyl)-L-alanine

PYR-Cytc	[$pyrAla^{82}$]cytochrome *c*
Quin 2	2-{[2-bis(carboxymethyl)amino-5-methylphenoxy]methyl}-6-methoxy-8-bis(carboxymethyl)aminoquinoline
SDS	sodium dodecylsulphate
SUV	small unilamellar vesicles
TEA	triethylamine
TFA	trifluoroacetic acid
TLC	thin layer chromatography
TNBS	2,4,6-trinitrobenzenesulfonic acid
Tris	tris(hydroxymethyl)aminomethane
tRNA	transfer ribonucleic acid
UV	ultraviolet
Xaa	nonnatural amino acid
Xaa-AMPA	[Xaa^3]AMPA
Z	*N*-benzyloxycarbonyl

INTRODUCTION

Proteins play fundamental roles in all living cells [1]. Almost all chemical reactions in the cellular system are catalyzed by proteins with strict specificity and remarkable efficiency. Therefore, these proteins are expected to be utilized for new molecular materials such as molecular device, sensing unit of analytical apparatus, drug delivery system, and bioreactor, etc. However, for application of proteins in a wide range of fields, modification of native proteins to create new proteins with novel structure and function is necessary. This has been purposed in protein engineering, which is based on protein chemistry to relate the primary structure, *i.e.,* the sequence of naturally occurring amino acids, with the tertiary structure (folding structure). The number of available amino acids is about 20 [2], restricting the nature of functional groups and hence the protein function. When one can increase the number of available amino acids, the possibility of yielding new proteins will be increased significantly. This is the motivation for the present author to start preparation of proteins having nonnatural amino acids in the sequence.

Information concerning the primary structure of a protein is stored in a gene, which is expressed in the protein produced in the ribosome of a cell [3]. In 1970s, genetic engineering started to use genes for production of proteins [4]. Recently, almost all kinds of naturally occurring proteins can be reproduced by means of the genetic engineering [5]. Amino acid sequence of proteins can be designed at will, in principle, through the genetic engineering technique. When the desired sequence is only slightly different from a native one, the necessary mutation can be easily introduced in the appropriate site of DNA coding the protein [6].

The relationship between protein structure and function has been extensively studied by genetic mutation technique, and the relationship is getting clearer in some cases [7]. Proteins are folded into a certain stable tertiary structure, in which three-dimensional locations of pendant groups are precisely determined to yield specific functions [8]. Protein functions are controlled by spatial arrangement of pendant groups. The limited number of amino acids available for genetic engineering is due to the translation system of genetic code [9]. There are two possible ways for incorporation of nonnatural amino acids into a protein; one is a modification of the gene translation system, and the other is a chemical synthesis. In order to obtain mutant proteins with novel and desired functions, both approaches were examined in the present thesis.

Bain et al. [10] succeeded in the synthesis of nonnatural proteins in 1989 by chemical synthesis of nonnatural aminoacyl-tRNA. A chemically synthesized tRNA carrying a functional nonnatural amino acid was added to *in vitro* protein synthesis system in the absence of competing tRNAs [11]. Several kinds of mutant proteins were obtained, in which the nonnatural amino acid was incorporated into the proteins. This method seemed promising for the synthesis of mutant proteins, but requires experienced and sophisticated skills for the chemical synthesis of modified aminoacyl-tRNA [12]. Furthermore, it is hard to obtain a sufficient amount of mutant protein for structural analysis due to difficulties in preparation of modified aminoacyl-tRNA and in keeping *in vivo* protein synthesis system active.

Instead of using chemically modified tRNA, an overproducing cell system was used in this thesis. Misacylation of tRNA with a nonnatural amino acid in the absence of a competing native amino acid might occur frequently in this system, because aminoacylation enzyme, aminoacyl-tRNA synthetase, is only

able to distinguish a correct natural amino acid from other inappropriate natural amino acids [13]. When a nonnatural amino acid is not recognized as an inappropriate substrate, aminoacyl-tRNA synthetase should aminoacylate the nonnatural amino acid to yield easily modified aminoacyl-tRNA. However, this method is unable to realize a site-specific incorporation of nonnatural amino acid.

Chemical modification of proteins using chemical reagents has been extensively investigated by many researchers [14,15]. However, the chemical reaction takes place only on the protein surface, where chemical reagents are easily accessible. In addition, it is difficult to modify a specific residue in the protein by this method. A semisynthetic method could be an alternative of the chemical synthesis of mutant proteins. In this technique, a protein is degraded into several fragments, and the fragments are recombined after necessary substitutions in appropriate fragments [16,17,18]. The most useful aspect of the semisynthetic method is a high yield of mutant proteins. Furthermore, this method is applicable to any kind of nonnatural amino acids.

This thesis consists of two parts including six chapters, concerning incorporation of nonnatural amino acid to several kinds of proteins and melittin derivative peptides. These proteins include β-D-galactosidase, cytochrome *c* and phospholipase A_2 (PLA_2). β-D-Galactosidase is an enzyme digesting oligosaccharide to supply carbon source for *Escherichia coli(E. coli)*, a prokaryote cell [19]. Cytochrome *c* transfers one electron from a reductase to an oxidase on mitochondrial membrane by changing the oxidation state of iron porphyrin, which plays essential roles in energy production systems such as respiratory system and photosynthesis [20]. PLA_2 hydrolyzes phospholipid molecules in the course of metabolic turnover of lipids [21]. The hydrolysis

products act as biochemical signals to induce cell responses. Melittin is a 26-residue peptide, and binds to cell membrane to cause cell lysis by disrupting the bilayer structure of cell membrane [22].

In part I of this thesis, 3-(1-pyrenyl)-L-alanine (pyrAla) or other nonnatural aromatic amino acid was incorporated into two kinds of proteins by different ways, and the effect of the substitution on the physical and chemical properties of the proteins was studied. pyrAla was chosen as a photosensitizer to make the protein photosensitive. In addition, the pendant group of pyrAla residue is highly hydrophobic and may improve the thermostability of the protein by strengthening the hydrophobic core of the protein. In chapter 1, fluorescent nonnatural amino acids such as 3-(2-naphthyl)-L-alanine (napAla), 3-(9-anthryl)-DL-alanine (antAla), and pyrAla were incorporated into β-D-galactosidase by using a genetically engineered *E. coli* strain in an overproduction state (Figure 1). A recombinant DNA was introduced into *E. coli* by genetic engineering techniques. The efficiency of incorporation and the change of thermostability of the protein were studied for each nonnatural amino acid.

In chapter 2, pyrAla residue was incorporated into cytochrome *c* at the position of Phe^{82} by a semisynthetic method (Figure 2). The electron transfer activity of the mutant cytochrome *c* was studied and compared with that of the native one (Figure 3). Since Phe^{82} is located near the heme moiety [23], it has been postulated that the orbital overlap and the oxidation-reduction potential difference between the heme and the aromatic side chain should influence the rate of electron transfer involving the cytochrome *c*. The electron transfer kinetics was examined spectroscopically, and discussed in relation with the change of accessibility of the reducing reagent to the heme induced by

incorporation of the nonnatural amino acid. Photosensitization effect was also examined in order to clarify the possibility to create a novel protein with photosensitive electron transfer activity. By examining the effect of photoirradiation on the electron transfer rate, photosensitization property of pyrAla residue can be discussed [24].

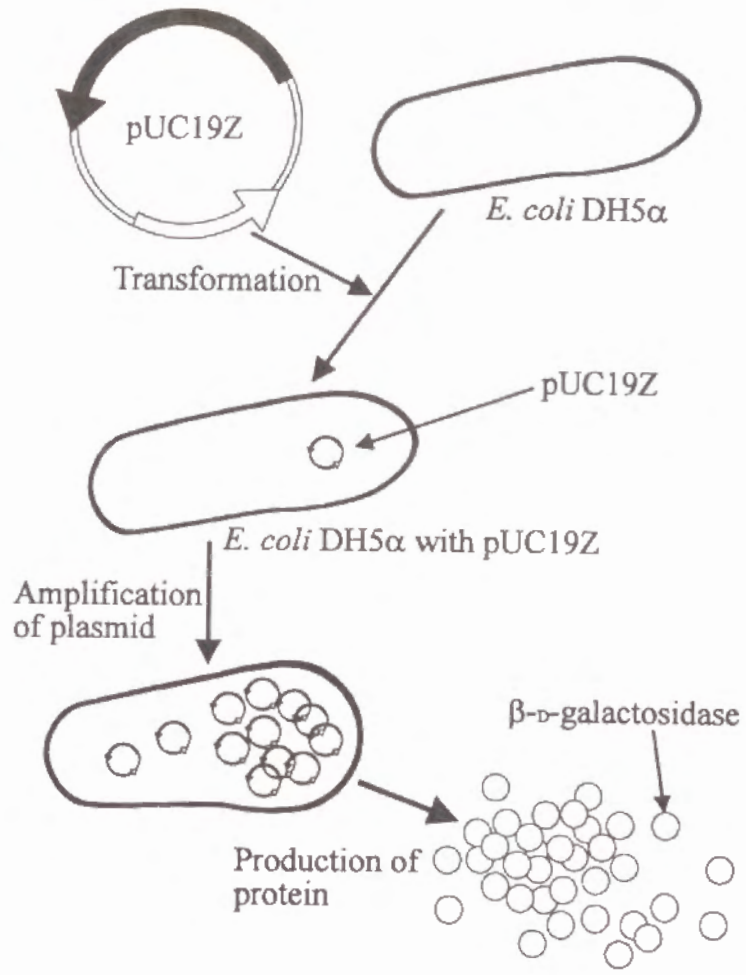

Figure 1. Schematic drawing of protein overproduction introduced by plasmid pUC19Z.

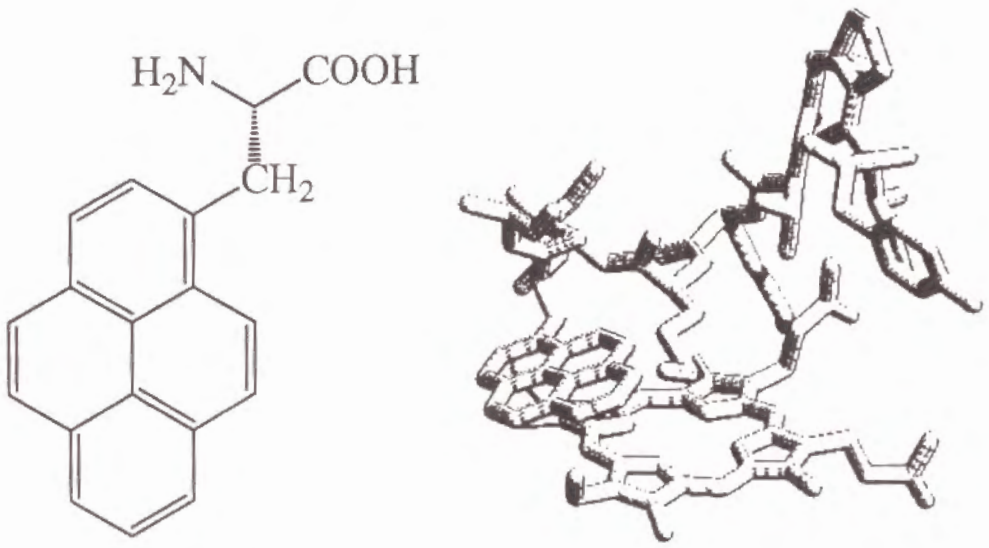

Figure 2. Structure of pyrAla (left) and a schematic drawing of the heme region of [pyrAla^{82}]cytochrome *c* (PYR-Cytc) (right) drawn by RasMOL Version 2.2 (see chapter 3).

Although, the semisynthetic method was found to be the best way to achieve a high yield of mutant cytochrome *c*, the incorporation of a bulky amino acid caused structural destabilization (Figure 3). In chapter 3, in order to evaluate the degree of structural distortion induced by bulky pendant groups, the stability of tertiary structure of the mutant cytochrome *c* was studied in detail. The structural change around the heme region, apart from the whole conformational change of backbone, can be observed by CD spectroscopy. The present author compared the effects of bulky pendant groups on local (around heme) and overall structure of the mutant proteins by examining chemical and thermal denaturation processes.

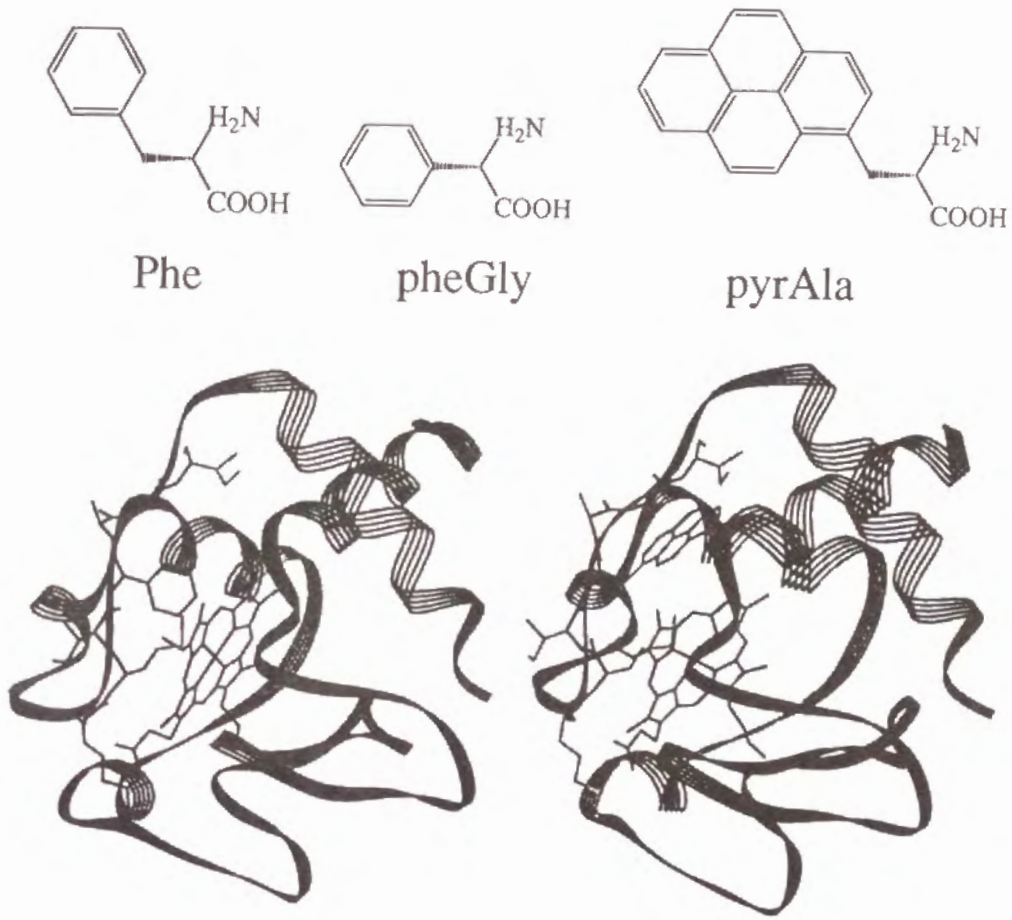

Figure 3. (Top) molecular structures of Phe, pheGly, and pyrAla. (Bottom) 3D ribbon drawing of [pheGly^{82}]cytochrome *c* (PGL-Cytc) (left) and PYR-Cytc (right) in the oxidized state. Protein main chain is illustrated in a sheet of ribbon, and an exact structure of backbone and side chains at 79-85 regions is superimposed. Ribbon drawings were created from the X-ray crystallographic data stored in the Protein Data Bank at Brookhaven National Laboratory (BNL), USA, by using MAGE, a 'kinemage' displaying program Version 2.5 for Windows System distributed from BNL.

In part II of this thesis, photocontrol of protein activity by photoisomerization of nonnatural amino acid was studied. Photosensitive nonnatural amino acids were incorporated to PLA_2, melittin or melittin fragment peptides by a semisynthetic method. Azobenzene and spiropyran are well-known as photosensitive chromophore which changes the structure by light irradiation. Azobenzene changes the molecular shape, and spiropyran the ionization state. Therefore, these chromophores might cause structural change of the protein backbone and the hydrophobicity of microenvironment of the protein. Through these structural changes induced by photoirradiation, the protein activity may be changed.

In chapter 4, a nonnatural amino acid carrying azobenzene was incorporated into the interfacial recognition site (IRS) of PLA_2 [25]. It was expected that the affinity of the IRS for lipid substrates might be changed by photoirradiation due to structural change [26], resulting in a change of hydrolysis activity (Figure 4). The structural change was represented by the change of enzymatic activities, and the time course of hydrolysis was analyzed in order to determine kinetic parameters. These parameters can be interpreted in two different aspects, one of them is activation energy, and the other is affinity toward aggregated substrates. The contribution of these two factors to the change of hydrolysis activity is discussed in relation to the structural transition of mutant PLA_2s observed by CD spectroscopy. [antAla^3]-N^{ε}-amidinated phospholipase A_2 (Ant-AMPA) and [napAla^3]-N^{ε}-amidinated phospholipase A_2 (Nap-AMPA) were also synthesized and the activity in lipid hydrolysis was compared with [azoPhe^3]-N^{ε}-amidinated phospholipase A_2 (AzoF-AMPA).

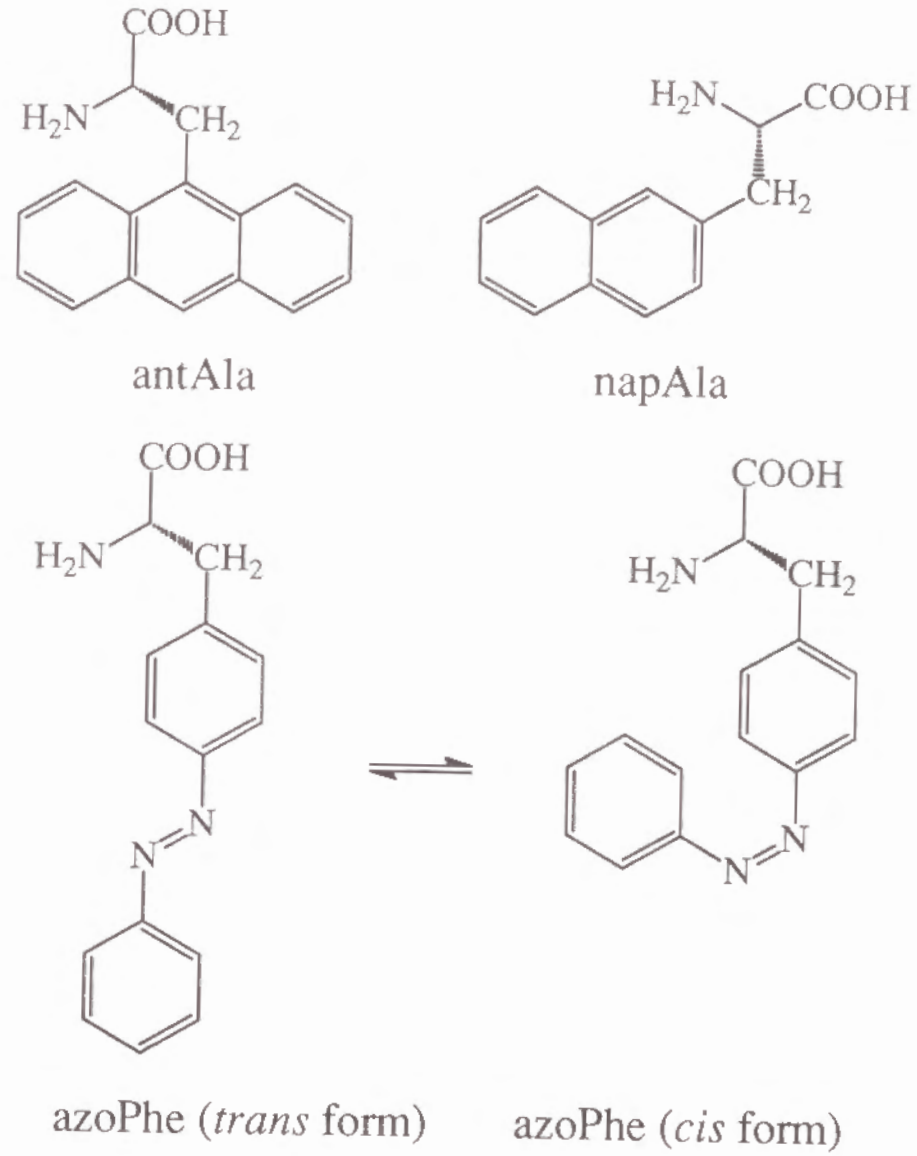

Figure 4. Molecular structures of antAla, napAla, and *p*-phenylazo-L-phenylalanine (azoPhe).

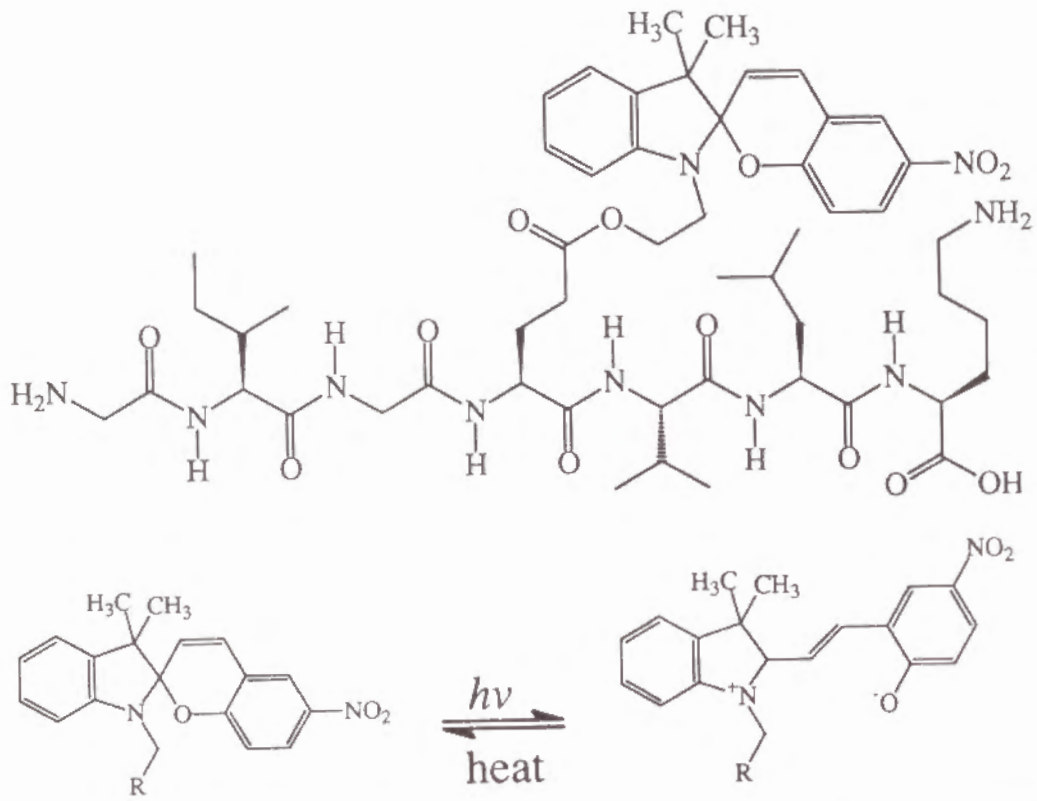

Figure 5. Molecular structure of melittin fragment carrying spiropyran group (top) and the photoisomerization / thermal isomerization between non-ionic spiropyran form and zwitterionic merocyanine form (bottom).

In chapter 5, a melittin fragment (1-7) carrying spiropyran at the 4th position was synthesized by a conventional chemical method (Figure 5), and the membrane-binding activity was studied. This fragment was synthesized, because the hydrophobic N-terminal fragment (1-7) of melittin has been thought to be essential for strong interactions with phospholipid membranes [27,28]. Spiropyran is isomerized to a merocyanine form by UV-light irradiation and gradually isomerizes back to spiropyran form. The latter rate depends on hydrophobicity of the surrounding microenvironment [29]. Therefore, the

location of the merocyanine group of the peptides in the membrane can be estimated from the kinetics of thermal isomerization from merocyanine to spiropyran form. The affinity of the melittin fragment carrying spiropyran group to membrane may be controlled by UV-light irradiation, and hence the lysis activity of the spiropyran derivative could be controlled by light irradiation. The leakage of 5/6-carboxyfluorescein(CF) was investigated under UV-light irradiation in the presence of the melittin fragment carrying a spiropyran group, and was discussed in relation with the change of binding activity of the melittin fragment.

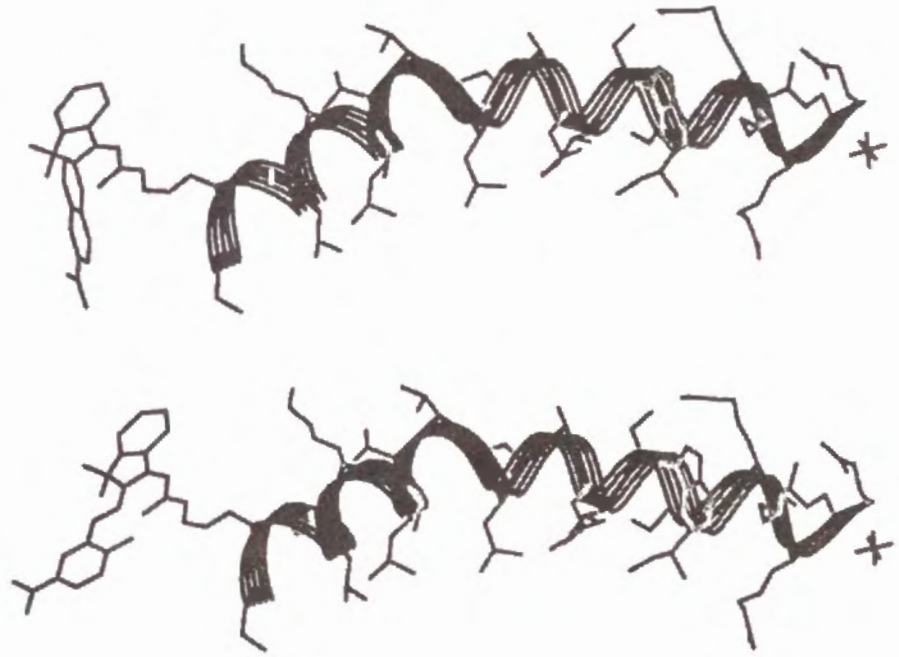

Figure 6. 3D ribbon drawing of melittin carrying a chromophoric group in spiropyran form (top) or merocyanine form (bottom). Backbone and side chains are superimposed on the ribbon. Ribbon drawings were created from the X-ray crystallographic data stored in the Protein Data Bank at BNL, USA, by using MAGE Version 2.5.

In chapter 6, a mutant melittin replaced by a nonnatural amino acid carrying spiropyran at the third position was synthesized by a semisynthetic method (Figure 6). The photoisomerization kinetics and irradiation effects on the membrane-disturbing activity of the mutant melittin were investigated. Upon UV-light irradiation, the highly polar zwitterionic merocyanine group appears at the N-terminal region of the mutant melittin, and they form a hydrophilic cluster there. Consequently, the orientation of the peptide in lipid membrane changes by photoirradiation, leading to a change in the membrane-disturbing activities as in the case of the melittin fragment carrying spiropyran group at the 4th position discussed in chapter 5. The effect of the mutant melittin carrying a spiropyran group on the phospholipid membrane was evaluated by measuring the CF leakage from liposomes. The rate of CF leakage can be analyzed as a sum of exponential decay factors, which are closely related to binding kinetics of the mutant protein and decoloration process of merocyanine. By comparing CF leakage kinetics with the decoloration kinetics, the main factor responsible for the CF leakage was discussed.

In the present thesis, several mutant proteins and peptides were synthesized by biological or chemical modification of naturally occurring proteins and peptide. The presence of nonnatural amino acid residue in the primary sequence affected the activity of protein. In the case of a bulky enzyme such as β-D-galactosidase, a small number of the incorporated nonnatural amino acids increased the thermostability. In contrast, less bulky proteins such as cytochrome *c* and PLA_2 lost thermostability by incorporation of a bulky nonnatural amino acid. However, incorporation of photoisomerizing amino acid made the enzymatic activity and the membrane-binding activity of

proteins photocontrollable. The experimental results will be described in detail in the following chapters.

References

1. D. Metzler, *"Biochemistry: The Chemical Reactions of a Living Cell.,"* 1977, Academic Press, New York.
2. J. W. B. Hershey, *"The Translational Machinery"* in *"Cell Biology: A Comprehensive Treatise,"* 1980, Eds. D. M. Prescott and L. Goldstein, Vol. 4, Academic Press, New York.
3. J. A. Lake, *Sci. Am.*, 1981, **245**, 84.
4. T. Maniatis, E. F. Fritsch and J. Sambrook, *"Molecular Cloning,"* 1982, Cold Spring Harbor, New York.
5. Y. Gluzman, *"Eukaryotic Viral Vectors,"* 1982, Cold Spring Harbor, New York.
6. D. L. Oxender and C. F. Fox, *"Protein Engineering,"* 1987, Alan R. Liss, Inc., New York.
7. (a) R. Wallace, M. Schold, M. Johnson, P. Dembek and K. Itakura, *Nucl. Acid. Res.*, 1979, **6**, 3543. (b) M. Zoller and M. Smith, *Methods in Enzymology*, 1983, **100**, 468.
8. J. S. Richardson, *Adv. Protein Chem.*, 1981, **34**, 167.
9. M. Nomura, A. Tissières and P. Lengyel, Eds., *"Ribosomes,"* 1974, Cold Spring Harbor, New York.
10. J. D. Bain, C. G. Glabe, T. A. Dix and R. Chamberlin, *J. Am. Chem. Soc.*, 1989, **111**, 8013.
11. J. D. Bain, D. A. Wacker, E. E. Kuo, M. H. Lyttle and R. Chamberlin, *J. Org. Chem.*, 1991, **56**, 4615.

12. J. D. Bain, E. S. Diala, C. G. Glabe, D. A. Wacker, M. H. Lyttle, T. A. Dix and R. Chamberlin, *Biochemistry*, 1991, **30**, 5411.
13. F. Naider, Z. Bohak and J. Yariv, *Biochemistry*, 1972, **411**, 3202.
14. D. W. Conrad and R. A. Scott, *J. Am. Chem. Soc.*, 1989, **111**, 3461.
15. R. Bechtold, C. Kuehn, C. Lepre and S. S. Isied, *Nature*, 1986, **322**, 286.
16. A. R. Rees and R. E. Offord, *Biochem. J.*, 1976, **159**, 467.
17. D. E. Harris and R. E. Offord, *Biochem. J.*, 1977, **161**, 21.
18. C. J. A. Wallace, G. Corradin, F. Marchiori and G. Borin, *Biopolymers*, 1986, **25**, 2121.
19. T. P. St. John and R. W. Davis, *J. Mol. Biol.*, 1981, 152, 285.
20. R. E. Dickerson, *Sci. Am.*, 1980, **242**, 136.
21. D. Bainton, *J. Cell Biol.*, 1981, **91**, 66.
22. H. Vogel and F. Jähnig, *Biophys. J.*, 1986, **50**, 573.
23. T. I. Poulos and J. Kraut, *J. Biol. Chem.*, 1982, **255**, 10322.
24. G. J. Kavarnos and N. J. Turro, *Chem. Rev.*, 1986, **86**, 401.
25. B. W. Dijkstra, J. Drenth, K. H. Kalk, *Nature*, 1981, **289**, 604.
26. M. C. E. Van Dam-Mieras, A. J. Slotboom, W. A. Pieterson and G. H. De Haas, *Biochemistry*, 1975, **14**, 5387.
27. C. R. Dawson, A. F. Drake, J. Helliwell and R. C. Hilder, *Biochim. Biophys. Acta*, 1978, **510**, 75.
28. E. Habermann and H. Kowallek, *Hoppe-Seyler's Z. Physiol. Chem.*, 1970, **351**, 884.
29. T. Seki and K. Ichimura, *J. Colloid Interface Sci.*, 1989, **129**, 353.

PART I

IMPROVEMENT AND PHOTOCONTROL OF PROTEIN ACTIVITY BY INCORPORATION OF NONNATURAL AMINO ACIDS

Chapter 1

Biosynthesis of Mutant β-D-Galactosidases Containing Nonnatural Aromatic Amino Acids by *Esherichia coli*

Introduction

Chemical treatment and protein engineering have produced many modified or mutant proteins, which are more effective in enzymatic activity than the original ones. In the meantime, the introduction of functional residues by means of chemical modification is limited only to functional groups on the protein surface, where modifying reagents are sterically reachable. On the other hand, site-directed mutagenesis provides a means of substitution at precise position of the sequence with natural amino acids. If protein engineering also enables utilization of nonnatural amino acids, we can design novelly functionalized enzymes more easily.

Proofreading system prevents protein biosynthesis from mistranslation in every step of biosynthetic process [1]. However, the system could not function properly against nonnatural amino acids because it works most strictly against naturally occurring amino acids. So far, many kinds of nonnatural amino acids, whose structure is very similar to a natural one, have been introduced into proteins by using *Escherichia coli* (*E. coli*). The substitution rate of a target amino acid with a nonnatural amino acid was found to be about 10 % to 90 % in the cases of alkaline phosphatase [2-8], aspartate transcarbamylase [9], β-D-galactosidase [10] and human epidermal growth factor (hEGF) [11]. Schlesinger and coworkers have

succeeded in incorporation of various amino acid analogs into bacterial alkaline phosphatase [2-7]. Alkaline phosphatase gene is expressed under the control of *phoA* promoter which is induced by lowering the phosphate concentration of the culture medium. The biosynthesis of the other probably toxic abnormal proteins is not active under these conditions except the production of abnormal alkaline phosphatase. In this method, Miyazawa and coworkers succeeded in preparing hEGF substituted with one norleucine for methionine by biosynthesis of alkaline phosphatase signal peptide-hEGF fusion protein [11]. On the other hand, incorporation of nonnatural amino acids, whose structure is very different from a natural one, is a difficult task. One of approaches to realize this purpose is that the protein-biosynthesis system is accelerated to obtain the mutant enzymes containing nonnatural amino acids as much as possible.

In this chapter, incorporation of fluorescent nonnatural amino acids into β-D-galactosidases was studied by using *E. coli* in an overproduction state on the protein synthesis. pyrAla was incorporated into β-D-galactosidases and relatively high thermostability was found in some of the mutant enzyme.

Experimental

Materials

o-Nitrophenyl β-D-galactopyranoside (ONPG), bovine serum albumin (BSA) and *E. coli* β-D-galactosidase (M.W. 130 kDa) were purchased from Sigma, USA. Bacterial endonucleases BamHI and EcoRV, bacterial alkaline phosphatase (BAP), and T4 DNA ligase were purchased from Toyobo Co. Ltd., Japan. Bacto-Trypton

and Bacto-Yeast-Extract were purchased from Difco Laboratory, USA. *E. coli* B357 (wild type) and *E. coli* DH5α (F^-, *endA*1, *hsdR*17(rk^-,mk^+), *supE*44, *thi*$^{-1}$, *recA*1, *gyrA*96, *relA*1, Δ(*argF*-laczya)U169, ϕ80d*lacZ*λM15, λ^-) were used for expression of β-D-galactosidase.

Measurements

Ultraviolet(UV) absorption spectra were recorded by a Hitachi Model 200-10 spectrometer. Fluorescence emission and excitation spectra were recorded by a Hitachi MPF-4 fluorescence spectrophotometer. Fluorescence excitation spectra were monitored at wavelength 397 nm for pyrAla and at wavelength 415 nm for 3-(9-anthryl)-DL-alanine.

Recombinant Plasmid

The recombinant plasmid pUC19Z was synthesized from the plasmid pUC19 and pMC1871 (Pharmacia, Sweden). A 3.0 kbp fragment containing the *LacZ* gene was excised from the pMC1871 plasmid with BamHI, and ligated into the pUC19, digested with BamHI and dephosphorylated with BAP. The resultant plasmid pUC19Z was transformed into DH5α strain and the transformants exhibiting β-D-galactosidase activity were picked on 2 % agar plates of Luria-Bertani(LB)-medium [1 % (w / w) bacto-trypton / 0.5 % (w / w) bacto-yeast-extract] in the presence of ampicillin, 5-bromo-4-chloro-3-indolyl β-D-galactopyranoside and isopropyl β-D-galactopyranoside. The plasmid DNA was isolated with the method of alkaline treatment [16].

Cell Cultivation

The *E. coli* strain DH5α harboring plasmid pUC19Z was precultured in a 500 ml flask containing 100 ml of LB-medium at 37 °C, with shaking for 16 h. The cells were collected by centrifugation at 3,000 rpm for 5 min and suspended in 30 ml of deionized water. An aliquot (1 ml) of the precultured cell suspension was inoculated into 100 ml of LB-medium in a 500 ml flask and cultivated to the exponential growth phase. Then 10 mg of CP was added and the flask was shaken for further 1 h. The cells were harvested by centrifugation and suspended in 30 ml of deionized water again. A portion of cell suspension (20 ml) was inoculated into 2.0 liter of LB-medium in the presence of 50 μg / ml of nonnatural fluorescent amino acid and 0.1 % lactose instead of glucose and cultured to the exponential growth phase at 37 °C. After cultivation, the cells washed with deionized water were suspended in 400 ml of 0.3 M (1 M = 1 mol dm^{-3}) potassium phosphate buffer (pH 7.2) in the presence of 3 mM $MgCl_2$. Cell growth was monitored at absorbance of 600 nm. One unit of the optical density(O.D.) corresponds to a cell density of 10^8 cells / ml.

Isolation of Proteins

Cell-free extracts were prepared by disintegrating the cells with a Braun cell homogenizer (Type 853023, B. Brown, Germany). The cell homogenate was centrifuged at 12,000 rpm for 5 min, the supernatant obtained being further centrifuged at 45,000 rpm for 60 min at 4 °C. The final cell-free extract obtained was concentrated through a Diaflow membrane filter (Ultrafiltration Cell Model 12, Amicon Corp., USA). The total amount of proteins was estimated by the Lowry's method [16]. The β-D-galactosidase protein was analyzed with sodium dodecyl sulfate-polyacrylamide gel electrophoresis (SDS-PAGE).

The proteins were recovered from the cell-free extracts with saturated ammonium sulfate. It was solubilized again with 100 mM potassium phosphate buffer (pH 7.2) and dialyzed for 24 h at 4 °C against 500-fold volume of the potassium phosphate buffer to remove ammonium sulfate. Thereafter, the fluorescence excitation spectra of the protein solution and the dialyzing buffer were measured at every 2.5 h of dialysis against 500-fold volume of the buffer at 4 °C. After ten-time repetition of dialysis for 25 h, the protein solution was added to the same volume of dimethyl sulfoxide (DMSO) and stirred overnight at 4 °C to wash out the nonnatural amino acid followed by further 20 times of the dialysis. The content of the nonnatural amino acid was monitored by following the fluorescence excitation spectrum during the dialysis treatment.

β-D-Galactosidase was purified with a gel-filtration chromatography followed by nondenaturing polyacrylamide gel electrophoresis. The proteins were applied to a Sephacryl S-300 column (2.5 × 85 cm) equilibrated with 100 mM potassium phosphate buffer (pH 7.2) containing 10 mM $MgCl_2$. A single peak of the β-D-galactosidase activity was found and the fractions were collected and concentrated. The concentrated solution was applied to a nondenaturing polyacrylamide gel electrophoresis (7 %) and the gel band corresponding to β-D-galactosidase was excised and eluted out with an Extraphore electrophoretic concentrator (Pharmacia, Sweden). The preparation finally obtained was used as a purified β-D-galactosidase.

Determination of Incorporated Nonnatural Amino Acids

The nonnatural amino acid content in the β-D-galactosidase was estimated by the fluorescence measurement. The fluorescence from the enzyme is attributed to both the original Trp residues and the incorporated nonnatural amino acid residues. Assuming that the fluorescence intensity of the Trp residues gives a maximum at wavelength λ_{trp} and the intensity of the nonnatural amino acid residues gives a maximum at wavelength λ_{aa}, a ratio (R) of the fluorescence intensity from the nonnatural amino acid residues to that from the Trp residues is represented by equation (3). The observed fluorescence intensity at wavelength λ, $F(\lambda)$, is composed of two components [equation (1)], one from the intrinsic fluorescence of protein, $F_{trp}(\lambda)$, and the other from the nonnatural amino acids, $F_{aa}(\lambda)$. X_{trp} and X_{aa} represent the contributions of each fluorescent residue.

$$F(\lambda) = X_{trp}F_{trp}(\lambda) + X_{aa}F_{aa}(\lambda) \qquad (1)$$

Introduction of working parameters as defined by equation (2), in which R_{obs} represents the ratio of observed fluorescence intensity at wavelength λ_{aa} to that at λ_{trp}, R_{aa}^0, the ratio of fluorescence intensity of the standard nonnatural amino acid solution at λ_{aa} to that at λ_{trp}, and R_{trp}^0, the ratio of fluorescence intensities for the standard protein solution at λ_{aa} to that at λ_{trp}, leads to equation (3).

$$R_{obs} = \frac{F(\lambda_{aa})}{F(\lambda_{trp})},\ R_{aa}^0 = \frac{F_{aa}(\lambda_{aa})}{F_{aa}(\lambda_{trp})},\ R_{trp}^0 = \frac{F_{trp}(\lambda_{aa})}{F_{trp}(\lambda_{trp})} \qquad (2)$$

$$R = \frac{X_{aa}F_{aa}(\lambda_{aa})}{X_{trp}F_{trp}(\lambda_{trp})} = R_{obs}\left(1 - \frac{R_{trp}^0}{R_{obs}}\right) \Big/ \left(1 - \frac{R_{obs}}{R_{aa}^0}\right) \qquad (3)$$

In the above equations, λ_{aa} and λ_{trp} represent a maximum fluorescence intensity of the nonnatural amino acid solution and the protein solution, respectively. The content of nonnatural amino acid C (mol / mol Trp residue) can be estimated from a calibration curve using 1 mg / ml BSA solution.

Enzyme Activity

The β-D-galactosidase activity was measured at 30 °C by following the increase in absorbance of *o*-nitrophenol produced through the hydrolysis of ONPG at 405 nm.

Results

The construction of plasmid pUC19Z to express β-D-galactosidase is illustrated in Figure 1. *E. coli* DH5α was transformed with the pUC19Z. Several transformants exhibiting β-D-galactosidase activity (blue-colored colonies) and having 5.7 kbp fragment of plasmid pUC19Z were obtained. The enzymatic activities of β-D-

galactosidase in various *E. coli* strains, grown in the absence of nonnatural amino acids, were measured and are summarized in Table 1. The activity of the wild strain B357 was 73-fold higher in lactose-grown cells than in glucose-grown cells. The protein produced in the presence of lactose from the DH5α strain, transformed with pUC19Z and treated with chloramphenicol (CP), showed two thousand-fold activity of that in the presence of glucose. The content of β-D-galactosidase in the total protein was estimated over 65 % judging from the calculation of specific activity (126 μmol / min mg in the cell free extract; 171 μmol / min mg in the purified preparation).

Table 1. β-D-galactosidase activity of various *E. coli* strains.

Strain	Plasmid[a]	Induction[b]	CP[c]	Specific activity[d]
B357	none	none	none	0.0645
B357	none	+	none	4.73
DH5α	pUC19Z	+	+	126
DH5α	none	+	+	0.00

[a]Transformation with the plasmid.

[b]Induction with lactose.

[c]Treated for 1 h.

[d]Specific activity is expressed in units per milligram of the β-D-galactosidase (μmol / min mg).

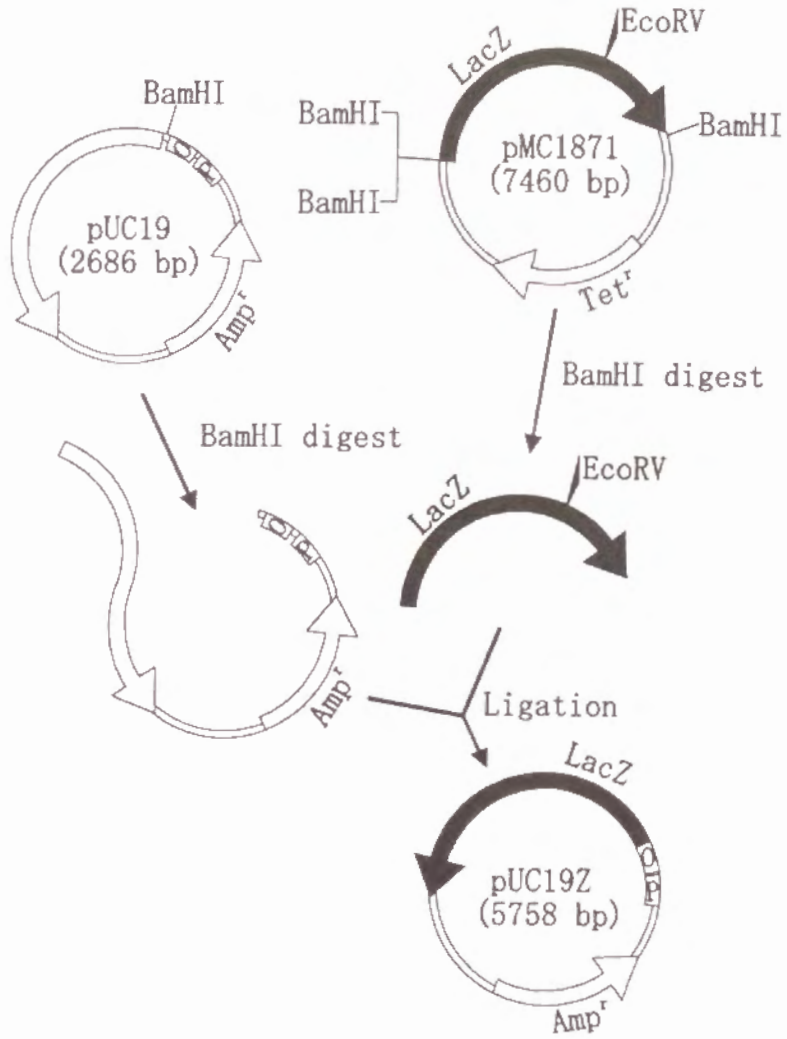

Figure 1. Construction of β-D-galactosidase expressing plasmid pUC19Z. BamHI and EcoRV represent the restriction sites on the plasmid. P is the promoter, and *LacZ* is the structural gene of β-D-galactosidase. Some of the colonies were screened for the presence of *LacZ* gene by agalose electrophoresis. A positive colony had a band corresponding to the open-circular plasmid DNA band digested at the site of EcoRV in *LacZ* gene.

The reduction in growth of strain B357 was within 20 % when the concentration of each nonnatural amino acid added in medium was lower than 50 μg / ml. The amount of produced proteins and β-D-galactosidase activity are shown in Table 2. In the presence of napAla, both the protein production and the activity per cell increased slightly. In this case, the effect of incorporation of napAla was not observed. In comparison, in the presence of antAla, the protein production per cell increased, while the activity per cell did not increase significantly, and in the presence of pyrAla, the protein production per cell did not decrease, while the activity per cell was reduced considerably. These results might be due to the incorporation of the nonnatural amino acid into β-D-galactosidase.

Table 2. The relative amount of proteins obtained from the cells of strain B357 and the relative β-D-galactosidase activity.

Nonnatural amino acid	Growth[b]	Amount of protein[c]	Specific activity[d]	Change[e]
none[a]	1.00	1.00	1.00	-
napAla	1.04	1.06	1.09	+9 %
antAla	0.91	1.38	0.95	-5 %
pyrAla	0.80	1.35	0.75	-25 %

[a]In the absence of any nonnatural amino acid.
[b]The relative growth of the cells.
[c]The relative amount of proteins per cell.
[d]The relative specific activity of β-D-galactosidases.
[e]The change in the specific activity.

The amount of a nonnatural amino acid in a protein was estimated by the fluorescence intensity of the nonnatural amino acid taking that of Trp in the protein as standard. For the calibration of fluorescence intensity, fluorescence of nonnatural amino acids was measured in the presence of BSA.

The fluorescence intensity ratio R and the residual content C were plotted on log-log graph paper and a calibration curve was obtained by the least-squares method. The curve was expressed by $C = 9.28\ R^{0.615}$ (mmol / mol Trp residue) for antAla in the range of $R < 15$ and by $C = 0.795\ R^{1.55}$ (mmol / mol Trp residue) for pyrAla in the range of $R < 10$.

The protein solution from the wild strain B357 grown in the presence of the nonnatural amino acid was added to the same volume of DMSO and the nonnatural amino acid which nonspecifically bound to the protein was removed by dialysis. The fluorescence intensity ratio during the dialysis was followed and is shown in Figure 2. The ratio was decreased exponentially, but a certain intensity was remained after the sufficient dialysis for 75 h. The minimum R was 0.30 for antAla and was 0.65 for pyrAla. The residual content C was obtained using the calibration curve as 4.5 mmol / mol for antAla and 0.42 mmol / mol for pyrAla. In comparison, the protein solution of the B357 grown without nonnatural amino acids was mixed with a solution of 40 μg / ml nonnatural amino acids and stirred at 4 °C for 24 h. The fluorescence intensity ratio during the dialysis was followed after washing with DMSO. As shown in Figure 2, the fluorescence of the nonnatural amino acids disappeared in 48 h, indicating that the nonspecifically bound nonnatural amino acids were completely removed by the dialysis.

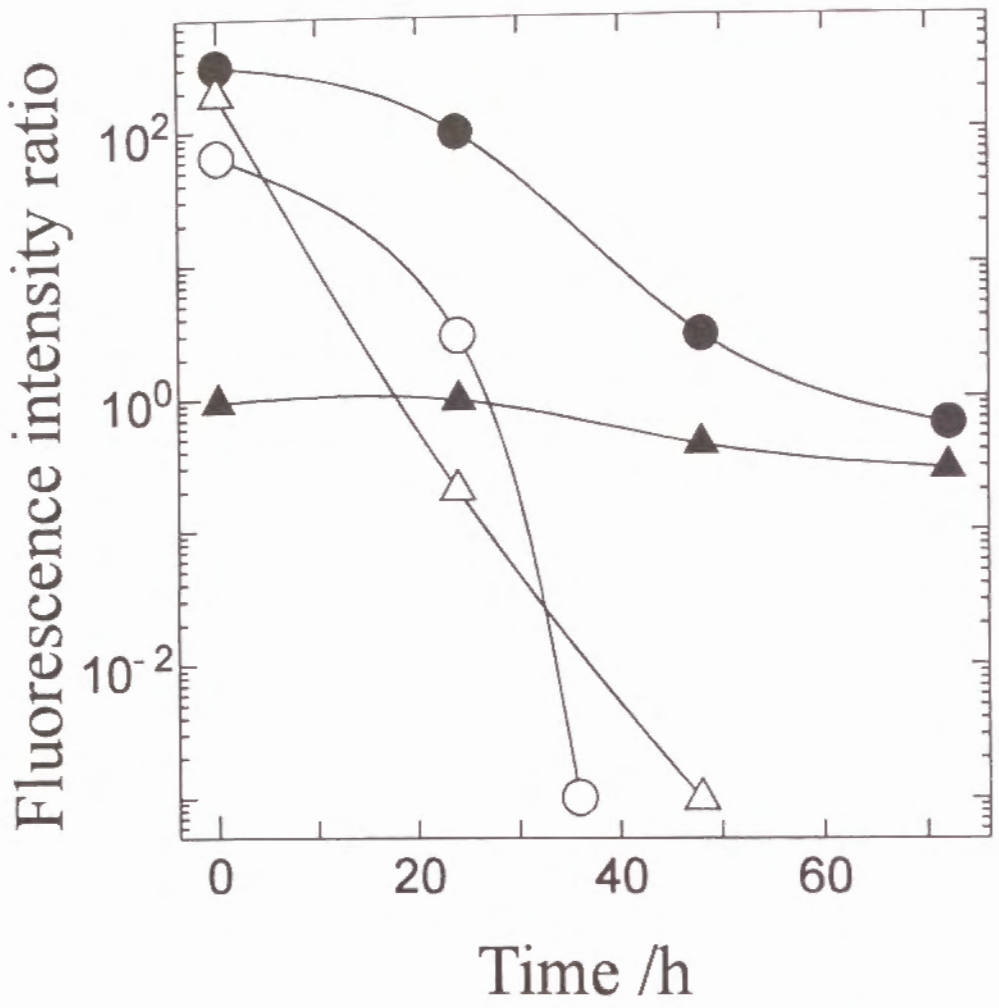

Figure 2. Change in fluorescence intensity ratio during dialysis treatment. The fluorescence intensity ratio of the protein solutions obtained from the cells of strain B357 was followed during the dialysis. ●, sample from the cells grown in the presence of pyrAla; ○, mixture of sample from the cells grown without nonnatural amino acid and 40 μg / ml of pyrAla; ▲, sample from the cells grown in the presence of antAla; △, mixture of sample from the cells grown without nonnatural amino acid and 40 μg / ml of antAla.

β-D-Galactosidase was purified from the protein solution obtained from the DH5α cells harboring pUC19Z without nonnatural amino acid (Figure 3). Similarly, β-D-galactosidase was purified from the protein solution obtained from the DH5α cells harboring pUC19Z grown in the presence of 50 μg / ml nonnatural amino acids. Each 200 μg of purified β-D-galactosidase was obtained from 1 mg of the crude preparation through the nondenaturing PAGE.

Figure 3. The SDS-PAGE profile of produced β-D-galactosidases. β-D-Galactosidase was obtained from various strains without nonnatural amino acid. Mr, Marker; lanes 1 and 4, DH5α strain harboring pUC19Z; lanes 2 and 5, DH5α strain harboring pUC19; lanes 3 and 6, DH5α without transformation. Lanes 1, 2, and 3, 20 μg protein each; lanes 4, 5, and 6, 10 μg protein each.

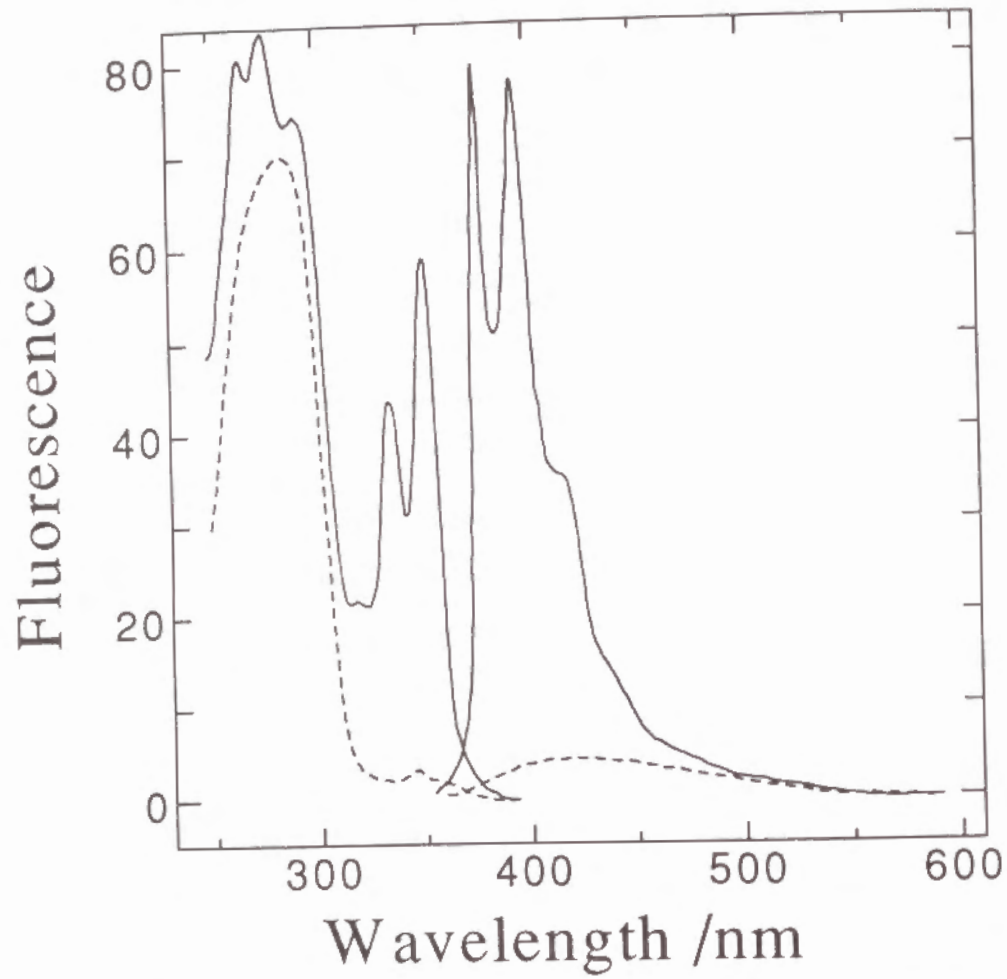

Figure 4. Fluorescence emission and excitation spectra of the purified β-D-galactosidase obtained from the cells of strain DH5α grown with or without pyrAla. The 360-580 nm range, fluorescence emission spectra excited at 345 nm; the 250-380 nm range, fluorescence excitation spectra monitored at 395 nm. Solid lines, spectra of the purified β-D-galactosidase obtained from the cells grown in the presence of pyrAla; broken lines, spectra of that obtained from the cells without nonnatural amino acid.

A significant fluorescence of pyrenyl moiety was observed in the purified β-D-galactosidase obtained from the cells grown in the presence of pyrAla (Figure 4). It was found that the fluorescence intensity ratio R_{obs} was 0.796 from the fluorescence excitation spectrum of the purified β-D-galactosidase monitored at wavelength 397 nm. The residual content C was determined as 0.556 mmol / mol from the calibration curve.

β-D-Galactosidases were incubated in a water bath at 60 °C. Aliquots were removed at various times over 180 s period, placed on ice and then measured for the residual activity (Figure 5). The activity of the purified β-D-galactosidases obtained from the cells grown in the presence of pyrAla or antAla remained after the incubation of 120 s at 60 °C, while that obtained from the cells grown without nonnatural amino acids was lost completely in 120 s. This indicates that the thermostability of β-D-galactosidase was improved by the incorporation of nonnatural amino acids.

It can be derived from the Michaelis-Menten's reaction kinetics that a specific activity of an enzyme is proportional to the rate constant k_{cat} in the case of sufficiently high substrate concentration. The activation energy of the catalytic reaction was calculated from the Arrhenius plot of log k_{cat} against $1 / T$ as shown in Figure 6. The activation energy of β-D-galactosidase obtained from the cells grown in the presence of various nonnatural amino acids was identical with that for β-D-galactosidase obtained from the cells grown without the nonnatural amino acids.

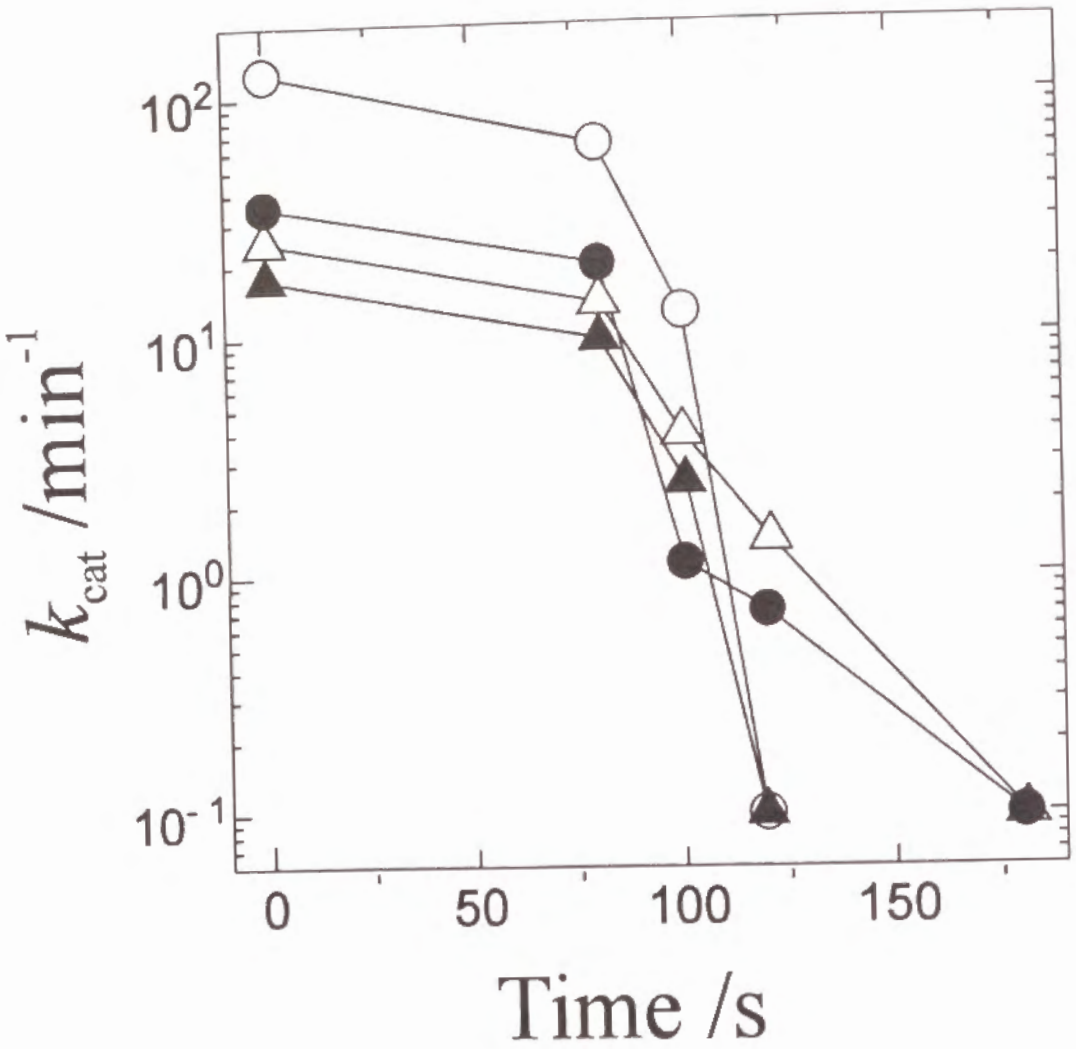

Figure 5. Thermostability of purified β-D-galactosidases. The specific activity is plotted against incubation times of 80 s, 100 s, 120 s, and 180 s. ○, sample obtained from the cells of strain DH5α grown without nonnatural amino acid; ●, △ and ▲, samples obtained from the cells of strain DH5α grown in the presence of pyrAla, antAla, and napAla, respectively.

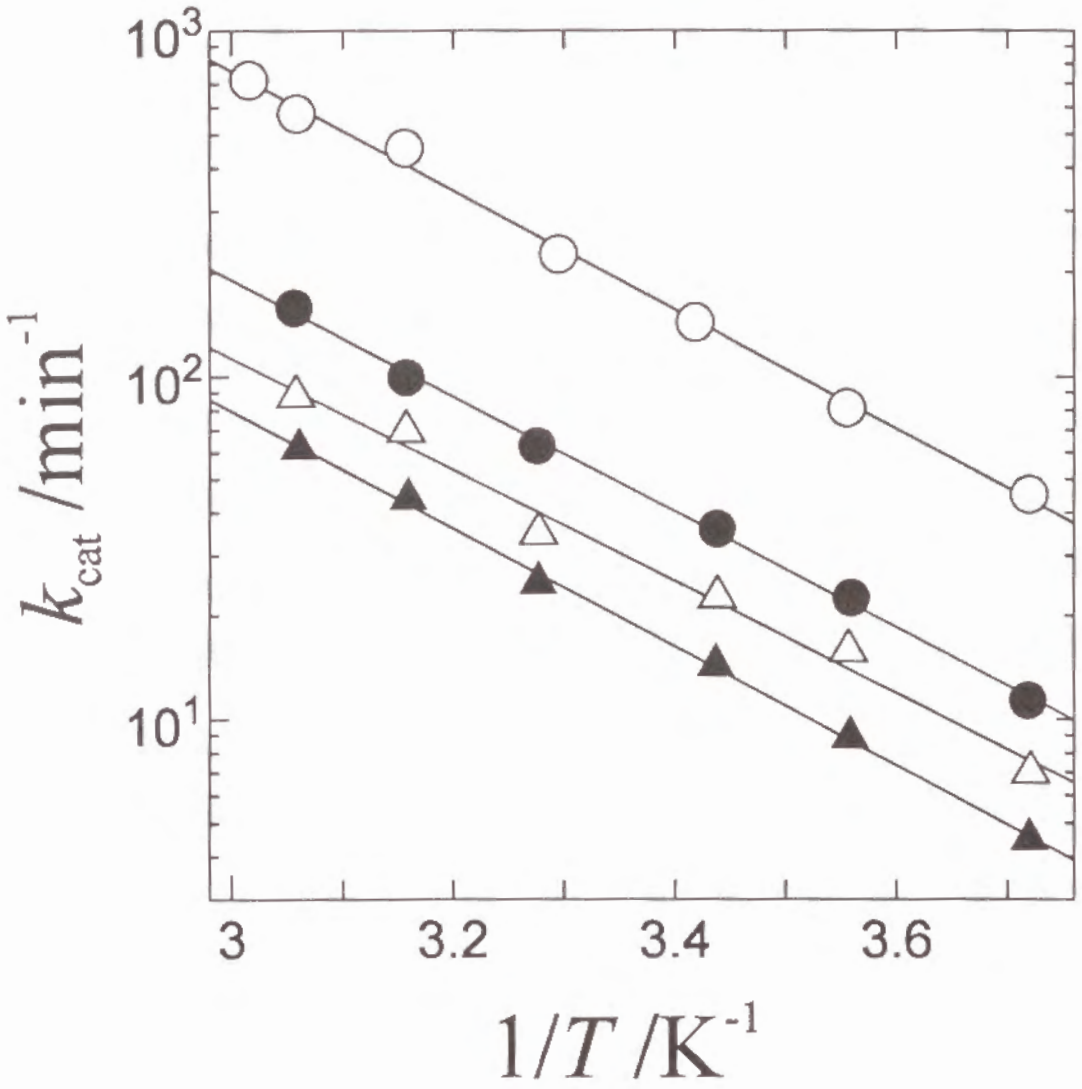

Figure 6. The specific activity *vs.* 1 / *T* plot of purified β-D-galactosidases. ○, sample obtained from the cells of strain DH5α grown without nonnatural amino acid; ●, △ and ▲, samples obtained from the cells of strain DH5α grown in the presence of pyrAla, antAla, and napAla, respectively.

Discussion

In general, a tRNA is not mischarged with nonnatural amino acids, because aminoacyl-tRNA synthetase precisely discriminates the corresponding amino acid from the others. Nonnatural amino acids found in natural polypeptides is usually formed in the process of the posttranslational modification. In some cases, the nonnatural amino acid-containing proteins show resistance to the digestion by proteases. The natural amino acid analogs, such as canavanine, 2-azetidinecarboxylic acid, and 4-fluorophenylalanine, were shown to be incorporated during the accelerated biosynthesis of protein after viral infection of bacteria [12]. The mutant proteins inhibited the self-assembly of the viral proteins. On the other hand, it has been reported that cleavage of the signal sequence of pre-prolactin synthesized in the presence of hydroxynorvaline is inhibited by incorporation of the analog [12]. In most cases, incorporation of analogs resulted in reduction of protein functions. Abnormal (mutant) proteins accumulated in a cell are known to be digested by intracellular proteases. The accumulation of abnormal proteins leads to an expression of protease La, which digests the abnormal proteins [13]. In addition, cell growth will be inhibited because high frequency of production of abnormal proteins may cause reduction of normal protein production. For these reasons, it was difficult to prepare abnormal proteins incorporated with nonnatural amino acids.

Parker reported that the amino acid substitutions did not lead to proteins recognized as grossly abnormal by the proteolysis systems in cells. Abnormal proteins in which substitution frequency was under 10 % were not eliminated in a cell, and abnormal subunits of ribosome were found in cells grown normally [14].

Taking these results into consideration, abnormal proteins may be prepared by lowering substitution frequency. Abnormal β-D-galactosidase was prepared in the presence of various fluorescent nonnatural amino acids with low frequency of incorporation. In order for the protein not to be recognized as a foreign abnormal protein, β-D-galactosidase was synthesized in *E. coli*. The nonnatural amino acids used in this study were not analogous to any natural amino acids, so that the nonnatural amino acids were mischarged to tRNAs to be incorporated into proteins in sufficiently low frequency. Fluorescent amino acids can be detected in abnormal proteins even in low frequency of incorporation.

Table 3. Amino acid sequence of β-D-galactosidase.[a]

	1234567890	1234567890	1234567890	1234567890	1234567890	1234567890
1	TMITDSLAVV	LQRRDWENPG	VTQLNRLAAH	PPFASWRNSE	EARTDRPSQQ	LRSLNGEWRF
61	AWFPAPEAVP	ESWLECDLPE	ADTVVVPSNW	QMHGYDAPIY	TNVTYPITVN	PPFVPTENPT
121	GCYSLTFNVD	ESWLQEGQTR	IIFDGVNSAF	HLWCNGRWVG	YGQDSRLPSE	FDLSAFLRAG
181	ENRLAVMVLR	WSDGSYLEDQ	DMWRMSGIFR	DVSLLHKPTT	QISDFHVATR	FNDDFSRAVL
241	EAEVQMCGEL	RDYLRVTVSL	WQGETQVASG	TAPFGGEIID	ERGGYADRVT	LRLNVENPKL
301	WSAEIPNLYR	AVVELHTADG	QLIEAGTCDF	REVRIENGLL	LLNGKPLLIR	GVNRHQHHPL
361	HGQVMDEQTM	VQDILLMKQN	NFNAVRCSHY	PNHPLWYTLC	DRYGLYVVDE	ADIETHGMVP
421	MNRLTDDPRW	LPAMSERVTR	MVQRDRNHPS	VIIWSLGNES	GHGANHDALY	RWIKSVDPSR
481	PVQYEGGGAD	TTATDIICPM	YARVDEDQPF	PAVPKWSIKK	WLSLPGETRP	LILCEYAHAM
541	GNSLGGFAKY	WQAFRQYPRL	QPGFVWDWVD	QSLIKYDENG	NPWSAYGGDF	GDTPDDRQFC
601	MNGLVFADRT	PHPALTEAKH	QQQFFQFRLS	GQTIEVTSEY	LFRHSDNELL	HWMVALDGKP
661	LASGEVPLDV	APQGKQLIEL	QELPQPESAG	PLWLTVRVVQ	PNATAWSEAG	HISAWQQWRL
721	AENLSVTLPA	ASHAIPHLTT	SEMDFCIELG	NKRWQFNRQS	GFLSQMWIGD	KKQLLTPLRD
781	QFTRAPLDND	IGVSEATRID	PNAWVERWKA	AGHYQAEAAL	LQCTADTLAD	AVLITTAHAW
841	QHQGKTLFIS	RKTYRIDGSG	QMAITVDVEV	ASDTPHPARI	GLNCQLAQVA	ERVNWLGLGP
901	QENYPDRLTA	ACFDRWDLPL	SNMYTPYVFP	SENGLRCGTR	ELNYGPHQWR	GDFQFNISRY
961	SQQQLMETSH	RHLLHAEEGT	WLNIDGFHMG	IGGDDSWSPS	VSAEFQLSAG	RYHYQLVWCQ
991	K					

[a] Aromatic amino acids, Phe (F), Tyr (Y) and Trp (W), which have potential contribution to protein stabilization through hydrophobic interaction with pyrAla, are doubly underlined.

The overproduction of β-D-galactosidase using the DH5α strain with plasmid pUC19Z was in the level of two thousand times higher than the wild strain (Table 1). antAla and pyrAla were found in the proteins of the wild strain synthesized in the presence of these nonnatural amino acids (Figure 2), indicating that *E. coli* utilized these nonnatural amino acids to some extent in protein biosynthesis. Fluorescence emission of pyrenyl moiety was observed in the purified β-D-galactosidase synthesized in the presence of pyrAla, and the residual content was estimated to be 0.556 mmol / mol Trp residue. Thus, one pyrAla residue per 46 molecules of β-D-galactosidase was found because there are 39 Trp residues in a β-D-galactosidase molecule. However, pyrAla may be attached to the hydrophobic surface of BSA used in the calibration experiment, so that this value is the minimum in the case of the absence of pyrenyl moiety quenching by surrounding charges or dipoles.

The specific activity of the proteins obtained in the presence of antAla or pyrAla was reduced (Table 2), while the amount of proteins per cell was not affected. This indicates that protein biosynthesis was not lowered by the addition of the nonnatural amino acids. The β-D-galactosidase content of the total proteins was found to increase continuously throughout the cultivation, indicating that the reduction of the specific activity was not the result of proteolytic digestion of abnormal β-D-galactosidase but the result of the production of β-D-galactosidase with low activity. On the other hand, the activation energy of the purified β-D-galactosidase did not decrease (Figure 6). Thus, it is considered that the nonnatural amino acids were incorporated into the active site of β-D-galactosidase and the activity of some β-D-galactosidase was lost. In the case of enzyme which lost the activity, incorporated amino acids are thought to be on the protein surface and easily quenched. In addition, incorporation of a highly hydrophobic amino acid into the hydrophilic surface may cause instabilization of β-D-galactosidase.

At least 2.2 % of β-D-galactosidase was estimated to have one pyrAla residue. As shown in Figure 5, several per cent of the mutant β-D-galactosidases resulted in the improved thermostability of the enzyme, indicating that the nonnatural amino acids were incorporated into the hydrophobic region of β-D-galactosidase and a higher-order structure of the enzyme was stabilized. Aromatic amino acid residues which could interact with the incorporated pyrAla residue are shown in Table 3. In the case of enzyme which retained the activity with higher thermostability, the incorporated nonnatural amino acids should be located apart from the protein surface and are hardly quenched.

In conclusion, the mutant β-D-galactosidases substituted by the nonnatural amino acids were successfully prepared. By lowering substitution frequency, cell growth and protein biosynthesis rate were not reduced.

References

1. G. L. Igloi, F. Haar and F. Cramer, *Biochemistry*, 1978, **17**, 3459.
2. S. Schlesinger and M. J. Schlesinger, *J. Biol. Chem.*, 1967, **242**, 3369.
3. S. Schlesinger, *J. Biol. Chem.*, 1968, **243**, 3877.
4. S. Schlesinger and M. J. Schlesinger, *J. Biol. Chem.*, 1969, **244**, 3803.
5. J. Attias, S. Schlesinger and M. J. Schlesinger, *J. Biol. Chem.*, 1969, **244**, 3810.
6. H. Morris and M. J. Schlesinger, *J. Bacteriol.*, 1972, **111**, 203.

7. B. D. Sykes, H. I. Weingarten, and M. J. Schlesinger, *Proc. Natl. Acad. Sci. USA*, 1974, **471**, 469.
8. D. T. Browne and J. D. Otvos, *Biochem. Biophys. Res. Commun.*, 1976, **468**, 907.
9. P. Gueguen, M. Padron, B. Perbal and G. Herve, *Biochim. Biophys. Acta*, 1980, **615**, 59.
10. F. Naider, Z. Bohak and J. Yariv, *Biochemistry*, 1972, **411**, 3202.
11. H. Koide, S. Yokoyama, G. Kawai, J. Ha, T. Oka, S. Kawai, T. Miyake, T. Fuwa and T. Miyazawa, *Proc. Natl. Acad. Sci. USA*, 1988, **485**, 6237.
12. M. J. Wilson and D. L. Hatfield, *Biochim. Biophys. Acta*, 1984, **781**, 205.
13. S. A. Goff and A. L. Goldberg, *Cell*, 1985, **441**, 587.
14. J. Parker, *J. Biol. Chem.*, 1981, **256**, 9770.
15. T. Maniatis, E. F. Fritsch and J. Sambrook, *"Molecular Cloning: A Laboratory Manual,"* 1982, Cold Spring Harbor, New York, pp. 90-91.
16. D. H. Lowry, N. J. Rosebrough, A. L. Farr and R. J. Randall, *J. Biol. Chem.*, 1951, **193**, 265.

Chapter 2

Semisynthesis of Mutant Cytochromes *c* Replaced by Nonnatural Aromatic Amino Acid at Phe^{82} and Photoregulation of Reduction Reaction with 2-Mercaptoethanol

Introduction

Cytochrome *c* is a heme protein, which is involved in the electron transfer reaction of the respiratory chain in cell membrane such as mitochondrial inner membrane. It is known that the arrangement of amino acid residues around the heme moiety is crucial for the electron transfer ability [1-4 and references therein]. The molecular mechanism for the electron transfer over a long distance is still controversial [5,6], but the polypeptide matrix should play an important role for providing a passage to the partner proteins [7].

Phe^{82} is an evolutionarily conserved residue within the interfacial region that has long been believed to be important for anchoring cytochrome *c* to its redox partners. Recently, it was suggested that the Phe^{82} is required not for electron transfer activity but for correct binding between cytochrome *c* and cytochrome *c* oxidase [8]. However, changing only this amino acid residue in yeast iso-1-cytochrome *c* produces nearly as large effect on the triplet decay rate as does the use of cytochrome *c* (*Drosophila. melanogaster*), which differs from yeast iso-1-cytochrome *c* in 40 % of its amino acid residues [9]. Since Phe^{82} is located near the heme moiety, it has been postulated that the orbital overlap and the oxidation-reduction potential difference between the heme and the aromatic

side chains should be influential in the early process of electron transfer reaction of the cytochrome *c* [10].

A useful way to investigate the role of specific amino acid residues of a protein is to study the activity of the protein analogs that are substituted at a specific site [11]. A relationship between the nature of the axial ligand of the heme and the redox potential of mutant cytochromes *c* that are replaced at Met^{80} by natural or nonnatural amino acids was discussed [12,13]. Although protein engineering has been employed for fundamental studies of protein structure-function relations, it has little been applied for developing novel functions of the protein [14,15]. In this chapter, Phe^{82} of cytochrome *c* was replaced with pheGly or pyrAla residue, in order to correlate the electron transport with the spatial arrangement of the large aromatic side chain at the position 82. Furthermore, it was expected that the electron transfer of the mutant protein containing pyrAla would be regulated by light irradiation, because the oxidation-reduction potential of the pyrenyl group is changed by the photoexcitation [16].

Experimental

Materials

Horse heart cytochrome *c* (Type VI), and carboxypeptidase A (diisopropylphosphorofluoridate-treated) were obtained from Sigma Chemical Co., USA. *N*-(*tert*-Butyloxycarbonyl)methionine hydroxysuccinimide ester (Boc-Met-OSu) and Boc-Ile-OH were obtained from Kokusan Chemical Works, Ltd., Japan. Methyl acetimidate hydrochloride was prepared by the method reported by Hunter & Ludwig [17]. Optically pure pyrAla was prepared by the

method of Egusa and coworkers [18]. Other chemicals used in this work were commercially available highest purity products.

The mutant cytochromes *c* were prepared by using a semisynthetic method as shown in Scheme 1. The preparation procedure was as follows.

Horse heart cytochrome *c* (100 mg) was first subjected to gel filtration on a Sephadex G-50 column to remove polymeric substances. Acetimidylation of the cytochrome *c* was carried out by the method of Wallace and Harris [19]. Acetimidyl-cytochrome *c* was obtained as a red powder (95 mg) after gel chromatography. Amino group analysis showed over 95 % of ε-amino groups were blocked.

The protected cytochrome *c* was split into three fragments I(1-65), II(66-80), and III(81-104) by the established method [20]. A 30-fold excess of CNBr over Met residues was added to a 0.8 mM solution of acetimidyl-cytochrome *c* in 70 % (v / v) aqueous formic acid. The reaction was performed at 20 °C in the dark for 24 h. The mixture was then lyophilized and was redissolved in 7 % (v / v) aqueous formic acid, and subjected to gel filtration on a Sephadex G-50 (super-fine grade) column (4.0 × 55 cm). Fragment I lactone was purified by removing unreactive derivative of the fragment that had been hydrolyzed at the carboxyl terminal homoserine lactone (yield, 57 mg) [21]. Fragment II was dissolved in 0.01 M sodium phosphate buffer containing 4 M urea (pH 6.9, 10 ml) and applied to a diethylaminoethyl(DEAE)-Sephadex column (1.5 × 30 cm), with a linear sodium phosphate gradient (0.01-0.05 M) at a flow rate of 25 ml / h (yield, 9 mg) [21]. HPLC analysis showed a single peak of 66-80 fragment. Fragment III was purified on a CM-Sephadex column (1.5 × 35 cm), with a linear sodium phosphate gradient (0.01-0.15 M) at a flow rate of 25 ml / h (yield, 21 mg) [21]. HPLC analysis showed a single peak for the 81-104 fragment.

Two cycles of the Edman reaction [22] were carried out to split off the N-terminal residues Ile^{81} and Phe^{82} from the fragment III. The stepwise degradation of the fragment was monitored by TLC analysis [R_f = 0.72 of phenylthiohydantoin(PTH)-Ile for the first cycle, and R_f = 0.68 of PTH-Phe for the second cycle]. After two cycles, the degraded peptide was purified by gel filtration on a Sephadex G-50 column in 7 % formic acid and desalted by a Sephadex G-25 column. The required fraction was collected as a white powder (5 mg) after lyophilization.

N^{α}-Boc-$N^{72,73}$-diacetimidyl, des(Hse^{80})-fragment II O^{66},O^{69}-dimethyl ester was prepared as described in the literature [23] with several modifications. Fragment II O^{66},O^{69}-dimethyl ester was prepared by direct esterification of fragment II with 5 % methanolic HCl. The α-amino group was protected by treatment of a dimethylformamide (DMF) solution of the peptide ester with a 250-fold molar excess amount of di-*tert*-butyl dicarbonate. The C-terminal Hse^{80} lactone was selectively hydrolyzed in 2 % aqueous triethylammonium hydrogen carbonate (pH 9.0). The reaction mixture was adjusted to neutrality with 1 M acetic acid and the solution was lyophilized. The removal of C-terminal residue Hse^{80} was achieved by using carboxypeptidase A (50 units / ml) in 2 M aqueous ammonium hydrogen carbonate buffer (pH 7.5) [24]. The reaction mixture was applied directly to a Sephadex LH-20 column (2.0 × 100 cm) in chloroform / methanol (1:9, v / v). The collected fraction was concentrated.

The tripeptide IV (80-82) was prepared by a conventional method using dicyclohexylcarbodiimide (DCCD) and *N*-hydroxysuccinimide (HOSu) as coupling reagents. Fragment (83-104) was coupled with Boc-tripeptide(80-82)-

OSu, Boc-Met-Ile-pyrAla-OSu or Boc-Met-Ile-pheGly-OSu. Coupling reaction was performed in a DMF solution, at a peptide concentration of 1 mM, by using a 10- to 20-fold molar excess amount of active ester. The reaction was allowed to continue for 2 days at 20 °C. The product peptide was dried over silica gel under high vacuum and treated with anhydrous trifluoroacetic acid (TFA) (40 °C for 60 min, peptide concentration 5 mM). The product was purified by gel filtration on a Sephadex G-50 column using 7 % formic acid as eluent (yield, 5 mg).

The derivative of the fragment (66-79) was converted to *N*-hydroxysuccinimide ester and reacted with the fragment (80-104). Coupling was performed in a DMF solution, at a peptide concentration of 1 mM, by using a 10- to 20-fold molar excess amount of active ester. Reaction was allowed to continue for 2 days at 20 °C. The *tert*-butyloxycarbonyl (Boc) group was removed by treatment with anhydrous TFA at 40 °C for 1 h (peptide concentration, 1 mg / ml). After the treatment, the product was recovered by precipitation with 4-fold volumes of cold diethyl ether. The precipitate was washed once with cold diethyl ether and dried over silica gel (yield, 4 mg). The methyl groups were removed from purified fragment (66-104) by suspension, at a concentration of 0.5 mg / ml, in triethylamine (TEA) / water (1:49, v / v), which had been adjusted to pH 10.5 (at 20 °C) with 1 M acetic acid. After 24 h at 20 °C, the pH was adjusted to 7 with 1 M acetic acid, and the resulting solution was lyophilized (yield, 4 mg).

The technique of Corradin and Harbury [20] or its adaptation by Wallace and Rose [25] was used in the combination of the heme and nonheme fragments. The lactone of fragment I and the fragment (66-104) of horse cytochrome *c* form a complex in neutral aqueous buffers, in which the missing 65-66 peptide bond is reformed by aminolysis of C-terminal Hse^{65} lactone when the complex is maintained in a reducing state. Sufficient 2-mercaptoethanol was added to ensure

complete reduction of the degassed mixture, which was then sealed to exclude air completely. After 24 h in the reducing state, the mixture was purified by gel filtration [26] (yield, 1.2 mg). All the cytochrome *c* analogs prepared contain homoserine residue at the position 65. This substitution does not significantly affect chemical or physical properties of cytochrome *c* [20,27]. Lyophilized *N*-amidinated products were deprotected by treatment with aqueous NH_4OAc buffer(1 M, pH 11.5) at 20 °C in the dark [28]. After 18 h, the solution was subjected directly to a Sephadex G-25 fine column to remove low molecular weight salts. Heme-containing fractions were collected and lyophilized.

The lyophilized semisynthetic mutants of cytochromes *c* were renatured by the method reported by Babul and coworkers [29]. The lyophilized product was treated with 8 M urea in aqueous potassium phosphate buffer (0.1 M, pH 7.0), and then freed from urea on a gel-filtration column of Sephadex G-25 equilibrated with the potassium phosphate buffer. This treatment can renature proteins that might have been denatured by the freeze-drying procedure from 7 % formic acid.

Measurements

UV- and visible-absorption spectra were recorded on a Jasco Ubest-50 UV / Vis spectrophotometer with a cell of 1-cm path length. The concentration of proteins used in this study was determined by the intensity of the appropriate absorption maximum on the basis of molar extinction constants [ε_{550} (reduced) = 2.95×10^4 /M cm and ε_{409} (oxidized) = 1.10×10^5 /M cm for the heme-containing fragments, and $\varepsilon_{406} = 1.27 \times 10^5$ /M cm for the ferric heme fragment I and ε_{276} = 9.89×10^3 /M cm for the non-heme fragment (66-104)]. Circular dichroism

spectra were recorded on a Jasco J-600 CD spectrophotometer with a cell of 0.1-cm path length.

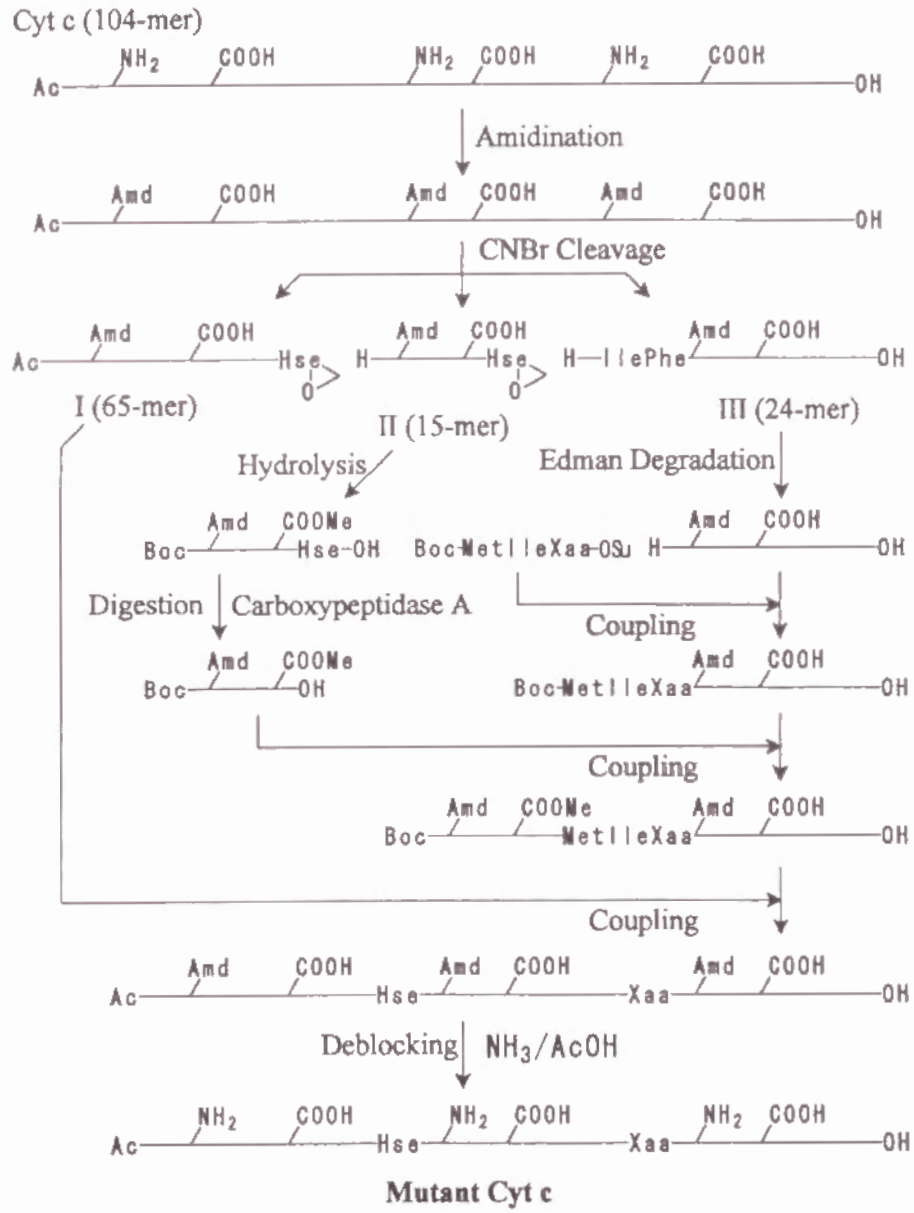

Scheme 1. Semisynthesis of mutant cytochromes *c*.

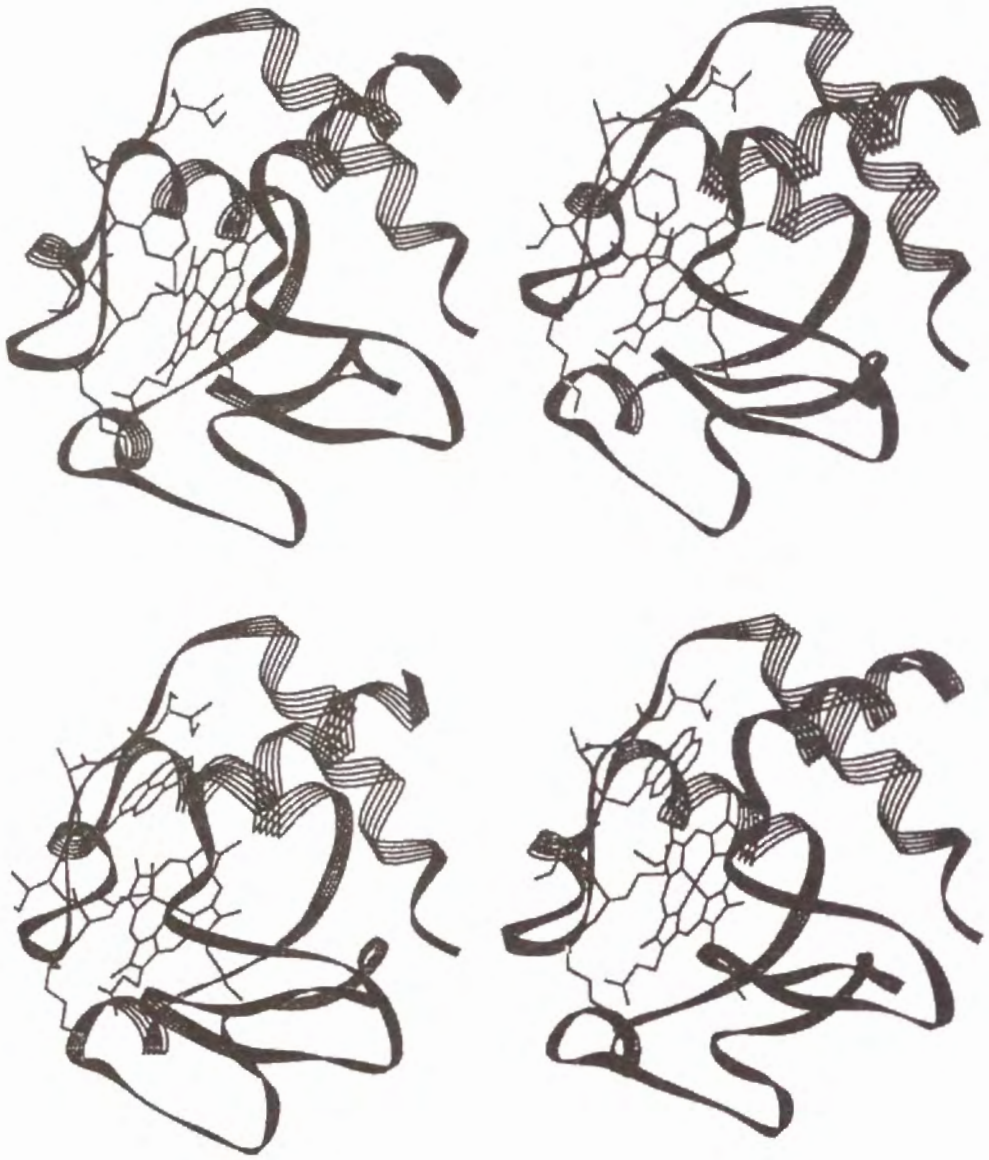

Figure 1. 3D Ribbon drawing of mutant cytochromes *c*.
Backbone structure was illustrated by ribbon model. Side chains at position 79-85 were drawn in stick model and were superimposed on the ribbon drawing. (Top) PGL-Cytc in oxidized (left) and in reduced (right) state. (Bottom) PYR-Cytc in oxidized (left) and in reduced (right) state.

High performance liquid chromatography (HPLC) was performed on Jasco LC-800 system (Japan Spectroscopic Co., Ltd., Japan). A $5C_{18}$ (4.6 × 150 mm) Cosmosil 390-46 column (Nacalai Tesque, Inc., Japan) was used at a flow rate of 1 ml / min. Solvent A was prepared by adding TFA (HPLC-grade, 1 ml) to filtered deionized water (1 liter). Solvent B was acetonitrile (HPLC-grade, Wako Pure Chem. Ind., Ltd., Japan) with 0.1 % (v / v) TFA.

Protein concentration was determined by the Lowry's method [30]. Free amino groups were determined by the method of 2,4,6-trinitrobenzenesulfonic acid (TNBS) assay [31].

The electron transfer activities of the mutant cytochromes *c* were evaluated by measuring the rate of reduction with 2-mercaptoethanol in aqueous solution. The absorbance at 415 nm assigned to the Soret band in the reduced form was monitored with the addition of 2-mercaptoethanol. The logarithm of absorbance, $\log (A_{415}(0) - A_{415}(t))$, was plotted against reaction time, and kinetic constants were determined by the least-squares fitting analysis.

Results

Semisynthesis

The technique of protein semisynthesis, in which fragments of a protein are condensed by chemical methods, has been established and employed by many authors [32-39]. The use of protein fragments produced by treatment with CNBr is important because it promises a spontaneous condensation of the fragments formed by aminolysis of the C-terminal homoserine lactone [27,40,41].

Horse heart cytochrome *c* was amidinated to block primary ε-amino groups and was subjected to CNBr treatment. CNBr cleaves the protected cytochrome *c*

at the two Met residues to give three fragments corresponding to residues, 1-65, 66-80, and 81-104. The fragment III containing Phe^{82} was subjected to Edman degradation. The nonnatural amino acids were incorporated by an active-ester method. The fragment was recombined with other two fragments, and finally the protecting groups were removed to obtain mutant cytochromes *c*. Figure 1 shows a schematic drawing of mutant cytochromes *c*, which was drawn by MAGE program of BNL, USA, using X-ray crystallography data of native cytochrome *c* and reconstructed with nonnatural amino acids.

Protein Structure

Figure 2 shows CD spectra of mutant cytochromes *c* at the Soret band. Almost the same spectra are observed for native cytochrome *c* and PGL-Cytc, but that of PYR-Cytc is somewhat different from the other two. A positive signal around 340 nm should overlap in the spectrum of PYR-Cytc due with the ^1L_a band of the pyrAla residue. The UV / visible spectrum of PGL-Cytc was virtually identical with the spectrum of native cytochrome *c* in the porphyrin absorption region: Soret band at 408 nm (1.1×10^5 /M cm); Q band at 528 nm (1.0×10^4 /M cm) (Figure 3). These results indicate that substitution of pheGly for Phe has little effect on the spatial arrangement of aromatic side chains around the heme, and the redox properties of PGL-Cytc and native cytochrome *c* might be nearly identical.

However, the Soret band of PYR-Cytc at 410 nm was broadened, reflecting relocation of aromatic side chains around the heme. UV / visible spectra showed a slight red shift at the Soret band by 2 nm, and some broadening was observed also in the Q band region (550 nm). This small shift is ascribed to interactions of the heme with the pyrenyl group at position 82 rather than to the structural change

around the heme region, since the Soret band peak has been reported not to shift for the largely disordered heme fragment I (1-65) [29] and even for urea-denatured cytochrome *c* [42,43].

The two mutants showed a double-minimum-type CD spectrum with peaks at 210 nm and 222 nm, which may reflect α-helical structures in the protein (Figure 4). Perturbation of the protein backbone structure was negligible with PGL-Cytc, supporting that the replacement of Phe with pheGly did not cause a significant change in the structure of PGL-Cytc. However, the apparent α-helix content in PYR-Cytc was reduced to half that of native cytochrome *c*. The conformation of PYR-Cytc changed to some extent, forming a different conformation in which a pyrAla residue is located near the heme and interacts with aromatic side chains around the heme. This conformational change by substitution of the Phe with a bulky pyrAla should cause a polarity change inside the heme pocket by solvent relocation [44], so that the redox properties might be affected [2,3].

Reduction Reaction

The heme moiety in a native ferrocytochrome *c* was slowly reduced by 2-mercaptoethanol having an oxidation potential of about 0.30 V (Figure 5a). Mutant cytochromes *c* in oxidized form were reduced by addition of 2-mercaptoethanol in 100 mM sodium phosphate buffer (pH 6.9) at 25 °C. The kinetic constant was smaller in PGL-Cytc than in the native cytochrome *c*, indicating that the redox potential gap between the heme moiety and the reductant is reduced by the substitution. On the other hand, ferric PYR-Cytc was reduced faster than was native cytochrome *c* (Figure 5b). There are two possible mechanisms to explain the accelerated electron transfer reaction observed in this

experiment. First, the redox potential of the heme moiety decreased and an enhanced potential gap between ferric PYR-Cytc and the reductant (free-energy controlling). Second, substitution for bulky pyrAla residue induced a structural change in the heme crevice, which probably facilitates access of reductant to the heme moiety (frequency-factor controlling). Spectroscopic analysis indicated a direct interaction between the heme and the pyrenyl group, suggesting that the free-energy term is controlling the electron transfer. However, since a conformational change is observed in PYR-Cytc, the frequency factor may be another important factor determining the reduction rate in this case.

Table 1. The rate constant of electron transfer from various reductants to PGL-Cytc, PYR-Cytc and cytochrome *c*.

Reductants	Rate constant (10^{-3} / s)		
	Cytochrome *c*	PGL-Cytc	PYR-Cytc
$HSCH_2CH_2OH$	2.94	1.79	5.31
$HSCH_2CH_2CH_3$	4.18	-	1.16
$HSCH(CH_3)CH_2CH_3$	2.44	-	4.09
$HSCH_2COOH$	0.07	-	15.3
$HSCH_2CH_2NH_2$	1.84	-	3.51

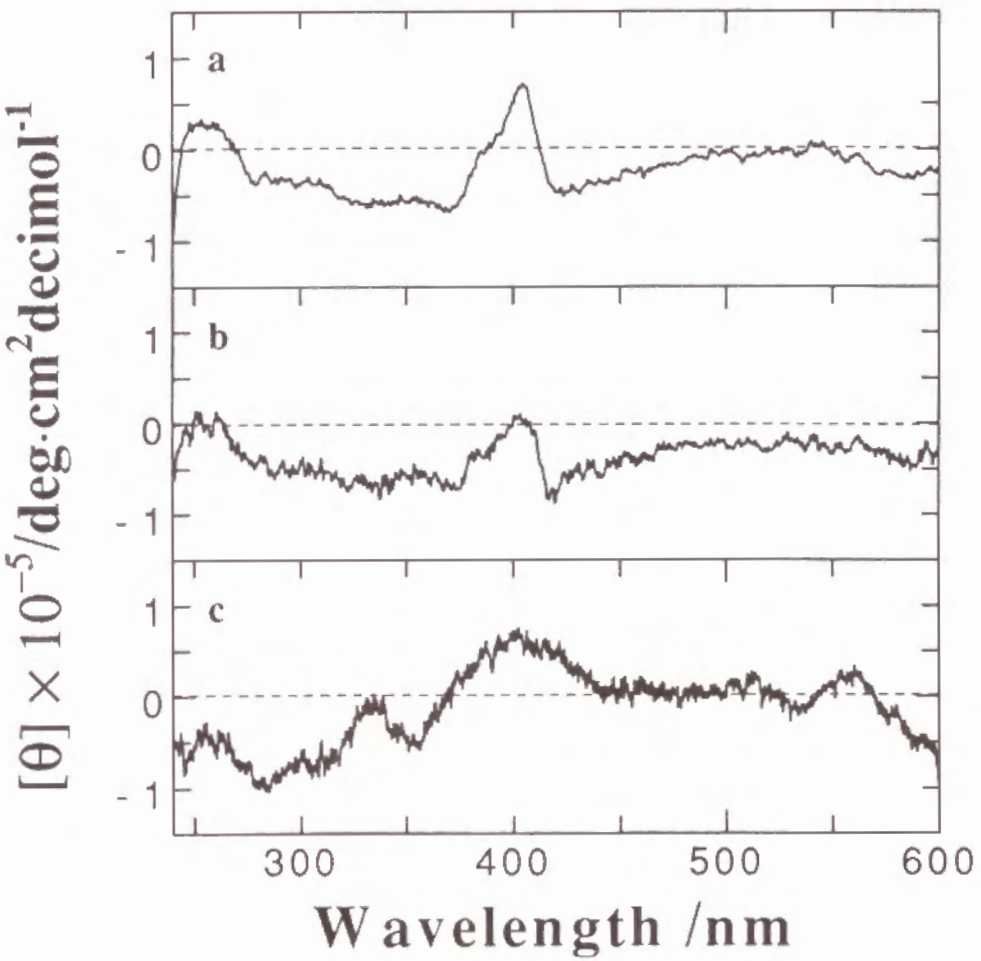

Figure 2. Circular dichroism spectra in the Soret band region.
a, native cytochrome *c*; **b**, PGL-Cytc; **c**, PYR-Cytc. Concentration of each cytochrome *c* was 1.10 μM.

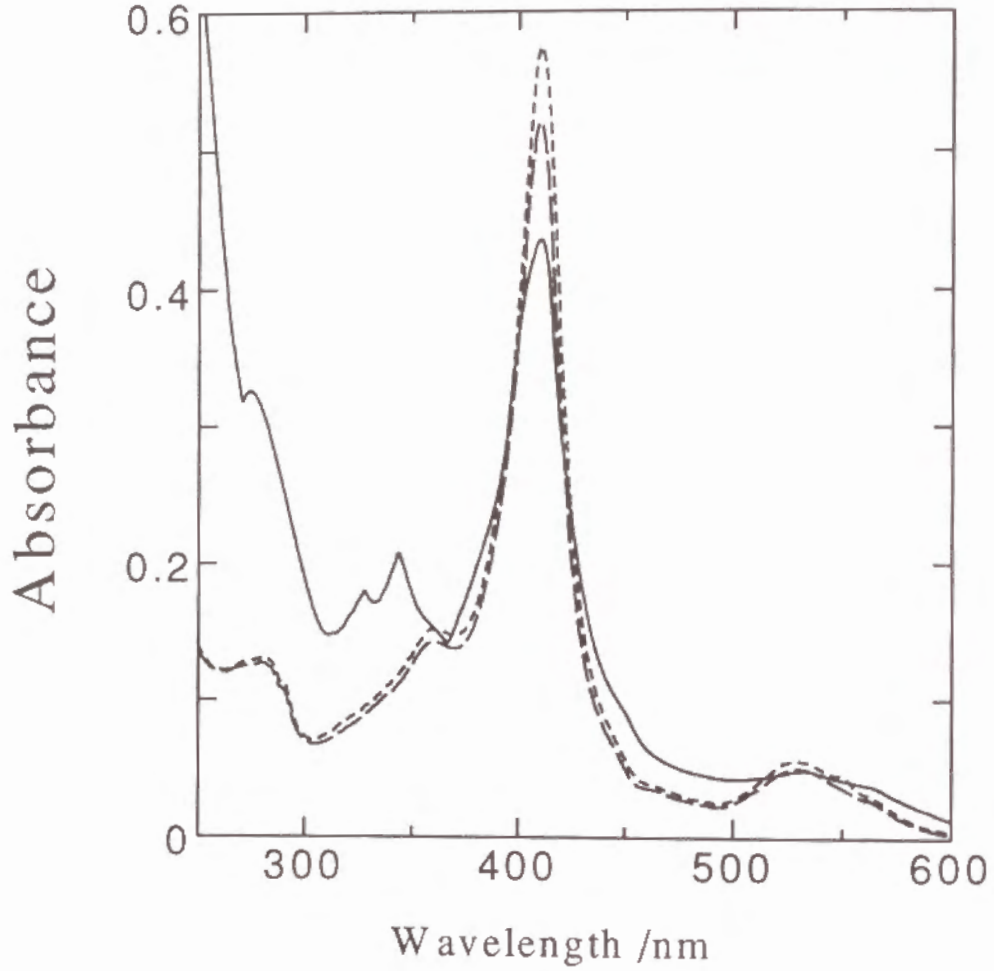

Figure 3. Absorption spectra of mutant cytochromes *c*.

(———), native cytochrome *c*; (- - - - -), PGL-Cytc; (———), PYR-Cytc.
Concentration of each cytochrome *c* was 1.10 μM.

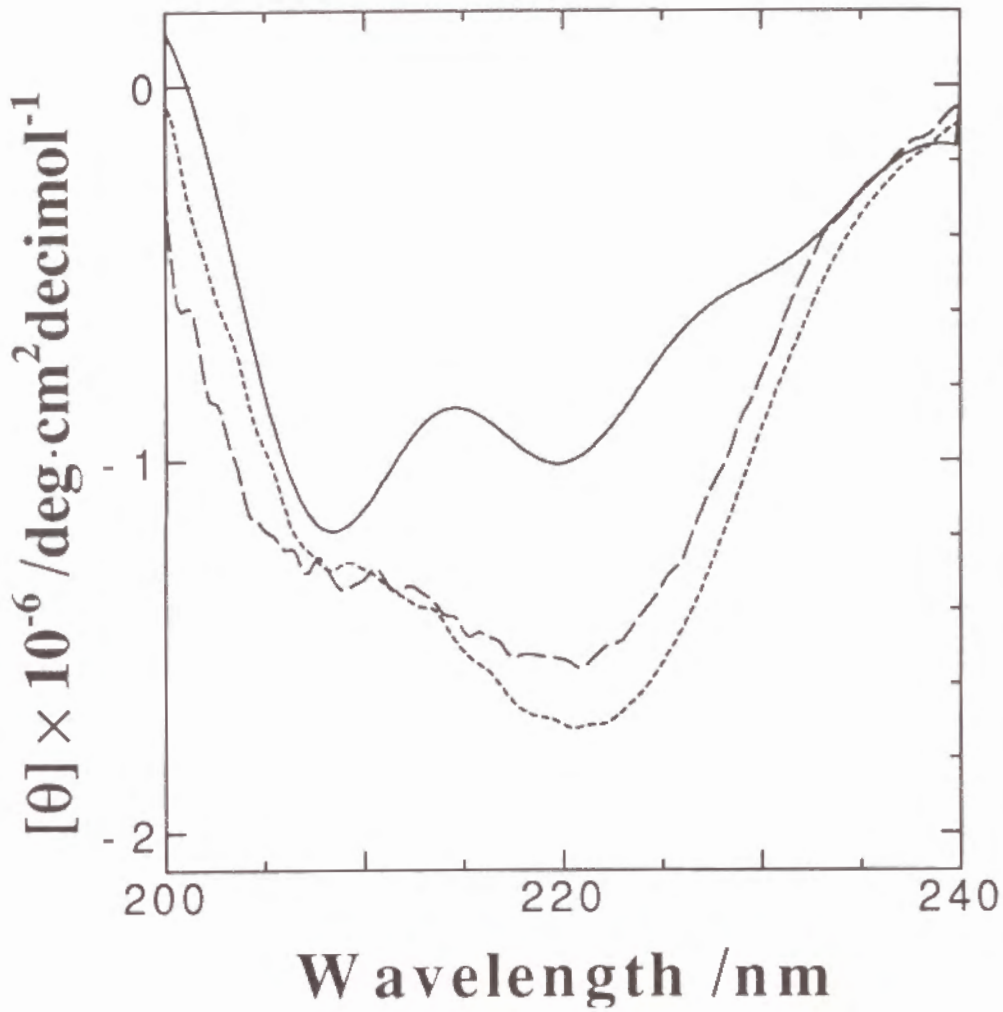

Figure 4. Circular dichroism spectra of mutant cytochromes *c* (200-240 nm region).

(———), PYR-Cytc; (- - - - -), native cytochrome *c*; (———), PGL-Cytc.
Concentration of each cytochrome *c* was 1.10 μM.

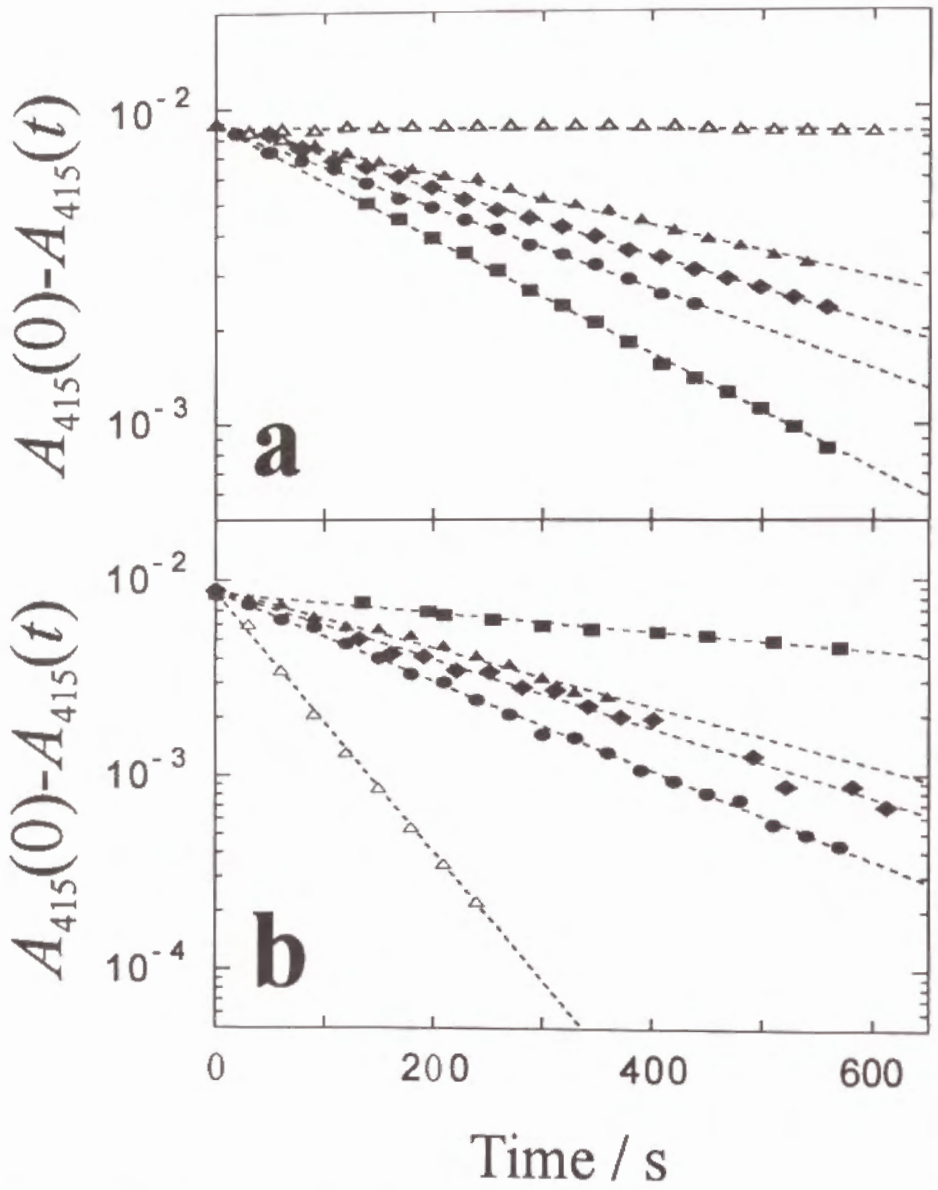

Figure 5. Reduction kinetics of native cytochrome *c* and PYR-Cytc with various reductants.

a, Reduction kinetics of native cytochrome *c*; **b**, reduction kinetics of PYR-Cytc. ●, 2-mercaptoethanol; ■, *n*-propylmercaptane; ◆, *sec*-butylmercaptane; ▲, 2-mercaptoethylamine; △, 2-mercaptoacetic acid.

The contribution of the frequency factor to the electron transfer process of native cytochrome *c* or PYR-Cytc was examined. Two kinds of reductants, *sec*-butylmercaptane and *n*-propylmercaptane, were used for reduction of PYR-Cytc. The reaction rates by these bulky reductants were smaller than that with 2-mercaptoethanol either in reduction of native cytochrome *c* or in reduction of PYR-Cytc (Table 1). Therefore, bulkier reductant molecules pass less easily through the heme crevice than does 2-mercaptoethanol, indicating that the heme of PYR-Cytc is not exposed to the surface of protein.

Next, another two kinds of reductants, 2-mercaptoethylamine and 2-mercaptoacetic acid were examined. These reductants have positive or negative charge, respectively, in a solution buffered at pH 6.9, while they are almost the same as 2-mercaptoethanol in molecular volume. In the case of native cytochrome *c*, the reduction rate with negatively charged 2-mercaptoacetic acid was very low. In contrast, positively charged 2-mercaptoethylamine reduced the cytochrome *c* at a rate comparable with 2-mercaptoethanol (Table 1). Native cytochrome *c* is a positively charged protein ($pI = 11$), which has lysine residues around the heme crevice [45], but negatively charged Asp or Glu residues were located around or inside the heme crevice (Figure 6). So, 2-mercaptoacetic acid has difficulty passing through the crevice probably because of repulsive electrostatic interactions.

In comparison, PYR-Cytc was reduced by either positively or negatively charged reductants. The passage found in PYR-Cytc was not affected by electrostatic interactions. This result indicates that substitution by the bulky pyrAla residue changed the polypeptide conformation and provided a novel passage of reductant in PYR-Cytc that was different from that in the native cytochrome *c*. This new passage might be either a new crevice through which

reductants can access the heme, or a new electron transport pathway through the polypeptide matrix of PYR-Cytc provided by incorporation of aromatic side chain of pyrAla located at the position 82 near the heme.

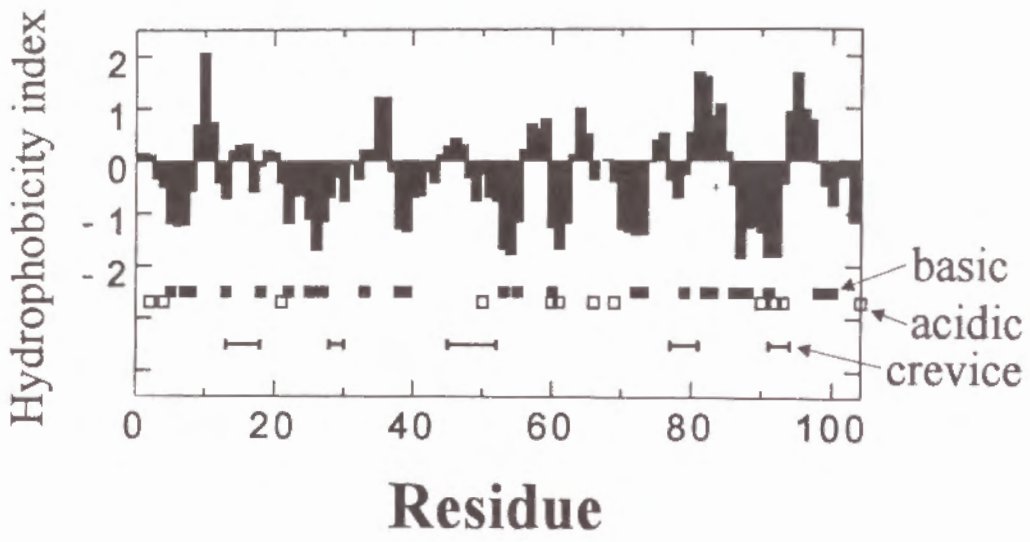

Figure 6. Hydrophobicity profile of native cytochrome *c*. The amino acid positions are indicated on the *x*-axis; the hydrophobic (+) or hydrophilic (−) indices are shown on the *y*-axis. Bar chart, the hydrophobicity index of amino acid residues. ■, location of basic amino acid residue; □, location of acidic amino acid residue; horizontal bar (⊢⊣), the heme crevice is made up from the amino acids located in this region. The heme crevice has acidic and hydrophilic amino acid residues.

Effect of Photoirradiation

A pyrenyl residue is known to be a catalytic photosensitizer [16]. The effect of photoirradiation on the reduction reaction of PYR-Cytc was examined. A

reaction cuvette was irradiated by a UV-light source (λ_{max} = 330 nm) during reduction of the ferric mutant cytochromes *c* by 2-mercaptoethanol. Before and after irradiation, concentration of ferrous heme was monitored for 10 min (Figure 7).

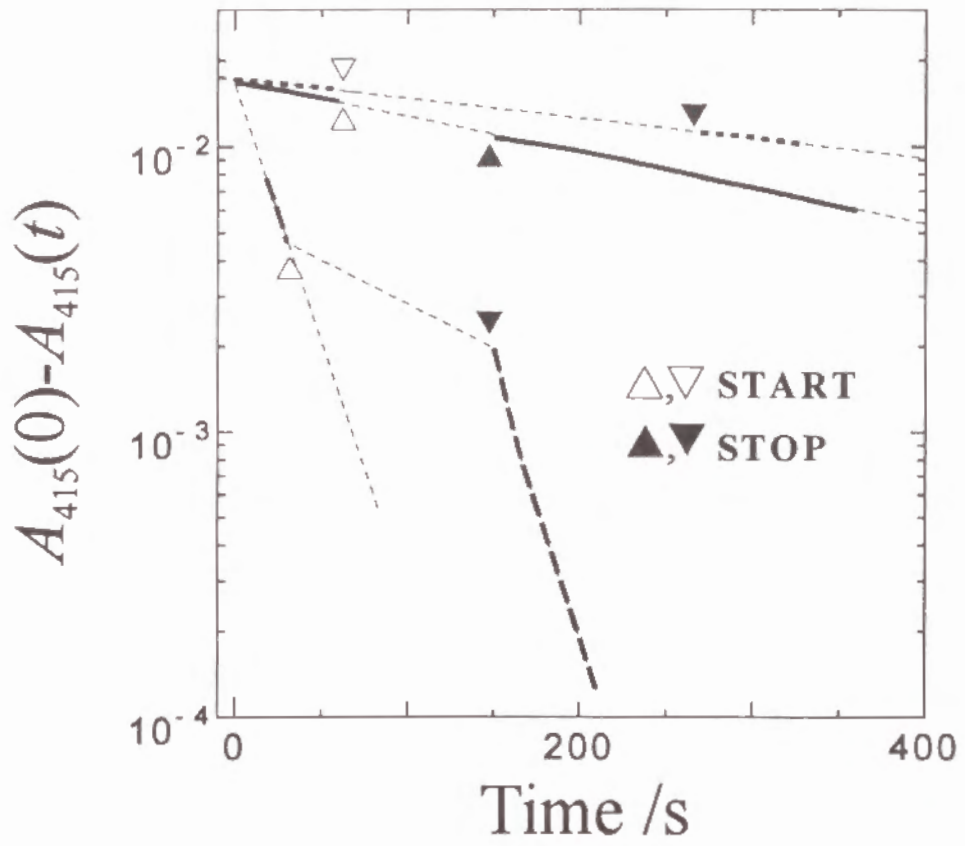

Figure 7. Reduction kinetics of native and mutant cytochromes *c* with or without light irradiation. (------), PGL-Cytc; (——), native cytochrome *c*; (— — —), PYR-Cytc. Light irradiation was started at the time shown by open triangles (△, ▽), and was stopped at the time indicated by filled triangles (▲, ▼). During light irradiation, the reduction reaction could proceed as represented by thin broken lines (– – –).

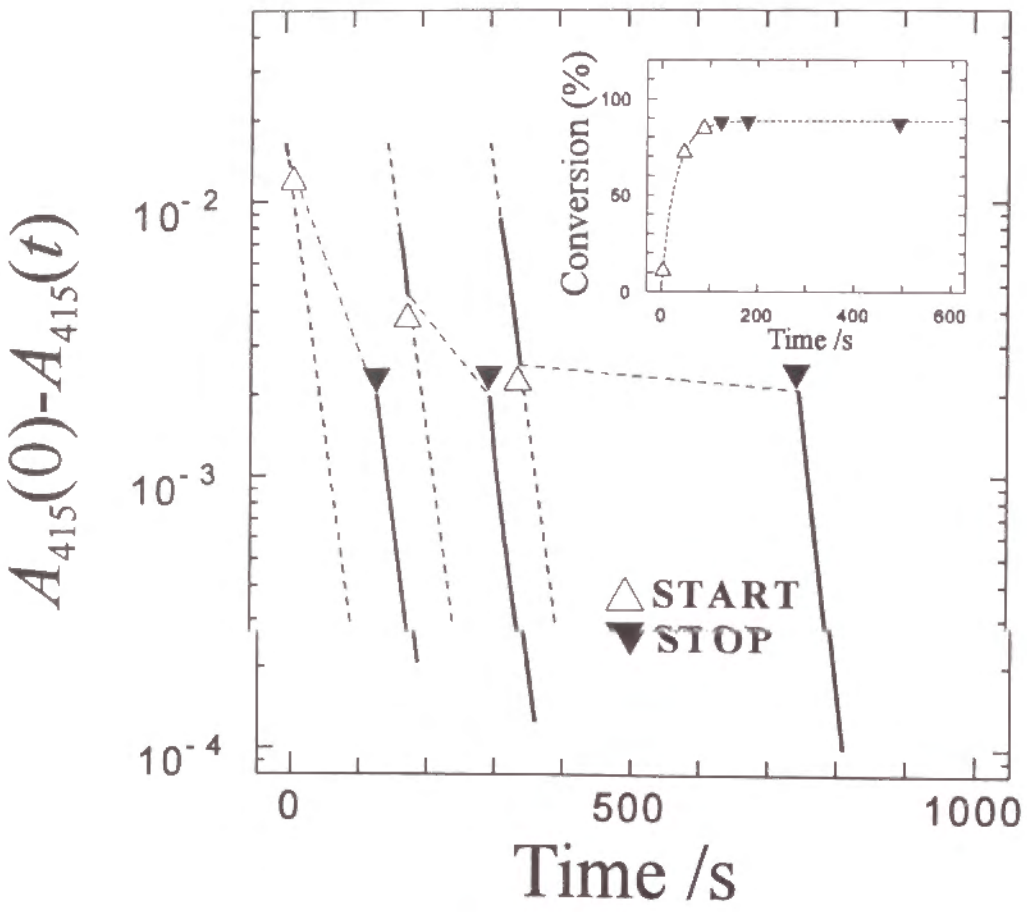

Figure 8. Dependency of the reduction reaction of PYR-Cytc on duration of light irradiation. (——), the absorbance change on keeping in the dark. The light irradiation was started at the time indicated by open triangles (△), and was stopped at the time indicated by filled triangles (▼). The thin broken lines (– – –) represent reduction reactions during light irradiation. The inset shows the calculated time-conversion (%) curve of reduction of PYR-Cytc by light irradiation.

Neither acceleration nor deceleration effects were observed for the native cytochrome *c* and PGL-Cytc. On the other hand, the reduction rate during the photoirradiation decreased with PYR-Cytc. The duration of photoirradiation was changed, and the reduction rate of PYR-Cytc was determined. After 100 s, 120 s and 350 s of photoirradiation, PYR-Cytc was reduced to almost the same degree of about 88 % conversion (Figure 8), indicating that the system reached equilibrium under photoirradiation. Since the irradiation effect was not observed in the native cytochrome *c* and PGL-Cytc, excitation of the heme moiety is not the main reason for the observed deceleration of the reduction reaction. Therefore, the heme should be oxidized through photosensitization by pyrenyl group in PYR-Cytc. The potential gap of about 3 V between the ground state and the excited state of the pyrenyl residue [16] is sufficient to reduce an ferric heme moiety that has redox potential of 0.25 V.

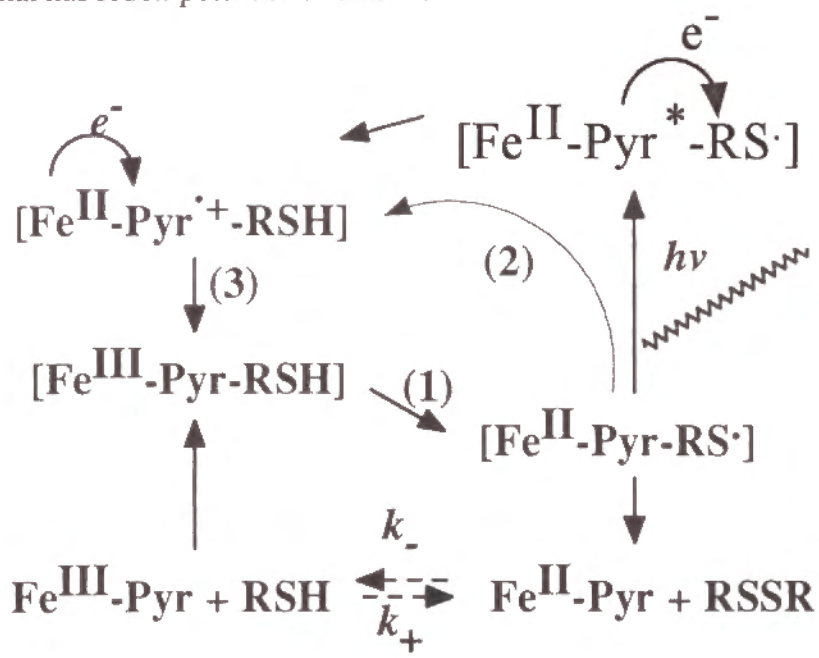

Scheme 2. Proposed reaction pathways of photoirradiated PYR-Cytc.

Discussion

A possible reaction pathway is summarized in Scheme 2. First, a reductant (R-SH) binds to PYR-Cytc (Pyr-Fe(III)) and an electron is transferred from the reductant to heme (Step 1). When the pyrenyl residue is excited by light irradiation, an excited electron on the pyrenyl residue (Pyr^{*}-Fe(II)) is transferred to the radical R-S· (Step 2). This step generates a radical cation of pyrenyl residue ($Pyr^{\bullet+}$-Fe(II)) and R-SH. Finally, a ferric heme is reformed through electron transfer from Fe(II) to the pyrenyl radical cation (Step 3). The route passing through the Steps 2 and 3 forms a reverse oxidation pathway of the heme during photoirradiation. However, this scheme remains to be tested by various spectroscopic methods.

References

1. E. Stellwagen, *Nature*, 1978, **275**, 73.
2. R. J. Kassner, *Proc. Natl. Acad. Sci. USA*, 1972, **69**, 2263.
3. R. J. Kassner, *J. Am. Chem. Soc.*, 1973, **95**, 2674.
4. C. C. Moser, J. M. Keske, K. Warncke, R. S. Farid and P. L. Dutton, *Nature*, 1992, **355**, 796.
5. D. S. Wuttke, M. J. Bjerrum, J. R. Winkler and H. B. Gray, *Science*, 1992, **256**, 1007.
6. D. S. Wuttke, M. J. Bjerrum, J. R. Winkler and H. B. Gray, *Biochim. Biophys. Acta.*, 1992, **1101**, 168.
7. S. L. Mayo, W. R. Ellis, Jr., R. J. Crutchley and H. B. Gray, *Science*, 1986, **233**, 948.

8. J. T. Hazzard, A. G. Mauk and G. Tollin, *Arch. Biophys. Biochem.*, 1992, **298**, 91.
9. J. M. Nocek, E. D. A. Stemp, M. G. Finnegan, T. I. Koshy, M. K. Johnson, E. Margoliash, A. G. Mauk, M. Smith and B. M. Hoffman, *J. Am. Chem. Soc.*, 1991, **113**, 6822.
10. T. L. Poulos and J. Kraut, *J. Biol. Chem.*, 1980, **255**, 10322.
11. A. Schejter, T. L. Luntz, T. I. Koshy and E. Margoliash, *Biochemistry*, 1992, **31**, 8336.
12. A. L. Raphael and H. B. Gray, *J. Am. Chem. Soc.*, 1991, **113**, 1038.
13. C. J. A. Wallace and I. Clark-Lewis, *J. Biol. Chem.*, 1992, **267**, 3852.
14. D. Hilvert, Y. Hatanaka and E. T. Kaiser, *J. Am. Chem. Soc.*, 1988, **110**, 682.
15. E. T. Kaiser, *Angew. Chem. Int. Ed. Engl.*, 1988, **27**, 913.
16. G. J. Kavarnos and N. J. Turro, *Chem. Rev.*, 1986, **86**, 401.
17. M. J. Hunter and M. L. Ludwig, *J. Am. Chem. Soc.*, 1962, **84**, 3491.
18. S. Egusa, M. Sisido and Y. Imanishi, *Macromolecules*, 1985, **18**, 882.
19. C. J. A. Wallace and D. E. Harris, *Biochem. J.*, 1984, **217**, 589.
20. G. Corradin and H. A. Harbury, *Proc. Natl. Acad. Sci. USA*, 1971, **68**, 3036.
21. P. J. Boon, G. I. Tesser and R. J. F. Nivard, *Proc. Natl. Acad. Sci. USA*, 1979, **76**, 61.
22. J. D. Peterson, *J. Biol. Chem.*, 1972, **247**, 4866.
23. R. E. Offord and C. Dibello, Eds., "Semisynthetic Peptides and Proteins," 1978, Academic Press, New York, p. 101.
24. C. J. A. Wallace and R. E. Offord, *Biochem. J.*, 1979, **179**, 169.
25. C. J. A. Wallace and K. Rose, *Biochem. J.*, 1983, **215**, 651.

26. P. J. Boon, A. J. M. Van Raay, G. I. Tesser and R. J. F. Nivard, *FEBS Letters*, 1979, **108**, 131.
27. G. Corradin and H. A. Harbury, *Biochem. Biophys. Res. Commun.*, 1974, **61**, 1400.
28. M. J. Hunter and M. L. Ludwig, *Methods in Enzymology*, 1972, **25**, 585.
29. J. Babul, E. B. McGowan and E. Stellwagen, *Arch. Biochem. Biophys.*, 1972, **148**, 141.
30. D. H. Lowry, N. J. Rosebrough, A. L. Farr and R. J. Randall, *J. Biol. Chem.*, 1951, **193**, 265.
31. R. Fields, *Biochem. J.*, 1971, **124**, 581.
32. A. R. Rees and R. E. Offord, *Biochem. J.*, 1976, **159**, 467.
33. A. R. Rees and R. E. Offord, *Biochem. J.*, 1976, **159**, 487.
34. D. E. Harris and R. E. Offord, *Biochem. J.*, 1977, **161**, 21.
35. C. J. A. Wallace, G. Corradin, F. Marchiori and G. Borin, *Biopolymers*, 1986, **25**, 2121.
36. G. Borin, F. Marchiori, A. Calderan, G. Corradin and C. J. A. Wallace, *Biopolymers*, 1986, **25**, 2271.
37. A. E. I. Proudfoot, C. J. A. Wallace, D. E. Harris and R. E. Offord, *Biochem. J.*, 1986, **239**, 333.
38. A. E. I. Proudfoot and C. J. A. Wallace, *Biochem. J.*, 1987, **248**, 965.
39. L. Gozzini, H. Taniuchi and C. DiBello, *Int. J. Pept. Protein Res.*, 1991, **37**, 293.
40. D. F. Dyckes, T. Creighton and R. C. Sheppard, *Nature*, 1974, **247**, 202.
41. L. E. Barstow, R. S. Young, E. Yakali, J. J. Sharp, J. C. O'Brien, P. W. Berman and H. A. Harbury, *Proc. Natl. Acad. Sci. USA*, 1977, **74**, 4248.
42. E. Stellwagen, *Biochemistry*, 1968, **7**, 2893.

43. E. Schechter and P. Saludian, *Biopolymers*, 1967, **5**, 788.
44. M. M. Frauenhoff and R. A. Scott, *Proteins: Struc. Func. Genet.*, 1992, **14**, 202.
45. R. E. Dickerson, R. Timkovich and R. J. Almassy, *J. Mol. Biol.*, 1976, **100**, 473.

Chapter 3

Destabilization of the Heme Region in Mutant Cytochrome *c* by Replacement of Phe^{82} with 3-(1-Pyrenyl)-L-alanine

Introduction

Cytochrome *c* is a peripheral protein, which has a heme group linked covalently to the polypeptide backbone. Cytochrome *c* has been engineered for structural analysis [1,2], enhancing thermostability [3] and so forth. The tertiary structure of cytochrome *c* is so flexible that a reversible unfolding was observed in a phospholipid bilayer membrane [4,5]. It is well known that cytochrome *c* takes a sub-state conformation, which is different either from native or from fully denatured conformation in the presence of denaturant or in a high pH medium. This state is called "molten globule" state, in which cytochrome *c* retains nearly the same secondary structure as those of native protein, while the tertiary structure is distorted. In chapter 2, PYR-Cytc was shown to preserve a high content of α-helix, but the structure was distorted (Scheme 1) [6]. As a result of the conformational deformation, the mutant cytochrome *c* possesses a new pathway for electron transfer, "the second crevice," through which small reductants interact with the heme directly or indirectly through the pyrenyl residue. In order to evaluate the degree of structural distortion induced by the incorporation of pyrAla into cytochrome *c*, the stability of tertiary structure of the mutant cytochromes *c* was studied in detail.

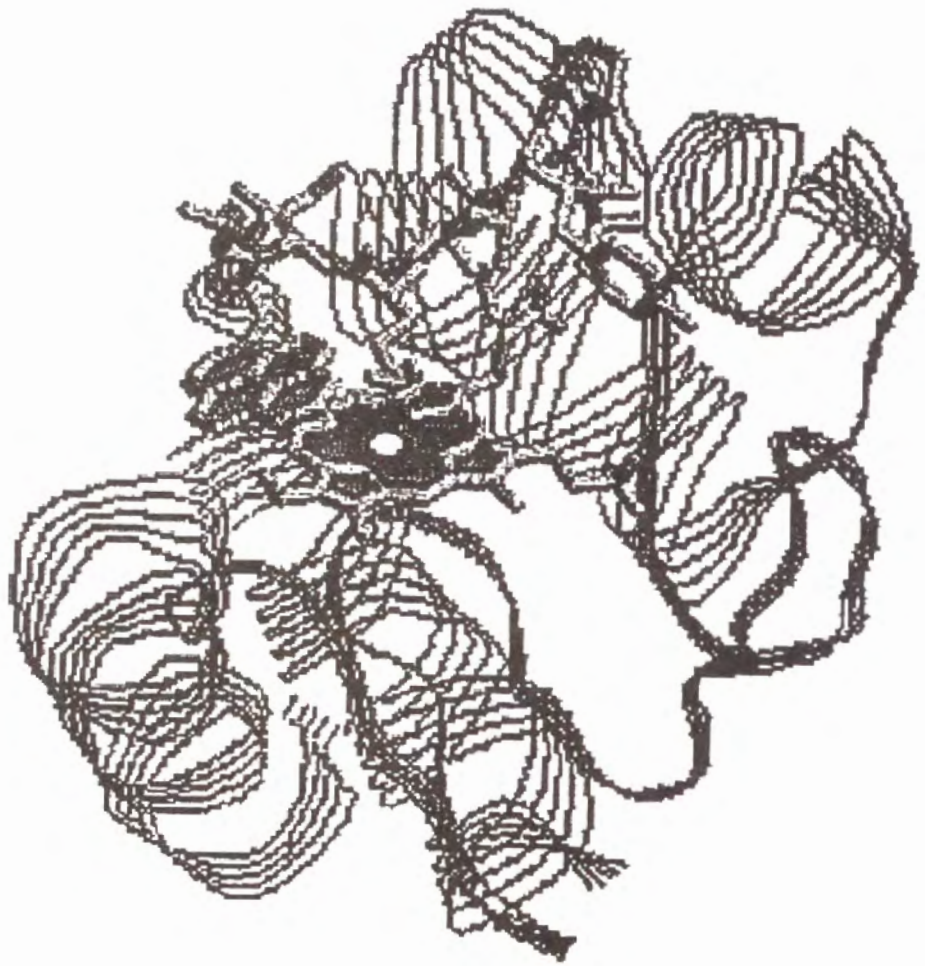

Scheme 1. Ribbon drawing of PYR-Cytc. The side chain and backbone at the range of 79-85, and the heme structures are drawn and superimposed by using RasWin Molecular Graphics Windows Version 2.3 with RasMOL Version 2.2 by Roger Sayle, 1993 [R. Sayle and A. Bissell., 'RasMOL: A program for fast rendering of molecular structures with shadows.' In *Proceedings of the 10th Eurographics UK '92 Conference*, University of Edinburgh, Scotland, April 1992].

Experimental

Materials

The mutant cytochromes *c* were prepared by a semisynthetic method as described in chapter 2 [6]. The native cytochrome *c* and the mutant cytochromes *c* were oxidized by oxygen bubbling in deionized water for 2 h at room temperature, and were subsequently lyophilized. All experiments were performed with ferricytochrome *c*. A stock solution of cytochrome *c* (4 mg / ml) in 10 mM potassium phosphate buffer (pH 7.2) was prepared and diluted before use. The concentrations of the mutant cytochromes *c* as well as the native cytochrome *c* in the oxidized state in 10 mM potassium phosphate buffer at 25 °C was determined spectrophotometrically using the molar extinction coefficient of $\varepsilon_{409} = 9.20 \times 10^4$ /M cm [7].

Other chemicals of the highest grade of purity available (Wako Pure Chem. Ind., Ltd., Japan) were used without further purification.

Spectroscopy

Absorption and fluorescence spectra were recorded on a Jasco Ubest-50 UV / Vis spectrophotometer and a Hitachi MPF-4 fluorescence spectrophotometer, respectively, using a cell of 1-cm path length. Circular dichroism spectra were measured by a Jasco J-600 CD spectrophotometer using a cell of 0.1-cm path length. Fluorescence from the pyrAla residue was measured with excitation at 345 nm. For the fluorescence-quenching experiments, a stock solution of acrylamide (1.0 M) was prepared and a small portion of the solution was added to the 1 ml of sample solution in 10 mM potassium phosphate buffer (pH 7.2).

Thermal Denaturation

Thermal denaturation experiments were carried out on the CD or UV spectrometer equipped with a water jacket to control the temperature of the sample solution. The temperature was raised with a rate of 1 degree / min from 10 °C to 80 °C. The signal strength at 222 nm in CD spectra and at 692 nm in UV spectra was monitored in 10 mM potassium phosphate buffer (pH 7.2) of 1.1×10^{-6} M cytochromes *c*. Melting curves were analyzed by using a linear least-squares program. The thermal unfolding equilibrium constant at temperature T, $K(T)$, in the cooperative transition region was calculated according to equation (1),

$$K(T) = \frac{A_N - A_{692}(T)}{A_{692}(T) - A_D} \quad (1)$$

where $A_{692}(T)$ represents the absorbance of 692 nm at temperature T, A_N and A_D the absorbance in the native state and the denatured state, respectively. The van't Hoff parameters ΔH_0 and ΔS_0 were obtained from the slope ($-\Delta H_0 / R$) and intercept ($\Delta S_0 / R$), respectively, of the plot of ln $K(T)$ against $1 / T$. T_m, the midpoint of the denaturation, was calculated from $T_m = \Delta H_0 / \Delta S_0$ where ΔG_0 = 0 kcal / mol. The difference of free-energy change in the thermal unfolding of the wild-type protein and the mutant protein, $\Delta\Delta G_0$, was calculated by equation (2),

$$\Delta\Delta G_0 = \frac{\Delta H_0^w \Delta T}{T_m^w} \quad (2)$$

where the superscript w represents the quantity for the native cytochrome *c*, and ΔT represents the difference of T_m between the two types of proteins [8].

Denaturation with Guanidium Hydrochloride (GdnHCl)

Unfolding of cytochrome *c* by the addition of GdnHCl was monitored by the change of the Cotton effect at 222 nm in CD spectra [9]. Measurements were done at 25 °C within approximately 10 min after mixing the protein with GdnHCl. The signal at 222 nm was measured at least for 2 min, and averaged by using a personal computer.

The denaturation curves obtained were analyzed by the standard procedure [10] according to Schellman's two-state model for the equilibrium N $\leftrightarrow$ U, in which N and U denote the native state and the denatured state, respectively [10].

The equilibrium constant, K_u, was calculated from the fractions of unfolded and folded proteins. K_u as a function of [GdnHCl] was analyzed by the equation, $\Delta G_u = \Delta G_u^0 - m$ [GdnHCl], to obtain the parameter ΔG_u^0 (free energy of unfolding in the absence of denaturant), m (cooperativity parameter of unfolding), and C_m ([GdnHCl] necessary to denature 50 % of protein) [11], which are summarized in Table 1.

Denaturation by pH Increase [12]

The pH of a solution of cytochrome *c* (3 ml) was adjusted by adding a 0.1 N NaOH solution in an optical cuvette at 25 °C under stirring. After each addition of NaOH solution, the absorbance at 692 nm was monitored until it reached a stable value.

The change in absorbance at 692 nm of the native cytochrome *c* and the mutant cytochrome *c* as a function of pH was analyzed by using the equation (3) [13],

$$\mathrm{p}K_{\mathrm{a}} = \log\left[\frac{A_{692}^{\mathrm{N}} - A_{692}}{A_{692} - A_{692}^{\mathrm{D}}}\right] + m\,\mathrm{pH} \qquad (3)$$

where $A_{692}{}^{\mathrm{N}}$ and $A_{692}{}^{\mathrm{D}}$ represent the absorbance of the native and the denatured (alkaline form) protein at 692 nm, respectively, and m is the number of deprotonation of the protein responsible for the absorbance change at 692 nm. The apparent pK_{a} of each protein for the equilibrium between the two states was determined from linear least-squares fitting of a $\log[(A_{692}{}^{\mathrm{N}}-A_{692}) / (A_{692}-A_{692}{}^{\mathrm{D}})]$ *vs.* pH. A free-energy difference between the native and the mutant cytochrome *c* in the alkaline form, $\Delta\Delta G_{\mathrm{alk}}$, was calculated by the equation $\Delta\Delta G_{\mathrm{alk}} = -2.3RT\,\Delta\mathrm{p}K$.

Results

Fluorescence Quenching of Pyrenyl Residue with Acrylamide

It has been shown that the α-helix content of PYR-Cytc was decreased

and the heme region was distorted as evidenced by the broadened Soret band [6]. Therefore, it was expected that the incorporation of the bulky pyrenyl group might result in loosening of the highly ordered structure due to steric effects and hydrophobic interactions between the pyrenyl group and the hydrophobic heme pocket. However, CD spectrum of far-UV region showed that the mutant protein retains a certain kind of ordered structure including a high content of α-helices [6].

The environment of the pyrenyl residue in PYR-Cytc was studied by fluorescence quenching using acrylamide. In the case of native cytochrome *c*, the phenyl group of phenylalanine residue at the position 82 reversibly changes the location depending on the redox state of cytochrome *c*. The phenyl group is packed in the hydrophobic heme pocket in ferrocytochrome *c*, while it is transferred to the protein surface accessible to aqueous medium upon one-electron oxidation to ferricytochrome *c* [14-17]. The fluorescence intensity of the pyrenyl group in the oxidized form of mutant cytochrome *c* was quenched by the addition of water-soluble quencher, acrylamide (Figure 1). On the other hand, no quenching was observed in the reduced form of the mutant cytochrome *c*. This result means that the conformational change in the heme region of the mutant cytochrome *c* occurs depending on the redox state of the heme, and takes place similarly to the native cytochrome *c*. It is interesting that the bulky pyrenyl group is fully buried in the hydrophobic pocket of the mutant protein in the reduced state.

Denaturation Investigated by CD

The stability of the tertiary structure of the mutant cytochrome *c* was analyzed on the basis of the change of CD spectra induced by raising

temperature or adding GdnHCl. Figure 2 shows the thermal stability and chemical unfolding of cytochrome *c*. Both experiments were monitored by the change of θ_{222}, which reflects the extent of denaturation of the helical region of cytochrome *c*. The native cytochrome *c* and PYR-Cytc similarly changed the intensity upon raising the temperature (Figure 2a). However, a minor conformational change was found at about 55 °C only in the case of PYR-Cytc, suggesting a structural perturbation of the heme environment [18]. It has been reported that the excess specific heat *versus* temperature curve for ferricytochrome *c* in an aqueous buffer solution (pH 7.4) showed a major endothermic transition at 81 °C, which is preceded by a minor endotherm centered at around 64 °C. While the transition at 81 °C is ascribed to a major conformational change of the polypeptide backbone, the minor transition is considered to be due to loosening of protein structure in the vicinity of heme crevice [18]. Thus, the structural perturbation in the heme region of PYR-Cytc might become significant compared with the native cytochrome *c*.

On the other hand, in the chemical unfolding by GdnHCl, the native cytochrome *c* and PYR-Cytc behaved in exactly the same way (Figure 2b). The curves were fitted by nonlinear least-squares analysis to determine thermodynamic parameters (Table 1). The minor transition at around 55 °C in the thermal denaturation of the mutant cytochrome *c* was not observed in Figure 2b. It is considered that GdnHCl of low concentrations, interacted only with the surface of the globular protein, and unfolding proceeded gradually from the surface to the bulk of protein molecule with increasing concentration of GdnHCl. Therefore, the preliminary unfolding of the heme environment could not have been detected by this procedure.

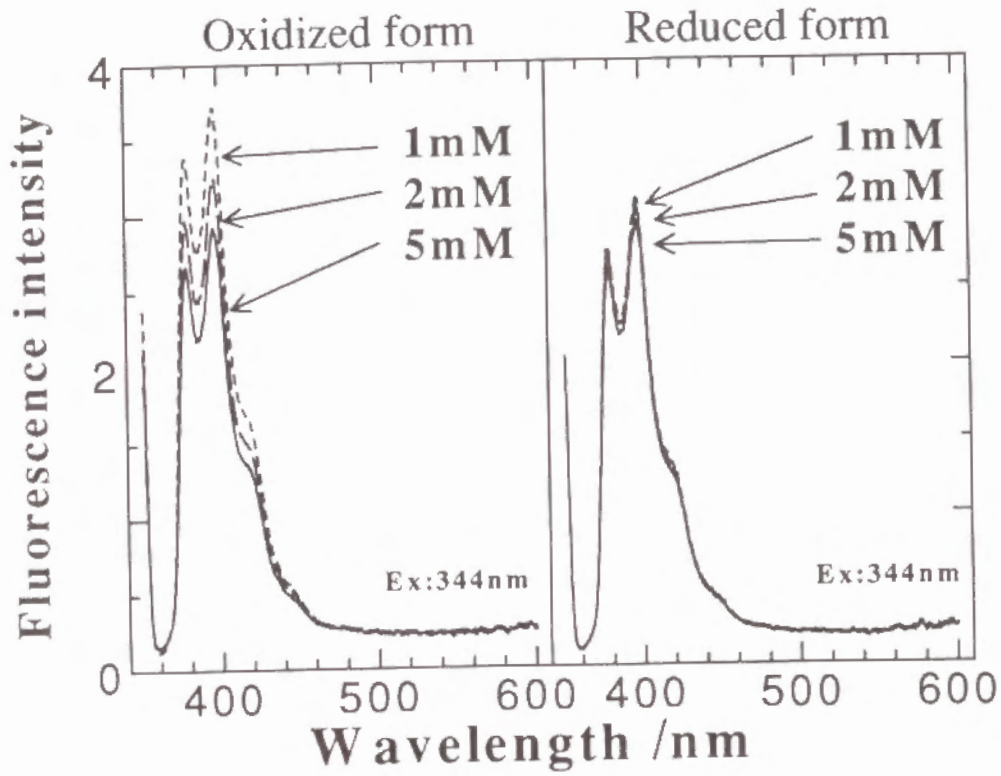

Figure 1. Fluorescence quenching of oxidized and reduced form of PYR-Cytc. Left: fluorescence spectra of ferricytochrome *c* in the presence of 1 mM, 2 mM, and 5 mM of acrylamide. Right: fluorescence spectra of ferrocytochrome *c* in the presence of acrylamide. PYR-Cytc was completely reduced by adding 1 % (v / v) of 2-mercaptoethanol followed by standing for 24 h at room temperature in the dark and subsequent gel permeation chromatography on a Sephadex G-25 (fine grade) column with potassium phosphate buffer solution (pH 7.2) as eluent. Excitation wavelength was 344 nm.

Denaturation Monitored by Absorbance at 692 nm

One of the most informative absorption bands on the heme environment is a weak charge-transfer band at 692 nm, which arises from the interaction of

the heme ferric iron and the sixth coordination ligand, the thioether of methionine 80 [20]. Though the extinction coefficient is relatively small, it is sensitive to pH- or temperature-induced perturbation of the heme environment. The mutant cytochromes *c* also show a weak absorption at 692 nm, which disappears completely at pH 11.0 (Figure 3). Therefore, this absorption is ascribed to the Fe-S bonding, and reflects the stability of the heme environment.

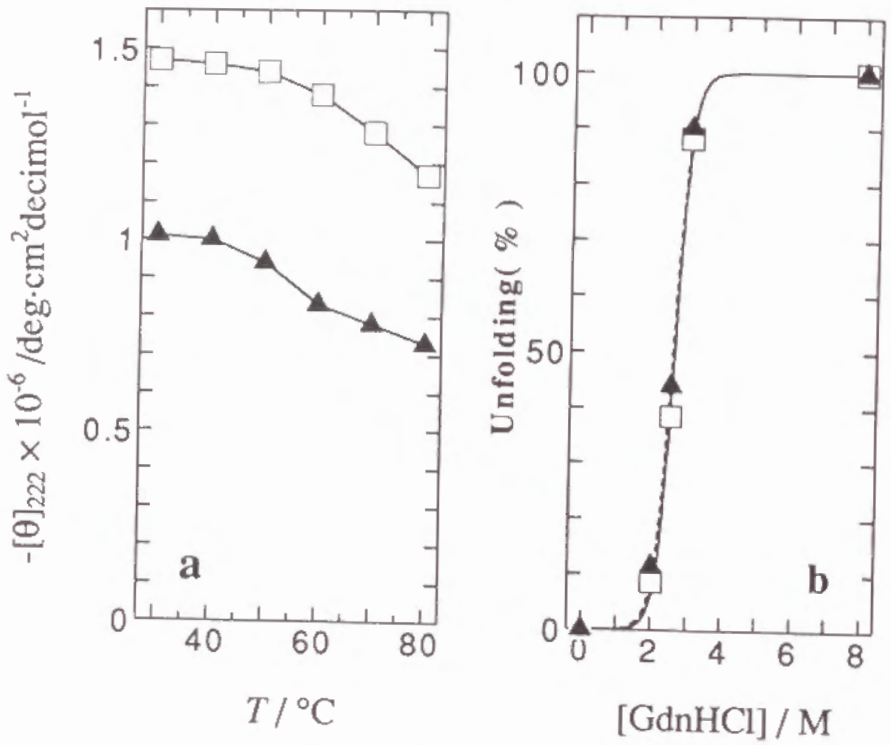

Figure 2. Secondary structure stability of the native cytochrome *c* and PYR-Cytc. (a) Thermostability of the cytochromes *c* was monitored by CD at the wavelength 222 nm. □, the native cytochrome *c*, ▲, PYR-Cytc. (b) Chemical unfolding of cytochromes *c* by the addition of GdnHCl as denaturant. (□, ——), the native cytochrome *c*, (▲, ------), PYR-Cytc. Fitting curves were calculated by nonlinear least-squares program.

Table 1. Thermodynamic parameters[a] for the conformational change of the protein backbone.

	Native	Mutant	Reported[b]
ΔG^0 (kcal / mol)[a]	6.47	6.21	6.2
m (kcal / mol^2)[a]	4.37	4.27	2.25

[a] Calculated from θ_{222} *vs.* [GdnHCl] plot.

[b] In 20 mM phosphate buffer solution (pH 7.0) at 25 °C [19].

The changes of absorbance at 692 nm of the native cytochrome *c*, PYR-Cytc and the fully N^{ε}-amidinated cytochrome *c* with increasing pH are shown in Figure 4. pK_a values were obtained by curve fitting of the data, and are shown in Table 2 with *m*, the numbers of deprotonation of the protein for pH-induced denaturation. The pK_a of the fully N^{ε}-amidinated cytochrome *c* increased by 3.8 pH unit compared with that of the native cytochrome *c*. This shift is qualitatively explained by the higher pK_a value of the amidinated group than the primary amino group of lysine. The pK_a of PYR-Cytc was calculated to be 8.8, which is slightly higher than 8.3 of the native cytochrome *c*. The increase of 0.5 pH unit corresponds to 0.65 kcal / mol stabilization of the heme iron-methionine bond, and is smaller than that reported for F82I and F82L mutants of yeast iso-1-cytochrome *c*, which showed a 1.3 pH unit increase [21].

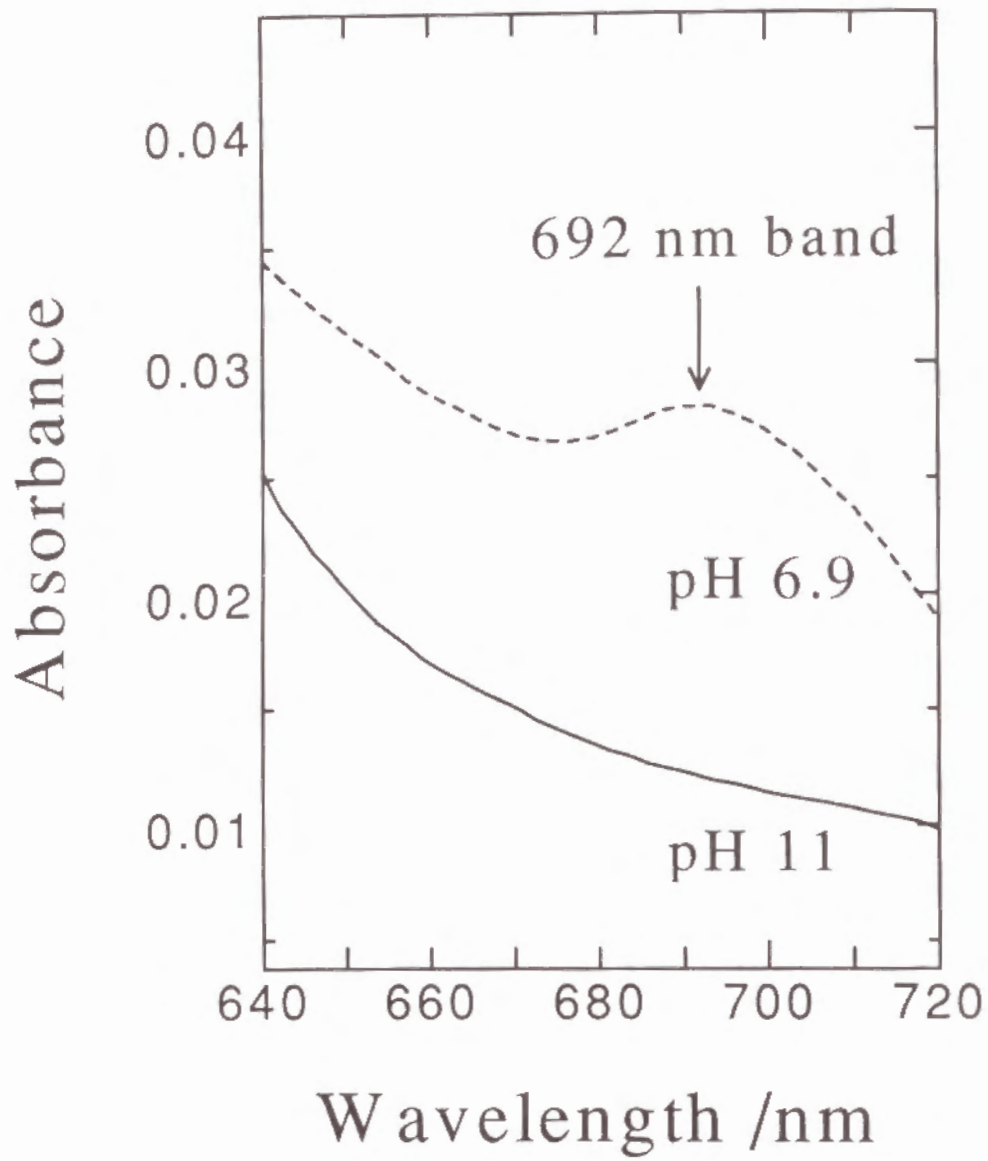

Figure 3. UV spectra in the far infrared region of PYR-Cytc. (– – –), PYR-Cytc of 40 μM in 10 mM potassium phosphate buffer solution at pH 6.9. (———), PYR-Cytc under the same conditions except pH = 11.0. The concentration of PYR-Cytc was 3.0×10^{-5} M.

The disappearance of the 692-nm band at high pH is generally interpreted as a result of the replacement of the normal methionine ligand with a deprotonated form of lysine residue due to conformational change in the heme crevice [22]. This explanation is also applicable to PYR-Cytc, because *m* values determined from the titration curves are approximately unity, suggesting that the structure change is accompanied by a one proton transfer. The increase of pK_a induced by replacement of Phe^{82} with pyrAla was not so large as that of F82I or F82L mutants. One possible explanation for the pK_a shift is that the access of the deprotonated amino group of lysine to the coordination site of the methionine with the heme group is hindered by the bulky pyrenyl group in the heme pocket.

Table 2. Thermodynamic parameters[a] for conformational change of the heme environment.

Transition parameters[a]	Cytochrome *c*			
	Native	Mutant	Amd-Cytc[b]	Reported[c]
pK_a	8.3	8.8	12	9.1[d]
m	0.91	0.95	1.3	-
$\Delta\Delta G_{alk}$ (kcal / mol)	0.0	-0.65	-5.1	-

[a] Determined by absorption change at 692 nm upon varying pH.

[b] Fully N^{ε}-amidinated cytochrome *c*.

[c] In 10 mM sodium cacodylate, 10 mM sodium chloride (pH 7.0) [23].

[d] In 0.1 M NaCl, 0.1 mM protein, at 25 °C [21].

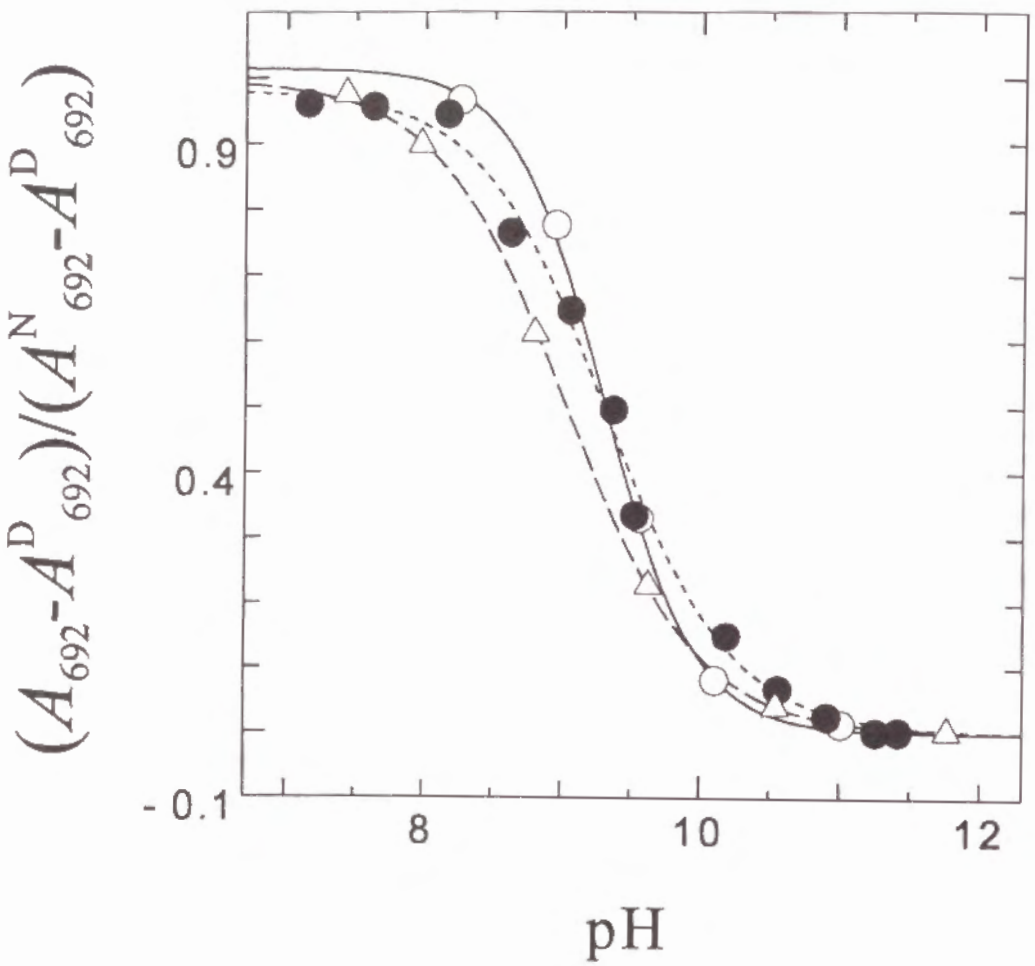

Figure 4. Alkaline transition of the native cytochrome *c* (●), PYR-Cytc (△) and fully N^{ε}-amidinated cytochrome *c* (○). The protein concentration was 40 μM. The titration was monitored by absorbance change at 692 nm at 25 °C.

Thermal Denaturation of the Heme Region

Thermal denaturation of the native and the mutant cytochromes *c* was monitored by the change of absorbance at 692 nm. The Arrhenius plots of the thermal denaturation are shown in Figure 5, and the thermodynamic parameters calculated from the plots are summarized in Table 3. The free-energy change for the conformational change of the heme environment, $\Delta G°$ reveals that PYR-Cytc and PGL-Cytc are less stable than the native cytochrome *c* by 0.7 and 1.5 kcal / mol, respectively. It should be noted that the instability of the heme region of PYR-Cytc is due to the large entropy change, $\Delta S°$. The enthalpy term of PYR-Cytc contributes to the conformational stability to a larger extent than that of the native cytochrome *c*. The large entropy change of the mutant cytochrome *c* might be explained by the lowered flexibility of the heme region, which is consistent with the crowdedness of hydrophobic heme pocket as described before. The melting temperature of 54 °C coincides well with the minor thermal transition at about 55 °C observed in the experiment of thermal denaturation (Figure 2a). Table 3 also shows thermodynamic parameters of PGL-Cytc. In the PGL-Cytc, one β-methylene of Phe^{82} was lost, resulting in a decrease of the melting point (T_m = 55 °C) as low as that of PYR-Cytc. In this case, a large difference of the enthalpy change ($\Delta\Delta H_0$ = −5 kcal / mol) was observed, while the entropy change was comparable to that of native cytochrome *c*. These results suggest that the aromatic group of Phe^{82} of the native cytochrome *c* contributes to the stability of the heme region probably due to a hydrophobic effect. Introduction of a large aromatic group should not impair the hydrophobic effect on the tertiary structure, but may destabilize the structure by putting high constraint on the structure.

Table 3. Thermodynamic parameters[a] for conformational change of the heme environment.

Transition parameters[a]	Cytochrome *c*			
	Native	PYR-Cytc	PGL-Cytc	Reported[b]
ΔS_0 (cal / mol K)	88	104	76	62
ΔH_0 (kcal / mol)	30	34	25	21.1
ΔG_0 (kcal / mol)	3.7	3.0	2.2	2.45
T_m (°C)	68	54	55	65

[a] Determined by absorption change at 692 nm upon varying temperature.

[b] In 10 mM sodium cacodylate, 10 mM sodium chloride (pH 7.0) [23].

Discussion

The conformational stability of protein is usually low (5-20 kcal / mol) and varies by the influence of the opposing factors of the hydrophobic effect and the entropy effect on the folded state [24]. Hydrophobic amino acid residues generally contribute to the stability of the hydrophobic region as shown by the conserved Trp residue of cytochrome *c* acting as a conformation-stabilizing unit [12]. The replacement of Phe^{82} with pyrAla^{82} of cytochrome *c* strengthened the hydrophobic effect as shown in the increase of ΔH for thermal denaturation, but destabilized the overall conformation due to the large ΔS for denaturation.

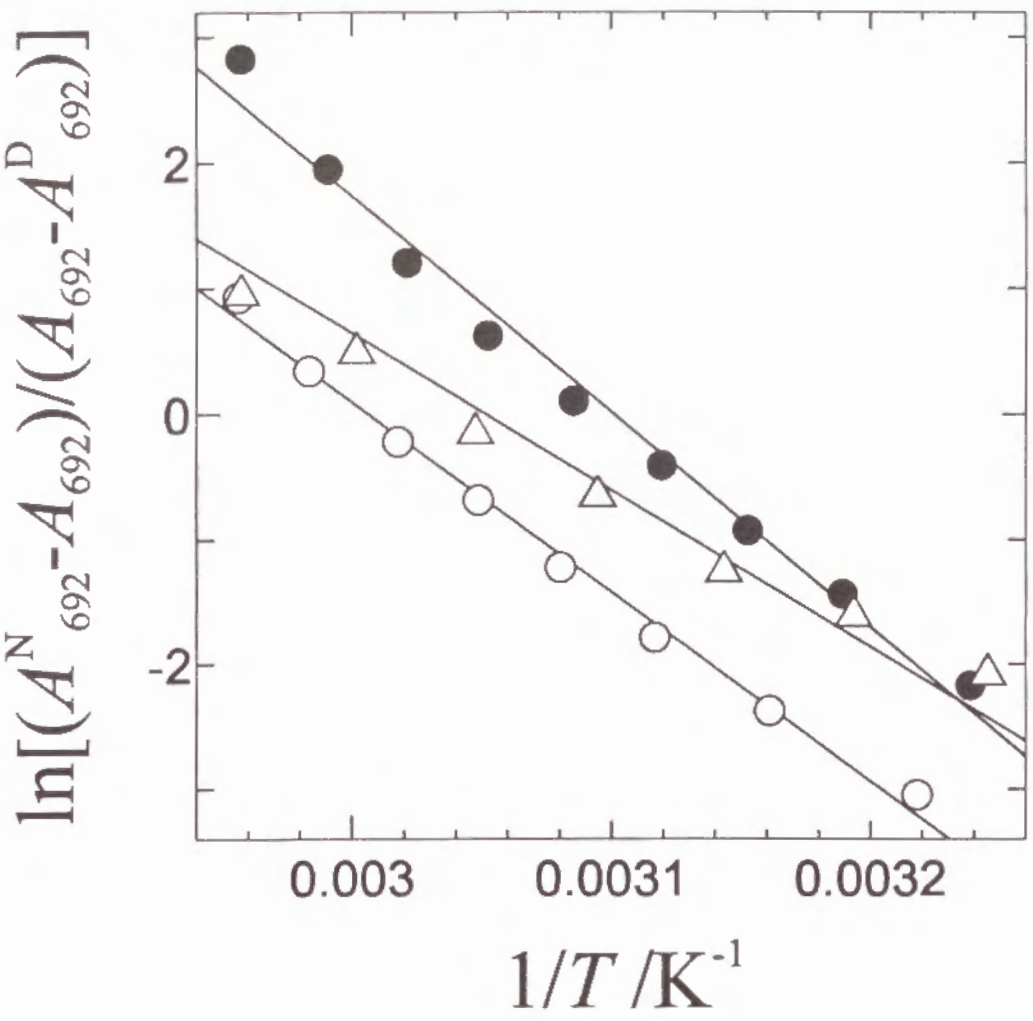

Figure 5. Thermostability of the native cytochrome *c* (○), PYR-Cytc (●) and PGL-Cytc (△). Sample solutions were prepared in 10 mM potassium phosphate buffer solution (pH 7.2). The denatured / native ratio, *K*, is plotted against the reciprocal of absolute temperature. The intercept at ln *K* = 0.0 gives the T_m.

Replacement of an amino acid residue of a protein may significantly affect its stability, but substitution of a conserved amino acid residue of cytochrome *c* does not always result in destabilization of the protein. It has been reported that the midpoints of GdnHCl denaturation for the mutant proteins (K32L, K32Q) are a little smaller than the wild type [24]. It has also been reported that hydrophobic interactions are the main factor for increasing stability of the Ile^{52} mutant of yeast iso-1-cytochrome *c* [25]. In the present study, a pyrAla residue was replaced for the conserved Phe^{82} residue. The overall backbone structure was not drastically altered, but the conformational change took place in the hydrophobic heme pocket. These results suggest that the mutant cytochrome *c* takes a kind of 'molten globule' structure. It is interesting, however, that a bulky pyrAla residue is accommodated in the hydrophobic heme pocket in the reduced state of the mutant cytochrome *c*, but that in the oxidated state, a significant deformation at the heme region is accompanied by exposure of the pyrAla residue to the medium. The structural change might yield another heme crevice, which acts as an alternative pathway for electron transfer as described in chapter 2 [6].

References

1. A. M. Davies, J. G. Guillemette, M. Smith, C. Greenwood, A. G. P. Thurgood, A. G. Mauk and G. R. Moore, *Biochemistry*, 1993, **32**, 5431.
2. Fredericks, Z. L. and G. J. Pielak, *Biochemistry*, 1993, **32**, 929.
3. S. F. Betz and G. J. Pielak, *Biochemistry*, 1992, **31**, 12337.
4. P. J. R. Spooner and A. Watts, *Biochemistry*, 1991, **30**, 3871.
5. P. J. R. Spooner and A. Watts, *Biochemistry*, 1991, **30**, 3880.

6. T. Ueda, S. Kimura and Y. Imanishi, *J. Chem. Soc. Perkin Trans. 1*, 1993, 219.
7. G. D. Fasman, *"Handbook of Biochemistry and Molecular Biology,"* 1976, 3rd ed., vol. 2, CRC Press, Boca Raton.
8. W. J. Becktel and J. A. Schellman, *Biopolymers*, 1987, **26**, 1859.
9. B. E. Bowler, K. May, T. Zaragoza, P. York, A. Dong and W. S. Caughey, *Biochemistry*, 1993, **32**, 183.
10. C. N. Pace, *Methods in Enzymol.*, 1986, **131**, 266.
11. J. A. Schellman, *Biopolymers*, 1978, **17**, 1305.
12. M. S. Caffrey and M. A. Cusanovich, *Arch. Biochem. Biophys.*, 1993, **304**, 205.
13. N. Oscherhoff, D. Borden, W. H. Koppenol and E. Margoliash, *J. Biol. Chem.*, 1980, **255**, 1689.
14. T. Takano and R. E. Dickerson, *Proc. Natl. Acad. Sci. USA*, 1980, **77**, 6371.
15. T. Takano and R. E. Dickerson, *J. Mol. Biol.*, 1981, **153**, 79.
16. T. Takano and R. E. Dickerson, *J. Mol. Biol.*, 1981, **153**, 95.
17. H. R. Bosshard and M. Zurrer, *J. Biol. Chem.*, 1980, **255**, 6694.
18. Y. P. Myer, S. Kumur, K. Kinnally and A. Pande, *J. Protein Chem.*, 1987, **6**, 321.
19. R. Santucci, A. Giartosio and F. Ascoli, *Arch. Biochem. Biophys.*, 1989, **275**, 2, 496.
20. R. E. Dickerson and R. Timkovitch, *"The Enzyme,"* 1975, Ed., P. D. Boyer, vol. 11, Academic Press, New York, pp. 397-547.
21. L. Pearce, A. Gartner, M. Smith and A. Mauk, *Biochemistry*, 1989, **28**,

3152.

22. B. Matthews, *Biochemistry*, 1987, **26**, 6885.
23. C. J. A. Wallace, P. Mascagni, B. T. Chait, J. F. Collawn, Y. Paterson, A. E. I. Proudfoot and S. B. H. Kent, *J. Biol. Chem.*, 1989, **264**, 15199.
24. D. R. Hickey, G. McLendon and F. Sherman, *J. Biol. Chem.*, 1988, **263**, 34, 18298.
25. D. R. Hickey, A. M. Berghuis, G. Lafond, J. A. Jaeger, T. S. Cardillo, D. McLendon, G. Das, F. Sherman, G. D. Brayer and G. McLendon, *J. Biol. Chem.*, 1991, **266**, 11686.

PART II

PHOTOCONTROL OF PROTEIN ACTIVITY THROUGH STRUCTURAL TRANSITION INDUCED BY PHOTOISOMERIZATION OF NONNATURAL AMINO ACIDS

Chapter 4

Photoregulation of Hydrolysis Activity of Semisynthetic Mutant Phospholipases A_2 Replaced by Nonnatural Aromatic Amino Acids

Introduction

A lipolytic enzyme PLA_2 cleaves specifically the 2-acyl linkage of phosphoglycerides. The reaction proceeds faster with substrates in aggregated states such as micelles and vesicles than in a molecularly dispersed state [1]. In contrast, the precursor of PLA_2, prophospholipase A_2, hydrolyses monomeric and aggregated substrates with similar rates. This difference between prophospholipase A_2 and PLA_2 is explained by the presence of an interface recognition site (IRS) in PLA_2 but not in the precursor [2,3]. The IRS is composed of amino acid residues involved in the N-terminal hydrophobic part of PLA_2, namely Ala^1, Leu^2, Trp^3, Arg^6, Leu^{19}, Met^{20}, Leu^{31}, and Tyr^{69}, and its function is to immobilize the enzyme at the lipid – water interface [4]. It has been shown that the N-terminal fragment of pancreatic PLA_2 takes an α-helical conformation, playing the key role in the activity of the IRS [5,6].

It has been reported that selective replacement of amino acid residues in the IRS region resulted in altered hydrolyis activity due to conformational changes [7]. In this chapter, a nonnatural aromatic amino acid was introduced into the IRS region for the purpose of developing a photosensitive mutant PLA_2. A number of mutant PLA_2s, which shows high affinity for bilayer membrane [8], high activity

[9,10], altered substrate specificity [11], and low specificity [12], have been prepared by site-directed mutagenesis and chemical modification. The present author employed a semisynthetic method for preparation of mutant proteins, because this method seemed to be more suitable for incorporation of nonnatural amino acids into proteins than did the gene technology. Several mutant proteins modified at the N-terminal region of the proteins such as trypsinogen [13], ferredoxin [14,15], and PLA_2 [7] have been successfully prepared by the semisynthetic method.

Three kinds of mutant PLA_2s, [napAla^3]-N^{ε}-amidinated phospholipase A_2 (Nap-AMPA), [antAla^3]-AMPA (Ant-AMPA), and [azoPhe^3]-AMPA (AzoF-AMPA), were synthesized by the semisynthetic method. Two different ways to develop photosensitive enzymes were employed for incorporation of these nonnatural aromatic amino acids into the protein. One is the adoption of napAla and antAla for the replacement. These amino acid residues might affect protein conformation upon UV-light irradiation for the polar photoexcited state. The other is the use of azoPhe. This amino acid residue might affect protein conformation due to variable steric situations induced by *cis* / *trans* photoisomerization. In either way, the mutant protein is expected to show a photosensitive hydrolytic activity.

Materials and Methods

Materials

Bovine pancreatic PLA_2 was purchased from Sigma Chemical Co., USA. NapAla and *p*-nitro-L-phenylalanine (pNO_2Phe) were purchased from Aldrich Chemical Co., USA. AntAla was synthesized by the method reported by Egusa

and coworkers [16]. Boc-Leu-OSu and Boc-Ala-OSu were purchased from Kokusan Chemical Works, Ltd., Japan. DCCD and HOSu were obtained from Peptide Institute, Inc., Japan. Methyl acetimidate hydrochloride was prepared by the method reported by Hunter and Ludwig [17]. 1-Palmitoyl-2-[1-^{14}C]palmitoylphosphatidylcholine ([^{14}C]-DPPC) was purchased from New England Nuclear Co., USA.

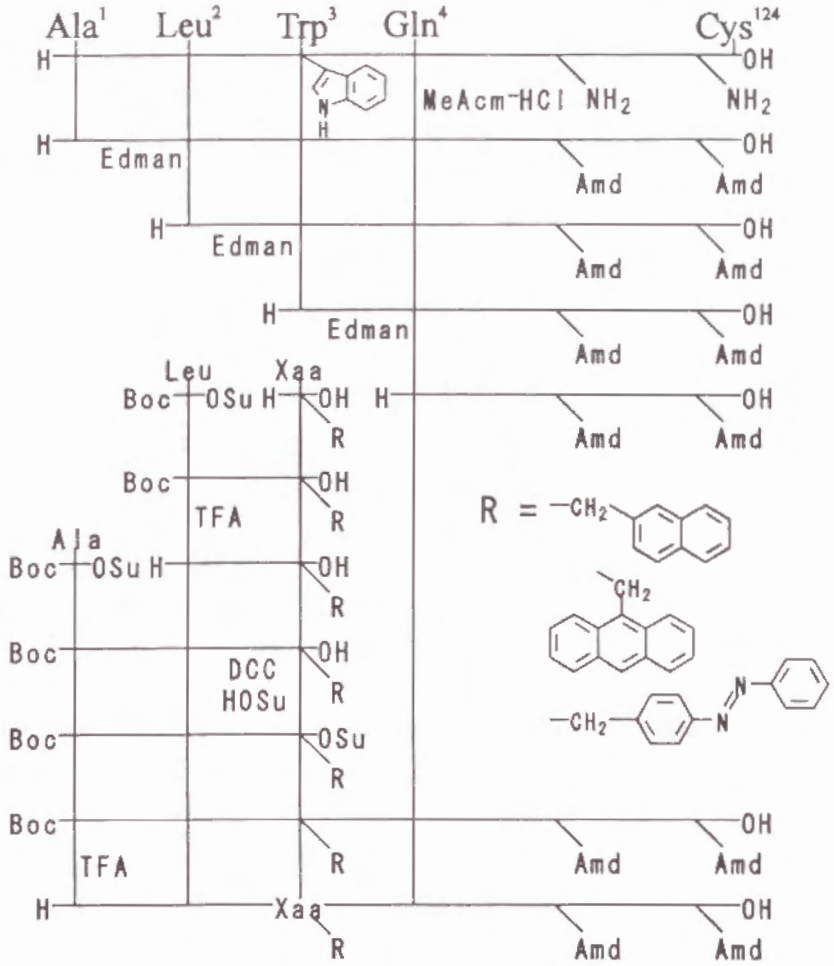

Scheme 1. Preparation of semisynthetic mutant PLA_2s.

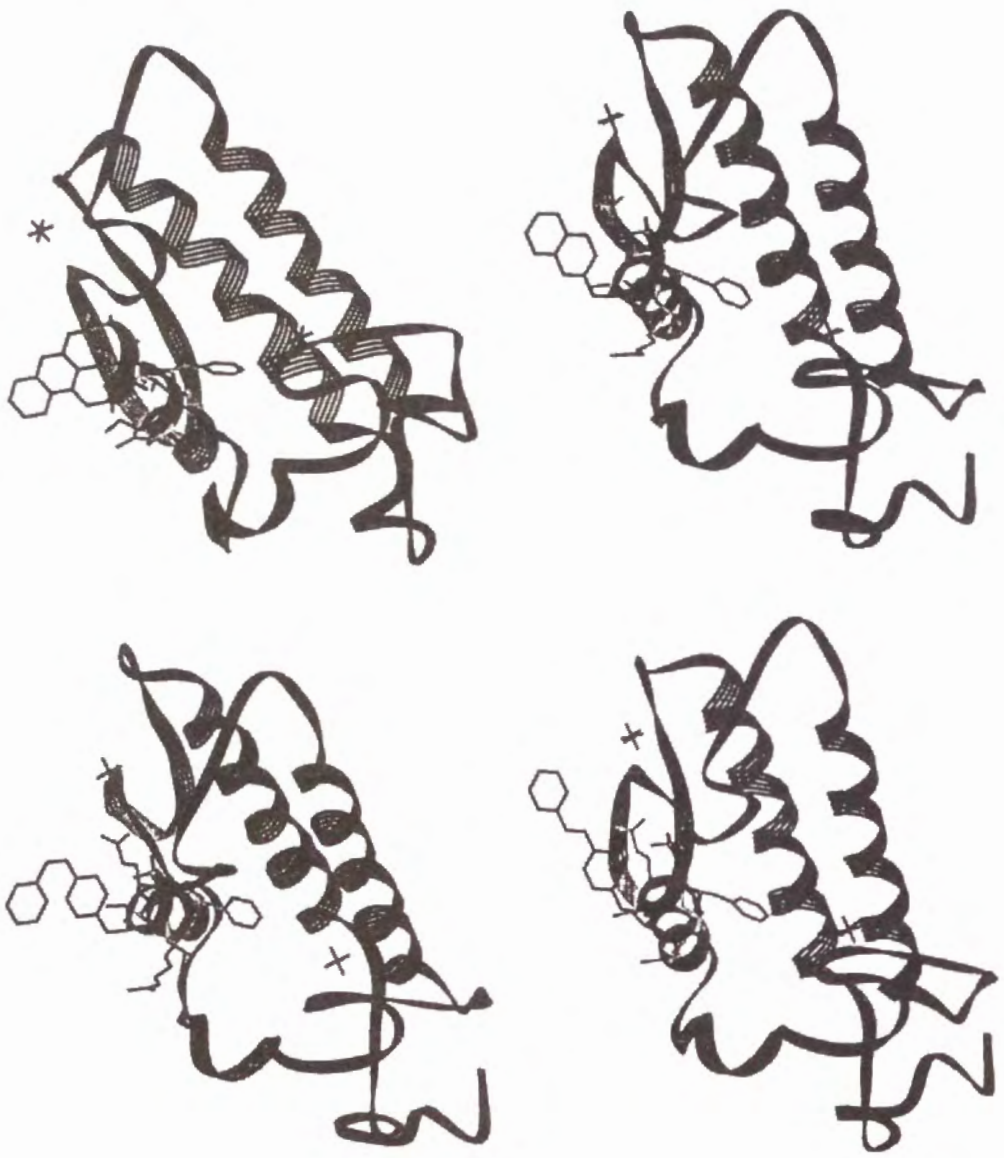

Figure 1. 3D Ribbon drawing of mutant PLA_2s.

Backbone structure is illustrated by a ribbon model. Side chains at positions 1-7 are drawn in stick model and superimposed on the ribbon drawing. (Top, left) Ant-AMPA, (top, right) Nap-AMPA, (bottom, left) AzoF-AMPA in *cis* form, (bottom, right) AzoF-AMPA in *trans* form.

Synthesis

The mutant proteins were prepared by the semisynthetic method as shown in Scheme 1.

Amidination of PLA_2

N^{ε}-Amidinated PLA_2 (AMPA) was prepared by principally the same method as those reported by Slotboom and De Haas [7] and Hunter and Ludwig [17]. PLA_2 (5.5 mg) was dissolved in distilled water (8 ml) and pH of the solution was adjusted to 9.8 with 5 N NaOH. Methyl acetimidate hydrochloride (125 mg) freshly prepared was added over a period of 2 h at room temperature and the mixture was stirred for another 2 h while the pH of the solution was maintained between 9.8 and 10.2. Excess reagents were then removed by gel chromatography of Sephadex G-25 with a Tris-HCl buffer solution (0.1 M, pH 9.5) as eluent. Fractions containing AMPA were collected and concentrated to a small volume. The pH of the solution was adjusted to 6.9 with 1 N hydrochloric acid, and the solution was desalted by a Sephadex G-25 column using deionized water as eluent. The collected fraction was lyophilized to obtain AMPA.

Preparation of Des[$Ala^1Leu^2Trp^3$]AMPA (DES3)

Ala^1, Leu^2, and Trp^3 in the N-terminal region of AMPA were eliminated by three cycles of Edman degradation [18]. Amino acid residues cleaved were identified by TLC analysis using two different solvent systems (chloroform / methanol (9:1 v / v) and chloroform / formic acid (20:1 v / v)). The product was purified by a Sephadex G-50 column to obtain DES3.

Synthesis of Tripeptide

Nonnatural amino acids (Xaa) were reacted with 3-fold molar excess of Boc-Leu-OSu and one molar equivalent of TEA in DMF for 1 day. The product, Boc-Leu-Xaa-OH, was solidified from ethyl acetate / diethyl ether mixture. The solid product was subjected to gel-filtration chromatography on a Sephadex LH-20 column using methanol as eluent. The dipeptides were treated with TFA in the presence of 1 vol % anisole at 0 °C for 30 min. Upon addition of diethyl ether, the dipeptides were obtained as solid TFA salt. Subsequently, the dipeptide salts were reacted with 3-fold molar excess of Boc-Ala-OSu and two molar equivalent of TEA in DMF for 1 day. Boc-Ala-Leu-antAla-OH was solidified from a diethyl ether / hexane solution, and Boc-Ala-Leu-napAla-OH and Boc-Ala-Leu-pNO_2Phe-OH from a methanol / diethyl ether solution. The obtained solid was subjected to gel-filtration chromatography on a Sephadex LH-20 column using DMF as eluent. Boc-Ala-Leu-pNO_2Phe-OH was converted into Boc-Ala-Leu-azoPhe-OH by the method reported by Goodman and Kossoy [19]. The carboxyl group of the tripeptides containing an nonnatural amino acid was esterified with HOSu by using DCCD as coupling reagent.

The purity of synthetic peptides was checked by TLC with a solvent system of chloroform / methanol / acetic acid (85:15:5 v / v / v). All the products were identified by ^{1}H NMR spectroscopy.

Semisynthesis of Xaa-AMPA

DES3 (2.0 mg) was dissolved in a mixture of 0.1 M 4-(2-hydroxyethyl)-1-piperazine ethanesulfonic acid (Hepes) buffer solution (0.4 ml, pH 8.0) and DMF (4 ml), and reacted with 50-fold molar excess of Boc-Ala-Leu-Xaa-OSu for

4 h at room temperature. An insoluble solid was removed by centrifugation, and the supernatant was subjected to a Sephadex G-25 column to obtain Boc-[Xaa^3]AMPA. The Boc group was removed by treatment with TFA (20 ml) at room temperature under nitrogen atmosphere for 20 min. A cold mixture (6 ml) of DMF / Tris-HCl buffer solution (10 mM, pH 7.8, 1:1 v / v) was added, and the solution was subjected to a Sephadex G-25 column and elution with a Tris-HCl buffer solution (10 mM, pH 7.8). Fractions containing the mutant protein were collected, and desalted by gel filtration on a Sephadex G-50 column to obtain Xaa-AMPA.

One dimensional SDS-PAGE was performed using a 7.5 % separation gel with 4 % stacking gel. An aliquot of the semisynthesized protein, after separation by a Sephadex G-25 column, was mixed with a buffer solution (50 mM Tris, pH 6.9; 10 % glycerol, 0.05 % bromophenol blue, 10 % SDS, 5 % 2-mercaptoethanol). After the sample had been heated at 95 °C for 5 min, it was applied to the SDS-polyacrylamide gel. The gel was stained with Coomasie Brilliant Blue R-250. AzoF-AMPA showed a band at a position nearly the same as that of the native PLA_2, indicating that the mutant protein has virtually the same molecular weight as the native one. Figure 1 shows a schematic drawing of mutant PLA_2s, which was drawn by MAGE program of BNL, USA, by using X-ray crystallography data of native PLA_2s and reconstructed with nonnatural amino acids.

Measurements

UV and fluorescence spectra were recorded on a Jasco Ubest-50 UV / Vis spectrophotometer and a Hitachi MPF-4 spectrophotometer, respectively. CD

spectra were recorded on a Jasco J-600 CD spectropolarimeter using a cell with 0.1-cm optical path length. The data are shown as the mean residue ellipticity, [θ]. The helix content of samples was calculated by $-[\theta]_{222} / 40000 \times 100$ (%).

Determination of Concentration

The concentrations of PLA_2 were determined from the absorbance at 280 nm by using a value for ε of 18200 /M cm, unless otherwise stated. Concentrations of mutant proteins were determined by the method reported by Lowry and coworkers [20], taking BSA as a standard protein. Amounts of free amino groups were determined by a colorimetric method using 2,4,6-trinitrobenzenesulfonic acid (TNBS) [21].

Hydrolytic Activity of Mutant PLA_2s with Quin 2-Encapsulated Vesicles as Substrate

The hydrolysis activity of mutant PLA_2s was assayed by the method reported by Nam and coworkers [22]. DPPC vesicles encapsulating 2-{[2-bis(carboxymethyl)amino-5-methylphenoxy]methyl}-6-methoxy-8-bis(carboxymethyl)aminoquinoline (Quin 2) were prepared and dispersed in a Hepes buffer solution (10 mM, pH 7.4; 100 mM NaCl) containing $CaCl_2$ (10 mM). Xaa-AMPA was added to give a final concentration of 1.65 μM. The increase in fluorescence upon addition of mutant PLA_2 was monitored.

The hydrolytic activity of mutant PLA_2s was also determined by using vesicles containing radiolabelled lipid as substrate. The activity was determined by principally the same method as reported by Zhang and Dennis [23]. A

chloroform solution of DPPC (4.05 mmol) and [^{14}C]-DPPC (1 μCi, 18.18 nmol) was dried under a stream of nitrogen. The film was dispersed in a Tris-HCl buffer solution (23.1 ml, 10 mM, pH 7.8, 5 mM $CaCl_2$), and was sonicated at 50 °C. The reaction was started by addition of mutant proteins to the dispersion (0.4 ml) (the final concentration was 21.4 μg / ml for Nap-AMPA and 34.6 μg / ml for the other two), and was continued for 60 min at 22 °C. The solution was irradiated with a high-pressure mercury lamp (150 W) through an optical cut-off filter of L-39 for Ant-AMPA and UV-29 filter for the other two. The reaction was stopped by the addition of 100 mM aqueous ethylenediammine-*N,N,N',N'*-tetraacetic acid (EDTA) solution (100 ml). A chloroform / methanol (9:1 v / v) mixture (1.3 ml) was added and the two phases were completely separated by centrifugation. The lower phase was dried under a nitrogen stream, and the residue was subjected to TLC analysis using a solvent system of chloroform / methanol / water (65:25:4, v / v / v). The radioactivity of the plate was counted by a scanning scintillation counter (Radiochromatoscanner).

Results

Semisynthesis of Mutant PLA_2

PLA_2 was amidinated on ε-amino groups to a conversion of 83 %. AMPA thus obtained was shown to be homogeneous electrophoretically. The average yield for one complete Edman cycle was about 80 %. The amino acid, which was cleaved at each Edman degradation operation, was identified. The elimination of three amino acid residues was confirmed by the absence of the Trp absorption in a UV spectrum of DES3 (Figure 2). On the other hand, Nap-AMPA and Ant-

AMPA showed absorption of naphthyl and anthryl groups, respectively, in a UV spectrum (Figure 2), indicating coupling of the tripeptide with DES3.

AzoF-AMPA showed a broad absorption around 325 nm due to the *trans* configuration of the azoPhe residue (Figure 3). UV-light irradiation on AzoF-AMPA decreased the intensity at 325 nm, indicating that photoisomerization of phenylazophenyl group from *trans*- to *cis*-configuration occurring in the mutant protein. It took nearly 20 min to reach the minimum absorbance at 325 nm under these conditions. On the other hand, visible-light irradiation on the mutant protein in the *cis*- configuration increased the absorption at 325 nm. This isomerization from *cis*- to *trans*-configuration completed within 20 s of the commencement of irradiation.

Conformation

CD spectra of AMPA, DES3, and mutant PLA_2s are shown in Figure 4. AMPA and DES3 showed negative Cotton effects at 208 and 222 nm with similar intensities, indicating the presence of a partial α-helical conformation in these proteins. Since the N-terminal region of PLA_2 is known to take α-helical conformation, the lower intensity of the Cotton effect for DES3 compared with that of AMPA should be due to removal of three amino acids from the N-terminal region, resulting in destabilization of the N-terminal α-helical structure. α-Helix content was calculated for AMPA and DES3 to be 17.8 and 6.5 %, respectively, from the Cotton effect at 222 nm.

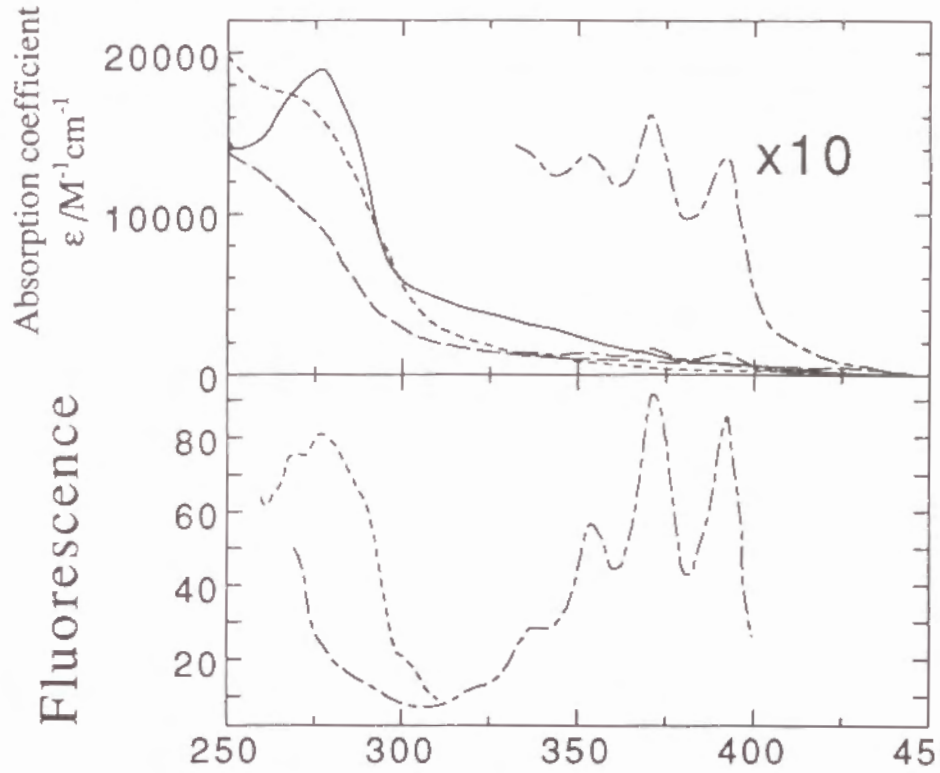

Figure 2. UV (bottom) and fluorescence excitation (top) spectra of AMPA (——), DES3 (— — —), Nap-AMPA (------), and Ant-AMPA (—·—·—). UV spectrum of Ant-AMPA is magnified by 10 in the wavelength range 330 to 450 nm. Fluorescence excitation spectra of Nap-AMPA and Ant-AMPA were monitored at 335 nm and 418 nm, respectively. All samples were measured in Tris-HCl buffer (10 mM, pH 7.8).

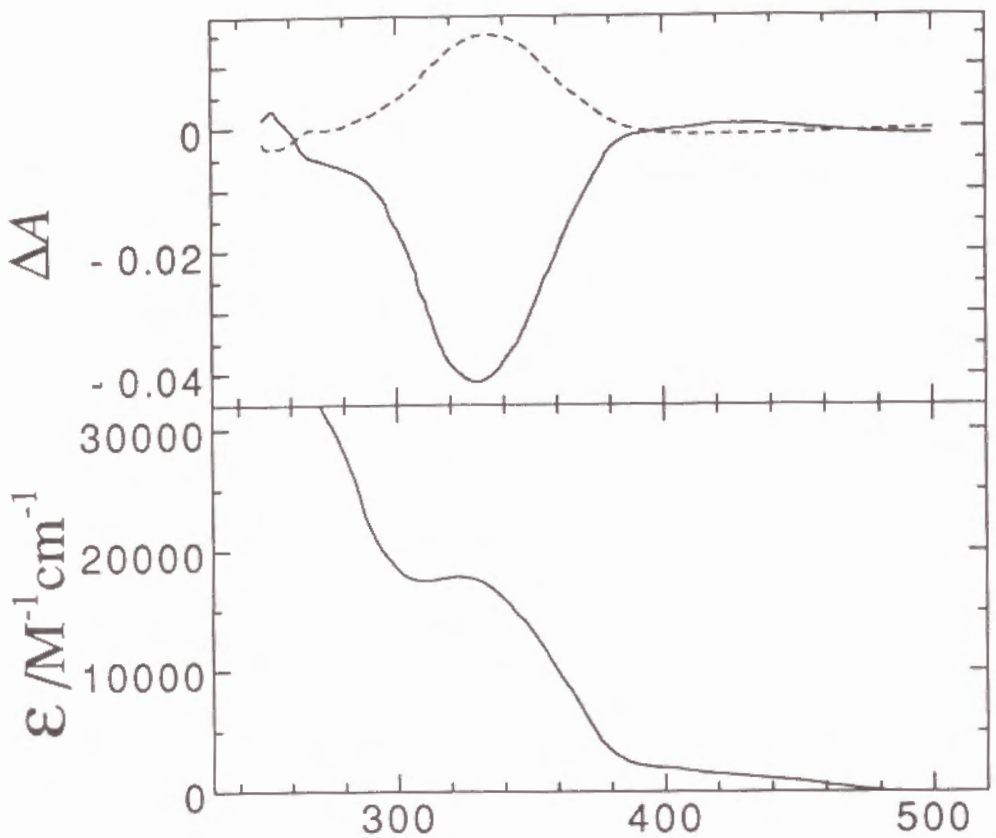

Figure 3. Photoisomerization of AzoF-AMPA monitored by UV spectroscopy. The bottom spectrum is AzoF-AMPA in Tris-HCl buffer (10 mM, pH 7.8). Difference spectra between after and before UV-light irradiation (——) and between after and before visible-light irradiation (— — —) are shown in the top figure. Photoisomerization from *trans*- to *cis*- configuration was induced by UV-light irradiation using a UV31 optical filter and a solution filter of nickel(II) sulfonate. Visible-light irradiation using an L39 optical filter was used for the *cis* to *trans* isomerization. Concentration of AzoF-AMPA was 1.13 μM.

α-Helix content of each mutant PLA_2 was as low as it was in DES3. However, Nap-AMPA is considered to take a secondary structure similar to that of PLA_2, because the Cotton effect at 200 nm is positive (probably due to a positive Cotton effect at the shorter wavelength of the α-helix), which is similar to PLA_2, but opposite to that found for other mutant proteins.

In particular, the Cotton effects at 208 and 222 nm for AzoF-AMPA increased in negative intensity upon UV-light irradiation, indicating that the α-helix content of AzoF-AMPA in the *cis* form is higher than that in the *trans* form.

Hydrolytic Activity

The hydrolytic activity of mutant PLA_2 was measured without removing the protecting groups of ε-amino groups, since AMPA retained *ca.* 60 % of the activity of the native enzyme [7]. The hydrolytic activity was assayed by using Quin 2-encapsulated vesicles. Quin 2 fluoresces strongly upon chelation with Ca^{2+}, and the extent of hydrolysis of lipid molecules by PLA_2 can be determined by measuring the fluorescence intensity [22]. The time course of increasing fluorescence intensity induced by AMPA is expressed by a single exponential curve (Figure 5). On the other hand, the increase of fluorescence intensity induced by Nap-AMPA and AzoF-AMPA was resolved into two components. One is slow and linearly related with time, and the other is fast and exponentially related with time as shown in the inset to Figure 5. The reaction profile (change of fluorescence intensity, F) was analyzed in terms of equation (1).

$$F = A_{\text{fast}}\left[1 - \exp(-k_{\text{fast}}t)\right] + A_{\text{slow}}t \qquad (1)$$

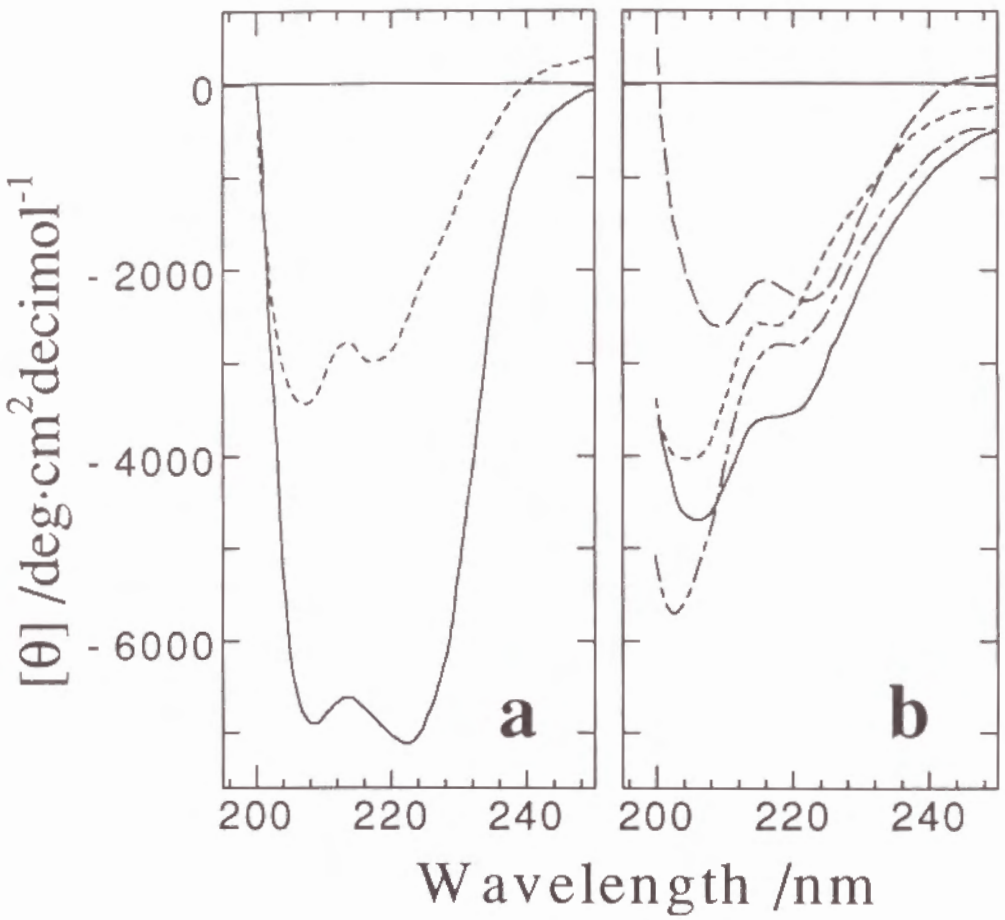

Figure 4. Circular dichroism spectra of (a) AMPA (———), DES3 (------), (b) Nap-AMPA (— — —), Ant-AMPA (— - — -), AzoF-AMPA in the *cis* form (———), and AzoF-AMPA in the *trans* form (------) in Tris-HCl buffer (10 mM, pH 7.8) at a concentration of 1.13 μM.

The solid lines in Figure 5 were obtained by the curve-fitting of the experimental data according to equation (1). Optimization of the three parameters was achieved by a nonlinear regression analysis. The standard deviation between the observed and calculated values was less than 1 %.

Jain and Berg have proposed equation (2) for the time course of hydrolysis reaction by PLA_2 [24],

$$\frac{P_t}{P_{\max}} = \frac{k_{\text{i}}}{k_{\text{i}} + k_{\text{d}}}\left[k_{\text{d}}t + \frac{k_{\text{i}}}{k_{\text{i}} + k_{\text{d}}}\left\{1 - \exp(-k_{\text{i}}t - k_{\text{d}}t)\right\}\right] \qquad (2)$$

where, P_t and $P_{\max}$ are the amounts of hydrolyzed lipid molecules at time t and at infinite time, respectively. The rate constant of the dissociation of PLA_2 from the vesicle is k_{d}. The rate constant k_{i} is for the first-order relaxation that describes the exponential curve of reaction progress, and is proportional to the maximal velocity per enzyme molecule, $k_{\text{cat}} / K_{\text{m}}$ [24,25]. Since equations (1) and (2) are in the same form, the following relations (equation 3) are obtained.

$$kA_{\text{fast}} = \frac{k_{\text{i}}^2}{(k_{\text{i}} + k_{\text{d}})^2}C$$

$$k_{\text{fast}} = k_{\text{i}} + k_{\text{d}} \qquad (3)$$

$$A_{\text{slow}} = \frac{k_{\text{i}}k_{\text{d}}}{k_{\text{i}} + k_{\text{d}}}C$$

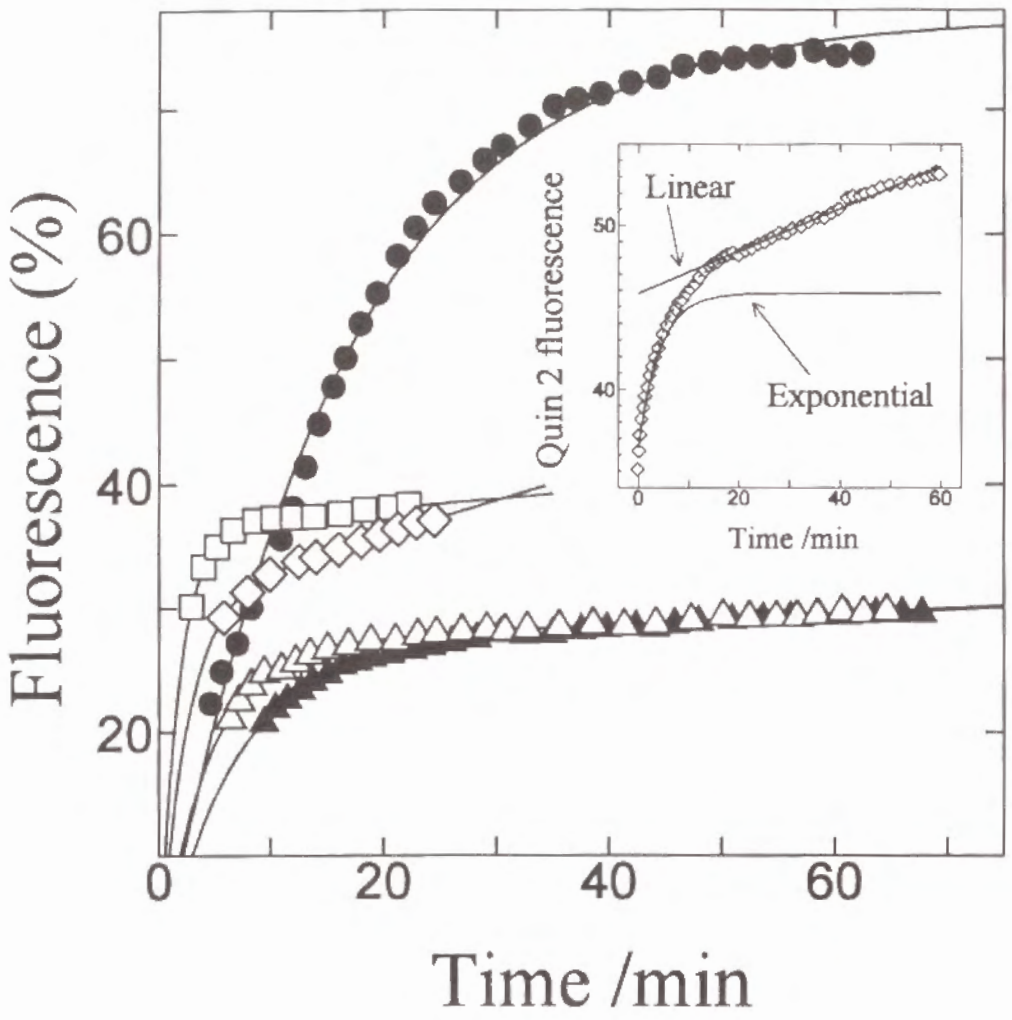

Figure 5. Change of fluorescence intensity of Quin 2-encapsulated DPPC vesicles upon addition of AMPA (●), DES3 (□), Nap-AMPA (◇), AzoF-AMPA in the *cis* form (△), and AzoF-AMPA in the *trans* form (▲). Concentrations of mutant PLA_2s were 0.64 mg / ml for AMPA and AzoF-AMPA, and 1.4 mg / ml for DES3 and Nap-AMPA, respectively. The solid lines represent the results of curve-fitting calculations according to equation (1). Linear and exponential components are shown in the inset.

The immediate change of fluorescence intensity on addition of PLA_2 is related to initial binding and catalysis by PLA_2 on lipid membranes. The subsequent slow increase of fluorescence represents the hydrolysis in a stationary state, where association and dissociation of PLA_2 to the membrane are equilibrated. The rate constants, k_i and k_d, were calculated according to equation (4), and are summarized in Table 1.

$$k_i = \frac{k_{fast}^2}{k_{fast} + \dfrac{A_{slow}}{A_{fast}}} \qquad (4)$$

$$k_d = \frac{k_{fast} A_{slow}}{A_{fast} k_{fast} + A_{slow}}$$

The hydrolysis rate, k_i, decreased in the order of DES3 > Nap-AMPA > AzoF-AMPA in the *cis* form > AzoF-AMPA in the *trans* form. On the other hand, residency times of these proteins ($1 / k_d$), which represents the rate of protein transfer from one site of a membrane to the other, were nearly the same with DES3 and AzoF-AMPA in the *cis* or *trans* form, but 4 – 5-fold that of Nap-AMPA. However, the residency time of Nap-AMPA is still much longer than that of the native PLA_2 (20 min) [26]. This long residency time may be one of the reasons for the fairly low activities of these mutant enzymes. The IRS region of the mutant proteins might be highly hydrophobic as a result of incorporation of the hydrophobic aromatic amino acid residue. This mutation

should take it difficult for the mutant protein to dissociate from the lipid membrane.

Table 1. Membrane perturbation by mutant PLA_2s.

PLA_2	Concn.[a]	Exponential		Linear	Kinetic constants		Residency time[b]
	(μg / ml)	A_{fast}	k_{fast}	A_{slow}	k_d	k_i	(min)
AMPA[c]	0.64	77.4[c]	0.0629[c]	–	–	–	–
DES3	1.4	36.5	0.581	0.0760	0.00207	0.579	483
Nap-AMPA	1.4	30.5	0.415	0.272	0.00873	0.263	115
AzoF-AMPA (*cis*)	0.64	26.8	0.242	0.0463	0.00172	0.240	581
AzoF-AMPA (*trans*)	0.64	26.4	0.158	0.0490	0.00183	0.156	546

[a]Concentration is based on the amount of mutant PLA_2 per total volume of assay cuvette.
[b]Residency time is given by the reciprocal of the dissociation rate constant, $1 / k_d$.
[c]The fluorescence increase of AMPA showed a single exponential curve probably due to the formation of large pores.

The change of fluorescence intensity of Ant-AMPA differs from others as shown in Figure 6. The intensity increased sharply immediately after the addition of Ant-AMPA (lifetime = 0.613 min), and decreased slowly (lifetime = 34 min). The turbidity of the dispersion also changed by addition of Ant-AMPA with a lifetime of 0.29 min, indicating aggregation of vesicles induced by bound Ant-AMPA. The aggregation obstacled the determination of kinetic constants for Ant-AMPA.

Effect of UV-Light Irradiation on Hydrolytic Activity

Hydrolytic activity was assayed by using radiolabelled lipid molecules, and the effect of UV-light irradiation on hydrolytic activity was investigated. Figure 7 shows the experimental results of AMPA, DES3, and three mutant PLA_2s. The hydrolytic activity of DES3 decreased to 20 % of that of AMPA. The reduced activity may be a result of distortion of the IRS of DES3. Nap-AMPA and Ant-AMPA were of considerably low activity, that is, 10 and 2 % of that of AMPA, respectively. Hydrolysis by AzoF-AMPA in the *trans* form did not exceed spontaneous hydrolysis under the same conditions. These results are consistent with those obtained by using Quin 2-encapsulated vesicles.

Discussion

Although the primary sequence of the mutant proteins is nearly the same as that of PLA_2, the hydrolytic activities of the mutant proteins are much lower than that of PLA_2. This is probably because the tertiary structure of the IRS region of the mutant proteins changed considerably from the native PLA_2, which is reflected on CD spectra (Figure 4). The catalytic activity of Nap-AMPA is the highest among the mutant proteins, but is only 10 % of that of AMPA. The napAla residue is considered to replace Trp^3 without disrupting the IRS structure so much as do others, because the size of the side group is not much different from those of natural amino acids.

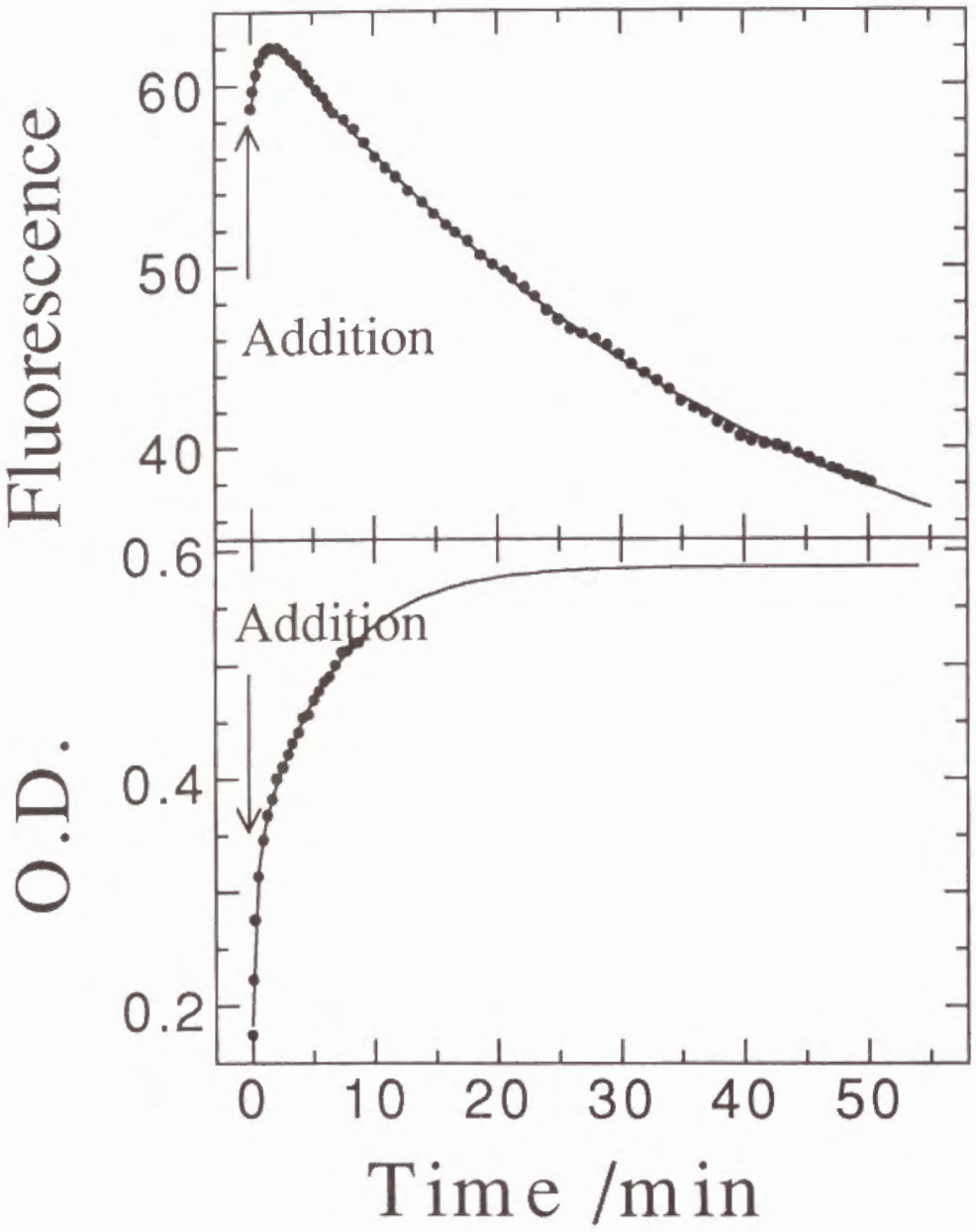

Figure 6. Changes of fluorescence intensity of Quin 2-encapsulated DPPC vesicles (top) and of absorption at 290 nm (bottom) on addition of Ant-AMPA (1.65 μM).

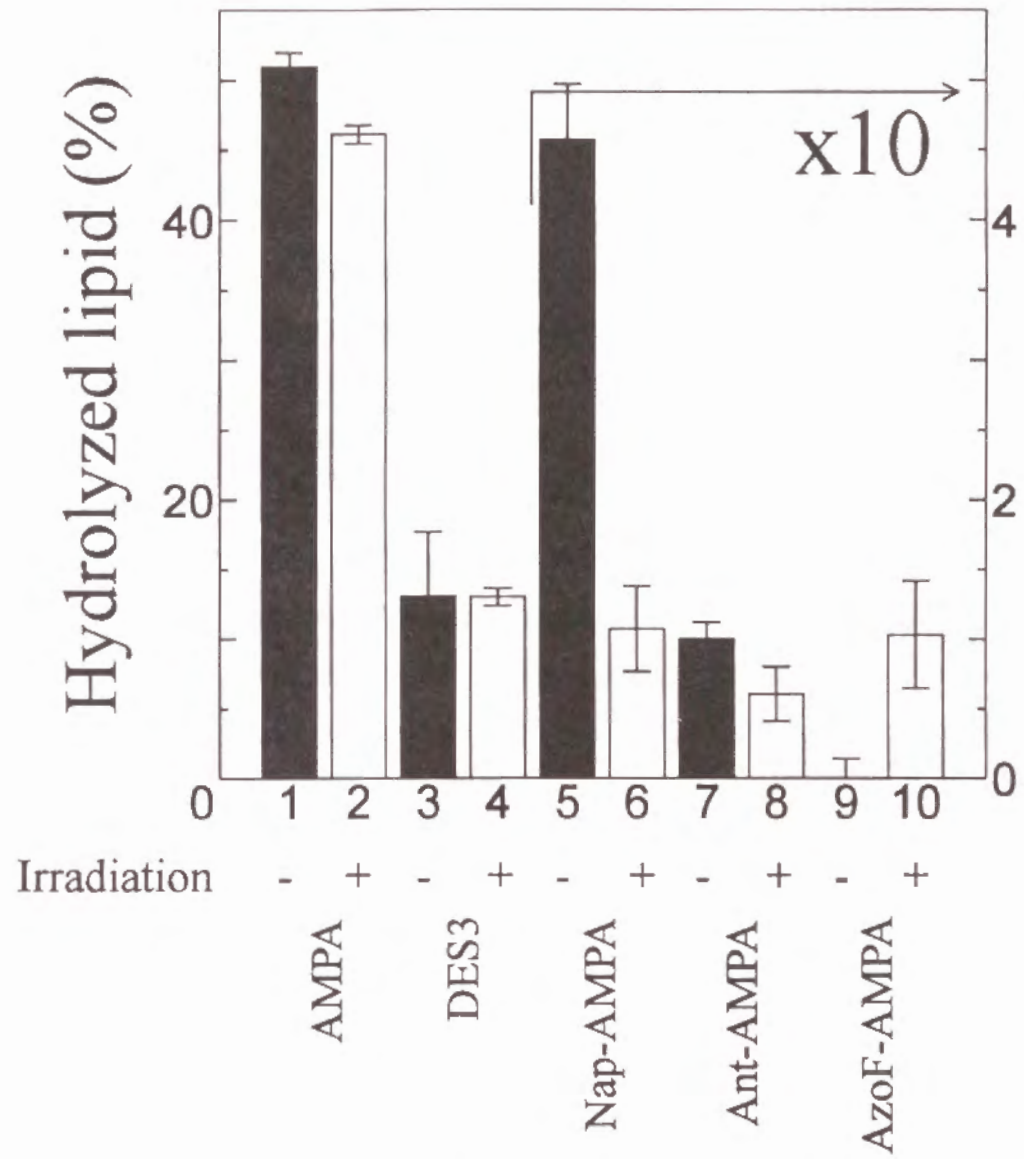

Figure 7. Effect of UV-light irradiation on hydrolytic activity of AMPA, DES3, and mutant PLA_2s. The ordinate represents the amount of hydrolyzed lipid molecules after 60 min. Without UV-light irradiation, ■. With UV-light irradiation, □. Standard errors of the mean (SEMs) are shown as I-bars.

UV-light irradiation showed very little effect on hydrolysis reaction catalyzed by AMPA or DES3. On the other hand, the activities of Nap-AMPA and Ant-AMPA were reduced by UV-light irradiation during hydrolysis. In particular, the activity of Nap-AMPA decreased to 25 % of that before UV-light irradiation. Since the naphthyl group in the excited state becomes more polar than in the ground state, the structure of IRS may be distorted by dislocation of the excited naphthyl group to a more polar environment during UV-light irradiation. This explanation for the photoregulation of the enzymatic activity, however, should be verified by mutant enzymes having much higher activity than the present mutant proteins.

The reduced activity of Ant-AMPA by UV-light irradiation may be explained by the same reasoning as for Nap-AMPA. The extent of activity decrease of Ant-AMPA by UV-light irradiation was less than that of Nap-AMPA. The anthryl group is so bulky that the structure of the IRS should be significantly distorted even in the ground state, resulting in a smaller effect, upon photoirradiation, on the tertiary structure.

AzoF-AMPA in the *cis* form is a little more active than in the *trans* form. This result is parallel with the result obtained by using Quin 2-encapsulated vesicles. Since the α-helix content increases by photoisomerization of azoPhe from *trans* to *cis* form as revealed by CD spectroscopy, the hydrolytic activity of AzoF-AMPA in the *cis* form is ascribable to a partial recovery of the native helical structure of the IRS in the mutant protein. However, azoPhe in the *trans* form cannot be accommodated into the native IRS because of its bulkiness along the longer molecular axis.

By incorporation of the bulky aromatic group into the IRS, the mutant PLA_2s changed their hydrolytic activity in response to UV-light irradiation. It is

believed that the protein structure is changed by UV-light irradiation, resulting in altered interactions of proteins with the phospholipid membrane.

References

1. G. H. De Haas, P. P. M. Bonsen, W. A. Pieterson and L. L. M. Van Deenen, *Biochim. Biophys. Acta*, 1971, **239**, 252.
2. R. Verger, M. C. E. Mieras and G. H. De Haas, *J. Biol. Chem.*, 1973, **248**, 4023.
3. W. A. Pieterson, J. C. Vidal, J. J. Volwerk and G. H. De Haas, *Biochemistry*, 1974, **13**, 1455.
4. M. C. E. Van Dam-Mieras, A. J. Slotboom, W. A. Pieterson and G. H. De Haas, *Biochemistry*, 1975, **14**, 5387.
5. B. W. Dijkstra, J. Drenth, K. H. Kalk, *Nature*, 1981, **289**, 604.
6. J. P. Abita, M. Lazdunski, P. P. M. Bonsen, W. A. Pieterson and G. H. De Haas, *Eur. J. Biochem.*, 1972, **30**, 37.
7. P. A. J. Slotboom and G. H. De Haas, *Biochemistry*, 1975, **14**, 5394.
8. F. C. Van der Wiele, W. Atsma, B. Roelofsen, M. V. Linde, J. V. Binsbergen, F. Radvanyi, D. Raykova, A. J. Slotboom and G. H. De Haas, *Biochemistry*, 1988, **27**, 1688.
9. O. P. Kuipers, M. M. G. M. Thunnissen, P. D. Geus, B. W. Dijkstra, J. Drenth, H. M. Verheij, G. H. De Haas, *Science*, 1989, **244**, 82.
10. J. P. Noel, C. A. Bingman, T. Deng, C. M. Dupureur, K. J. Hamilton, R.-T. Jiang, J.-G. Kwak, C. Sekharudu, M. Sundaralingam and M.- D. Tsai, *Biochemistry*, 1991, **30**, 11801.

11. J. P. Noel, T. Deng, K. J. Hamilton and M.- D. Tsai, *J. Am. Chem. Soc.*, 1990, **112**, 3704.
12. C. M. Dupureur, Y. Li and M.-D. Tsai, *J. Am. Chem. Soc.*, 1992, **114**, 2748.
13. N. C. Robinson, H. Neurath and K. A. Walsh, *Biochemistry*, 1973, **12**, 420.
14. E. T. Lode, *Fed. Proc., Fed. Am. Soc. Exp. Biol.*, 1973, **32**,542.
15. E. T. Lode, C. L. Murray, W. V. Sweeney and J. C. Rabinowitz, *Proc. Natl. Acad. Sci. USA*, 1974, **71**, 1361.
16. S. Egusa, M. Sisido, Y. Imanishi, *Bull. Chem. Soc. Jpn.*, 1986, **59**, 3175.
17. M. J. Hunter and M. L. Ludwig, *J. Am. Chem. Soc.*, 1962, **84**, 3491.
18. G. W. Anderson, I. E. Zimmerman and F. M. Callahan, *J. Am. Chem. Soc.*, 1964, **86**, 1839.
19. M. Goodman and A. Kossoy, *J. Am. Chem. Soc.*, 1966, **88**, 5010.
20. O. H. Lowry, N. J. Rosenrough, A. L. Farr and R. J. Randall, *J. Biol. Chem.*, 1951, **193**, 265.
21. J. N. Van Eijk, H. M. Verheij, R. Dijkman, G. H. De Haas, *Eur. J. Biochem.*, 1983, **132**, 183
22. K.-Y. Nam, A. Morino, S. Kimura, H. Fujiki and Y. Imanishi, *Biochem. J.*, 1990, **268**, 169-173.
23. Y. Zhang and E. A. Dennis, *J. Biol. Chem.*, 1988, **263**, 9965.
24. M. K. Jain and O. G. Berg, *Biochim. Biophys. Acta*, 1989, **1002**, 127.
25. O. G. Berg, B.-Z. Yu, J. Rogers and M. K. Jain, *Biochemistry*, 1991, **30**, 7283.
26. M. K. Jain, J. Rogers, O. Berg and M. H. Gelb, *Biochemistry*, 1991, **30**, 7340.

Chapter 5

Location of Melittin Fragment Carrying Spiropyran in Phospholipid Bilayer Membrane Determined by Thermal Isomerization

Introduction

Conformation, orientation, and location of membrane-bound peptides are key factors for understanding the biological activity of such peptides on the molecular basis [1]. For example, opioid peptide hormones with definite conformation are distributed to a specific region of the membrane. This process is considered to enhance encountering and binding to a certain type of opioid receptor embedded in the membrane [2]. The location of peptides in the membrane has been investigated by various methods such as fluorescence [3], fluorescence quenching [4], attenuated total reflection-infrared (ATR-IR) spectroscopy [5], nuclear magnetic resonance (NMR) spectroscopy [6], differential scanning calorimetry [7], and hydrophobic photolabelling [8], etc. Although the fluorescence method is very sensitive to the microenvironment, it provides average information on the location in the membrane. This point imposes several limitations on the application of the fluorescence method, when the location of peptide molecules in the membrane is variable according to conformation and they are distributed according to the Boltzman rule among several sites of similar potential energies. Parallax method based on the fluorescence quenching determines the location of the fluorophore in an angstrom unit [4]. However, the location of the quenching group fluctuates in some occasions strongly in the membrane [9]. Distance geometry using nuclear

Overhauser effect (NOE) measurement is a powerful technique to determine the location exactly. However, this method is applicable only to the case of micelles [6]. Since each method is not almighty, a novel method should be explored.

In this chapter, spiropyran was used as an environmental probe. Because the rate of thermal isomerization from merocyanine to spiropyran is very sensitive to the polarity of microenvironment [10], the location of merocyanine group in the membrane can be determined by the kinetics of thermal isomerization.

Melittin, the main component of bee venom, undergoes membrane-lysis. The interaction of melittin with phospholipid membranes has been extensively studied [11-24], and different types of distribution of melittin in the membrane have been proposed, wedge-like model [25] and transbilayer model [26]. The primary sequence of melittin possesses an amphiphilic property, in which the melittin 1-20 fragment is composed predominantly of hydrophobic residues and the rest 21-26 fragment hydrophilic. Since melittin 8-26 fragment did not show membrane-lysis activity, the hydrophobic melittin 1-7 fragment is essential for strong interactions with phospholipid membrane [27-29]. In this chapter, Ala^4 residue of the melittin 1-7 fragment was replaced with Glu residue having a spiropyran group in the side chain [Glu(OSp)], and interaction of the peptide with phospholipid membrane was studied by using the spiropyran group as a probe. A melittin 4-7 fragment having Glu(OSp) for the N-terminal residue and a protected Lys^7 at the C-terminal residue was synthesized as a reference compound. The location of the merocyanine group of these peptides in the membrane was estimated from the kinetics of thermal isomerization.

Experimental

Peptide Synthesis

The melittin fragments were synthesized by the conventional liquid-phase method (Scheme 1). All intermediates and final compounds were identified by ^{1}H NMR, and the purity was checked by TLC. Analytical TLC was performed on Merck silica gel 60 F_{254} aluminum plates, with detection by UV light and / or the ninhydrin test. Light was shut off during the evaporation procedure. Figure 1 shows a schematic drawing of melittin fragment carrying spiropyran.

Boc-Glu(OSp)-OBzl

A photochromic compound, 1-(β-hydroxyethyl)-3,3-dimethyl-6'-nitrospiro(indoline-2,2'-2H-benzopyran) (HO-Sp), was prepared by the reaction of 1-(β-hydroxyethyl)-3,3-dimethylindolenium iodide and 5-nitrosalicylaldehyde in the presence of piperidine [30,31]. HO-Sp (1 eq. mol) was reacted with Boc-Glu-OBzl (γ free, 1 eq. mol) in the presence of 4-pyrrolidinopyridine (0.1 eq. mol) using DCCD as coupling reagent. The product was purified by eluting through a silica gel column (Lobar Si60, Sigma Chemical Co., USA) using a mixture of ethyl acetate and toluene (1:1, v / v) as eluent. $R_f = 0.78$ (ethyl acetate / toluene, 1:1, v / v)

TFA·H-Glu(OSp)-OH (M1Sp)

Boc-Glu(OSp)-OBzl (100 mM) was dissolved in acetone and 1.5-fold molar excess of LiOH solution (0.4 N) was added dropwise under stirring over a period of 1 h. After stirring for further 1.5 h at 24 °C, the solution was acidified

with citric acid solution (10 %) and extracted with ethyl acetate. The combined extract was concentrated and eluted through a silica gel column (Lobar Si60) using ethyl acetate as eluent to obtain Boc-Glu(OSp)-OH (BocM1Sp). R_f = 0.43 (ethyl acetate / methanol, 7:3, v / v). The Boc group was removed by treatment with TFA containing 10 % anisole at 0 °C for 30 min. White precipitate was obtained by the addition of excess amount of diethyl ether.

TFA·H-Glu(OSp)-Val-Leu-Lys(Z)-OMe (M4Sp)

HCl·Val-Leu-Lys(Z)-OMe was synthesized according to the scheme shown in Scheme 1. BocM1Sp was coupled with H-Val-Leu-Lys(Z)-OMe using DCCD in DMF for 1 day. The product was purified by elution through a Sephadex LH-20 column using methanol as eluent to obtain Boc-Glu(OSp)-Val-Leu-Lys(Z)-OMe. R_f = 0.75 (ethyl acetate). The Boc group was removed by treatment with TFA containing 10 % anisole at 0 °C for 30 min. The solution was evaporated, and the residue was recrystallized from diethyl ether / petroleum ether mixture. R_f = 0.63 (chloroform / methanol / acetic acid, 95:5:3, v / v / v).

2HBr·Gly-Ile-Gly-Glu(OSp)-Val-Leu-Lys-OMe (M7Sp)

Boc-Gly-Ile-Gly-OH (R_f = 0.67 with butanol / acetic acid / water, 10:1:3, v / v / v) was prepared according to the scheme shown in Scheme 1. To a DMF solution of Boc-Gly-Ile-Gly-OH (22 mg) and TFA·Glu(OSp)-Val-Leu-Lys(Z)-OMe (71 mg), DCCD (16 mg), HOBt (13 mg) and TEA (9.1 ml) were added at 0 °C. After stirring overnight at room temperature, the solution was concentrated, and ethyl acetate was added. The precipitate was filtered off, and the filtrate was evaporated. The residue was purified by elution through a Sephadex LH-20

column using DMF as eluent. The main fraction was subjected to elution through a Silica gel column using a mixture of ethyl acetate and methanol (7:3, v / v) as eluent, and the fraction of R_f = 0.85 was collected.

The protected heptapeptide (20 mg) was dissolved in HBr / acetic acid (25 wt %, 200 ml) containing 1 % anisole. After standing for 1 h, diethyl ether was added. The precipitate was purified by elution through a Sephadex LH-20 column using methanol as eluent. The main fraction was further purified by elution through a reverse-phase HPLC column (Cosmosil 5C_{18} column) using a mixture of variable contents of acetonitrile (20 – 100 %) and water containing 0.1 % TFA. The final product was identified by amino acid analysis.

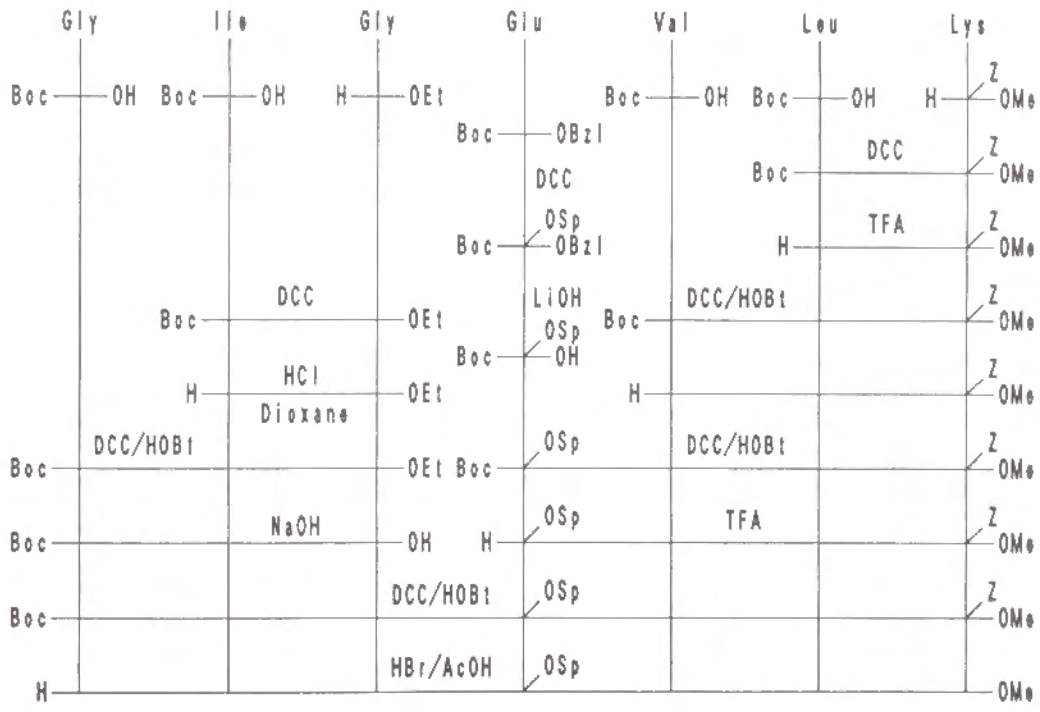

Scheme 1. Synthesis of three melittin fragments carrying a spiropyran group.

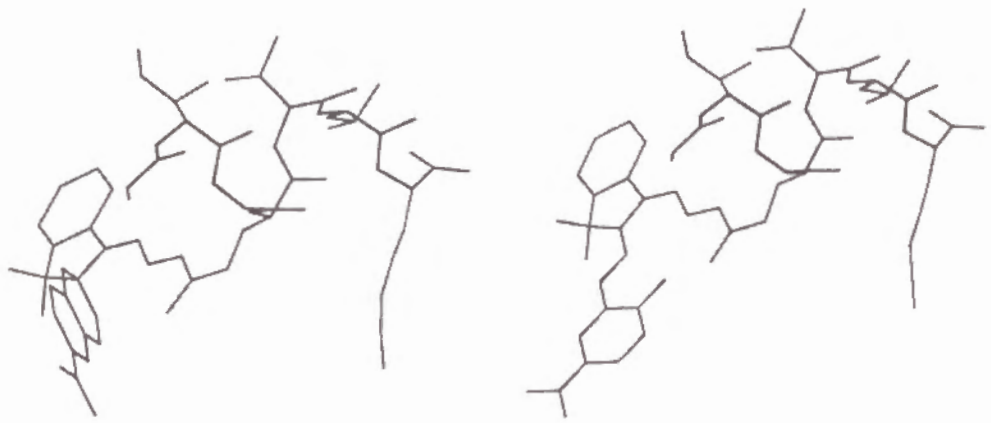

Figure 1. 3D wire frame drawing of melittin fragment carrying spiropyran. Backbone structure is illustrated by the wire frame model. Side chains are drawn in stick model. (Left) spiropyran form, (right) merocyanine form.

Measurements

Absorption and fluorescence spectra were recorded on a Jasco Ubest-50 UV / Vis spectrophotometer and a Hitachi MPF-4 fluorescence spectrophotometer, respectively. A high-pressure mercury lamp (100 W) was used for light source. Optical cut-off filters of UV-31, UVD-36C, and a nickel sulfate solution were used for UV-light irradiation, and a Y50 filter for visible-light irradiation.

Binding Constant

M1Sp, M4Sp or M7Sp, was incubated with multilamellar vesicles (MLV) of DPPC (potassium borate buffer, pH 9.0, 2 mM) at a molar ratio of [DPPC] / [peptide] = 100. The borate buffer was used because of the following

fluorescamine assay. For other experiments in buffer or DPPC dispersion, a Hepes buffer solution containing 0.1 M NaCl was used as standard. Under these conditions, melittin is shown to exist predominantly as monomer [32]. The dispersion was subjected to visible-light irradiation to convert merocyanine group completely into spiropyran group, and was divided into two portions. One portion was irradiated by UV light, and both portions were centrifuged (15000 rpm, 6 min) to sediment the peptide bound to MLV. Concentrations of the peptides in the supernatant were determined by the fluorescence method using fluorescamine for labeling free amino groups. Binding constants of melittin fragments to DPPC MLV were calculated according to equation (1),

$$K = \frac{[\text{peptide}]_0 - [\text{peptide}]_{\text{sup}}}{[\text{peptide}]_{\text{sup}} \cdot \ [\text{DPPC}]} \qquad (1)$$

where $[\text{peptide}]_0$ and $[\text{peptide}]_{\text{sup}}$ represent the initial concentration of peptide and the concentration of peptide in the supernatant, respectively.

Thermal Isomerization

A peptide solution (1.0×10^{-5} M) was subjected to UV-light irradiation for 30 min. The change of absorption intensity at the maximum wavelength of merocyanine group was followed at 25 °C. Thermal isomerization was also examined in the presence of small unilamellar vesicles (SUV) of DPPC, which were prepared as follows. Dried DPPC was dispersed in a Hepes buffer (10 mM

Hepes, 0.1 M NaCl, pH 7.4). The dispersion was sonicated at 50 °C under N_2 atmosphere. After centrifugation at 100000g, SUV was obtained.

Leakage of CF Encapsulated in DPPC Vesicles

CF-encapsulated DPPC vesicles were prepared by the method reported by Barbet and coworker [33]. The excitation and monitor wavelengths of CF were 470 and 515 nm, respectively. Complete release of CF was attained by addition of Triton X-100 (0.3 wt %). Peptides having a spiropyran group were dissolved in ethanol and kept in the dark. The peptide solution was added to the vesicle dispersion, keeping the ethanol content less than 1 % of the total volume. The temperature was regulated by circulating water thermostatted at 25 °C.

Results

Binding of Melittin Fragment to DPPC Membrane

The melittin fragment bearing either spiropyran or merocyanine group was incubated with DPPC vesicles, and the concentration of the peptide in aqueous phase was determined. The binding constant of the melittin fragment to DPPC membrane was calculated according to the method described in the experimental section, and is summarized in Table 1 together with the relative amount of melittin fragment bound to the membrane. M1Sp having either spiropyran or merocyanine group was practically insoluble in lipid membrane. In contrast, M4Sp was not detected in the aqueous phase, indicating a high affinity for DPPC membrane due to the hydrophobic property. On the other hand, M7Sp showed different membrane affinities depending on the nature of the chromophoric group (spiropyran or merocyanine). M7Sp having a spiropyran group possessed a high binding constant. However, upon UV-light irradiation about half of the bound

peptides was dissociated from the lipid membrane. The merocyanine form is zwitterionic and makes the peptide more hydrophilic, resulting in a reduced affinity for phospholipid membrane.

Table 1. Binding of melittin fragments to DPPC membrane[a]

	Without UV irradiation		After UV irradiation	
Fragment	K (M^{-1})	%[b]	K (M^{-1})	%[b]
M1Sp	126	0.75	120	0.71
M4Sp	large	> 99	large	> 99
M7Sp	116000	87.4	11600	41.1

[a][DPPC] = 60 μM, [peptide] = 0.6 μM, at 25 °C.

[b]The percentage of peptide distributed to DPPC membrane.

Location of Merocyanine-Carrying Peptide in Lipid Membrane Determined by Thermal Isomerization

The merocyanine form is sensitive to the polarity of microenvironment, and the maximum-absorption wavelength (λ_{max}) shifts towards shorter wavelength as the environmental polarity increases [10]. λ_{max} of BocM1Sp was measured in different compositions of dioxane / water mixtures (Table 2). A blue shift of λ_{max} is evidently observed with increasing water content in the solution.

More drastic change was observed in the rate of thermal isomerization from merocyanine to spiropyran of BocM1Sp. The rate of isomerization in 60 %

dioxane was 1 / 173-fold that in 97 % dioxane, and the isomerization in 50 % dioxane was very slow. The faster isomerization in less polar media can be explained in terms that the zwitterionic form of merocyanine is not stable in apolar media.

The kinetic studies of thermal isomerization of M1Sp, M4Sp, and M7Sp, however, revealed that the decay of merocyanine content could not be expressed by a single-component first-order reaction (Figure 2). In these cases, two, fast and slow, processes should be taken into consideration in the analysis of the experimental data shown in Figure 2, which were well fitted by equation (2),

$$\frac{A_t - A_{\text{inf}}}{A_0 - A_{\text{inf}}} = F\exp(-k_{\text{fast}}t) + (1-F)\exp(-k_{\text{slow}}t) \qquad (2)$$

where A_0, A_t, and A_{inf} are the absorbance at λ_{max} at time zero, t, and infinite, respectively. F is the fraction of peptides having the decay rate constant of k_{fast}. k_{fast}, k_{slow}, and F are summarized in Table 2.

Occurrence of two components in the kinetics of thermal isomerization indicates two different states of the merocyanine group in these peptides. Possible two forms of merocyanine are a contact ion-pair and a solvent separated ion-pair or free ions of merocyanine, which might be brought about by *cis-trans* isomerization of C^3-C^4 (numbering in a spiropyran form) double bond (Scheme 2). In the merocyanine form, other ionic species in the peptide molecule such as N-terminal ammonium group might interact with the anionic site of merocyanine. The thermal isomerization recombination in the form of

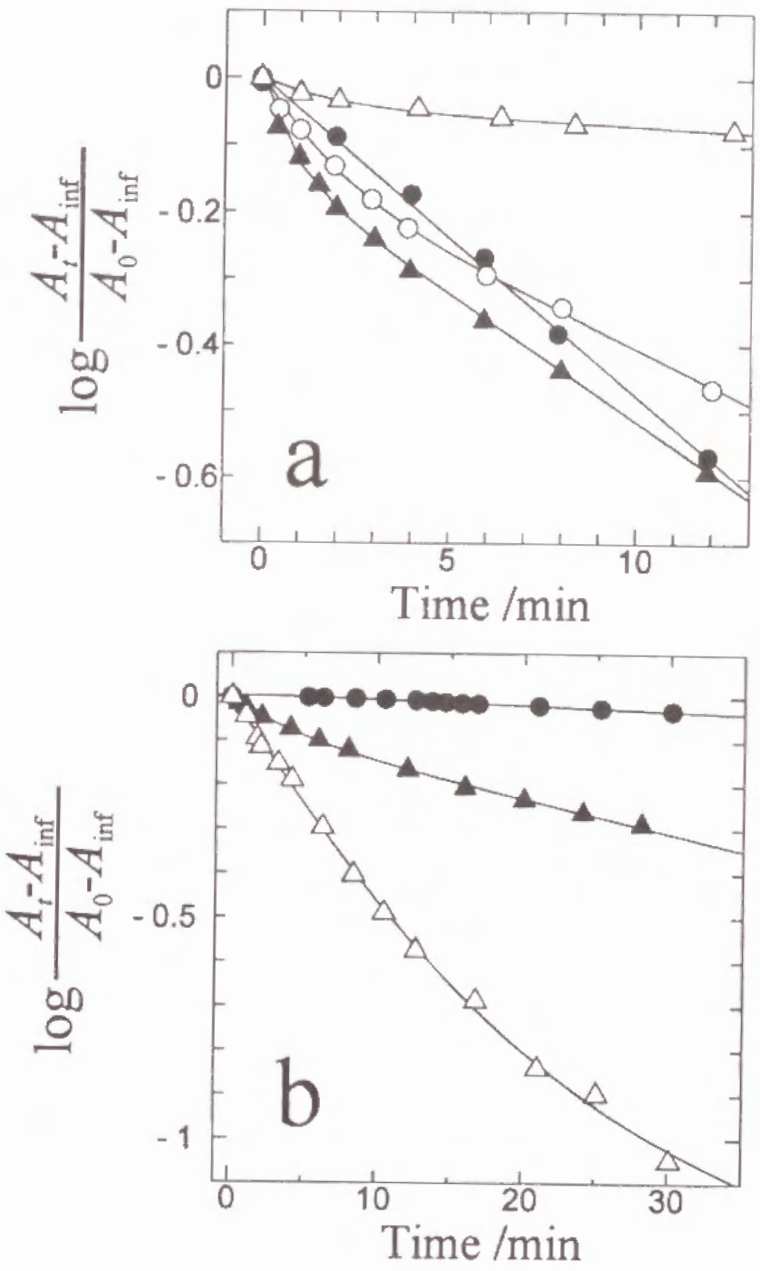

Figure 2. First-order plots for the thermal isomerization of the merocyanine group of HO-Sp (●), M1Sp (○), M4Sp (▲), and M7Sp (△), in ethanol (a) and in the presence of DPPC vesicles (b). [peptide] = 10 μM. [DPPC] = 1.6 mM.

Table 2. Thermal isomerization of merocyanine-containing peptides in various media

Fragment[a]	Solvent[b]	F[c.]	k_{fast}[c]	1-F	k_{slow}[c]	λ_{max}
HO-Sp	EtOH	1	0.110	-	-	540 nm
BocM1Sp	97 % DOx	1	4.33	-	-	572 nm
BocM1Sp	90 % DOx	1	0.642	-	-	562 nm
BocM1Sp	80 % DOx	1	0.186	-	-	551 nm
BocM1Sp	60 % DOx	1	0.025	-	-	548 nm
BocM1Sp	50 % DOx	-	<0.001	-	-	536 nm
M1Sp	EtOH	0.261	0.638	0.739	0.063	543 nm
M1Sp	DPPC	-	<0.001	-	-	-
M4Sp	EtOAc	0.497	2.59	0.503	0.676	-
M4Sp	EtOH	0.258	1.38	0.742	0.089	550 nm
M4Sp	DPPC	0.163	0.244	0.837	0.018	565-575 nm
M4Sp	DGOH	0.364	0.072	0.636	0.003	-
M7Sp	EtOH	0.097	0.551	0.903	0.006	520 nm
M7Sp	DPPC	0.836	0.135	0.164	0.024	545 nm

[a]Concentration of melittin fragments was 0.1 μM.

[b]EtOH, DOx, EtOAc, and DGOH represent ethanol, dioxane, ethyl acetate, and diglycerol, respectively.

[c]See the text for notations.

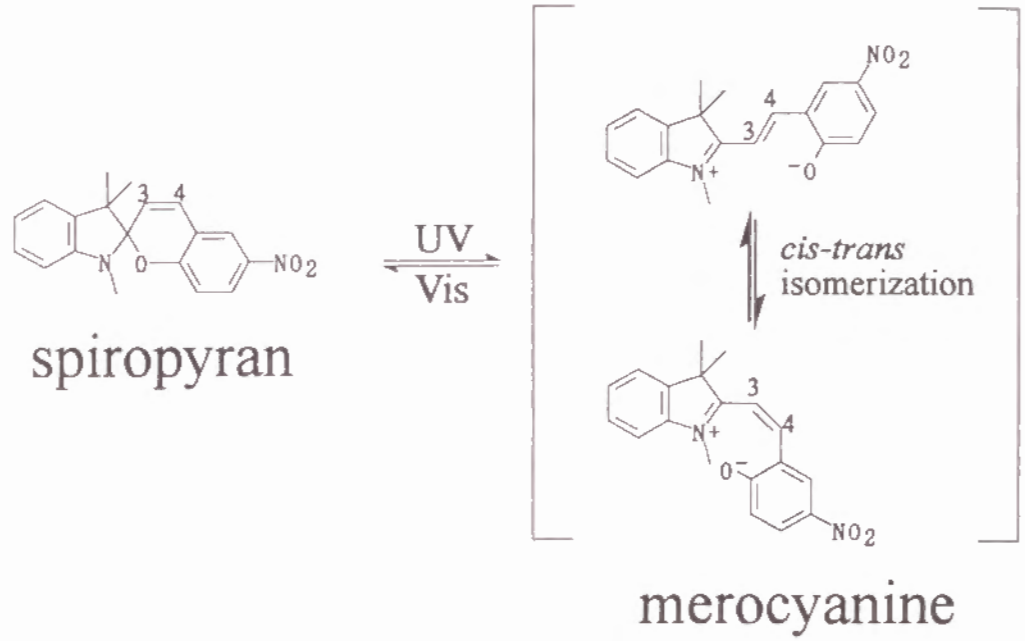

Scheme 2. Two forms of merocyanine on the basis of *cis-trans* isomerization.

the contact ion-pair must be faster than in the form of the free ions, because in the former two sites for recombination are in a close proximity. For example, the fraction of k_{fast} species of M4Sp is 49.7 % in ethyl acetate, which should be ascribed to the contact ion-pair species. The fraction decreases to 25.8 % in ethanol. The increasing solvent polarity may produce more free ions upon UV-light irradiation, since free ions should be stabilized in more polar environment. It should be noted that the conversion between the free ions and the contact ion-pair is hindered, because it requires the *cis-trans* isomerization. It is, therefore, conceivable that the microenvironment of a merocyanine group is probed from the fraction of k_{fast} species. The higher the fraction of k_{fast} species, the more hydrophobic the microenvironment of the merocyanine group.

When an aqueous solution of M1Sp was irradiated with UV lamp, the absorption intensity of the merocyanine group increased slightly. The rate of thermal isomerization of the merocyanine group was extremely slow. In the presence of DPPC vesicles, too, the absorption intensity of the merocyanine group of M1Sp produced by UV-light irradiation did not decay significantly, indicating that M1Sp stayed in the aqueous phase. The result is consistent with the binding assay, which showed that the fraction of M1Sp bound to DPPC vesicles was less than 1 %. M4Sp showed a high proportion of k_{slow} species (83.7 %), indicating that the merocyanine group is located in the polar region of phospholipid membrane. On the other hand, in the case of M7Sp, the k_{fast} species was predominant (83.6 %), indicating that the merocyanine group is located in the hydrophobic region of lipid membrane. Although the affinity of M7Sp for phospholipid membrane was lower than that of M4Sp, the merocyanine group of M7Sp was found to reside in the hydrophobic core region of lipid bilayer membrane. It is therefore concluded that the location of the merocyanine group in lipid membrane is determined by the interaction between the peptide moiety and the phospholipid membrane.

Maximum Absorption Wavelength of Merocyanine Group in DPPC Vesicles

Spectral changes with time of M4Sp and M7Sp under UV-light irradiation are shown in Figure 3. The absorption due to merocyanine group of M4Sp increased the intensity and underwent a blue shift. The blue shift of M4Sp from 575 nm to 565 nm suggests that the location of the merocyanine group in the lipid membrane changed from the hydrophobic core region of lipid bilayer membrane toward the hydrophilic membrane surface due to increased hydrophilicity upon UV-light irradiation. On the other hand, M7Sp increased the intensity of

maximum absorption with very little shift upon UV-light irradiation. Since about 60 % of M7Sp taking a merocyanine form stayed in aqueous phase (Table 1), the contribution of this fraction dominates over the absorption spectra, resulting in very little shift of maximum absorption.

Leakage of CF Entrapped in DPPC Vesicles

The effect of photo-isomerization of spiropyran group on the interaction of the spiropyran-carrying peptide with phospholipid membrane was examined by CF leakage from DPPC vesicles. The experimental results are shown in Figure 4. UV-light irradiation did not influence CF leakage by the M1Sp addition, which did not bind to the membrane. M4Sp taking a spiropyran form did not influence the leakage so much, although most of the peptides added were distributed to the membrane. However, a drastic increase of CF leakage was observed upon UV-light irradiation, and it slowed down by visible-light irradiation. On the other hand, the addition of M7Sp taking a spiropyran form induced a significant CF leakage, which was slowed down by UV-light irradiation. These results can be explained as follows. The spiropyran group of M4Sp is converted to a zwitterionic merocyanine group upon UV-light irradiation, and an amphiphilic property of M4Sp is strengthened. Amphiphilic peptides disturb the membrane structure resulting in enhancement of CF leakage [34]. M7Sp possesses strong amphiphilicity in spiropyran form, and the distribution of M7Sp disturbs the membrane structure significantly. However, upon UV-light irradiation, the fraction of M7Sp bound to the membrane was reduced to half that before irradiation as described before, resulting in the suppression of the CF leakage. These results demonstrate the photocontrol of peptide activity on phospholipid membrane using a nonnatural amino acid, Glu(OSp).

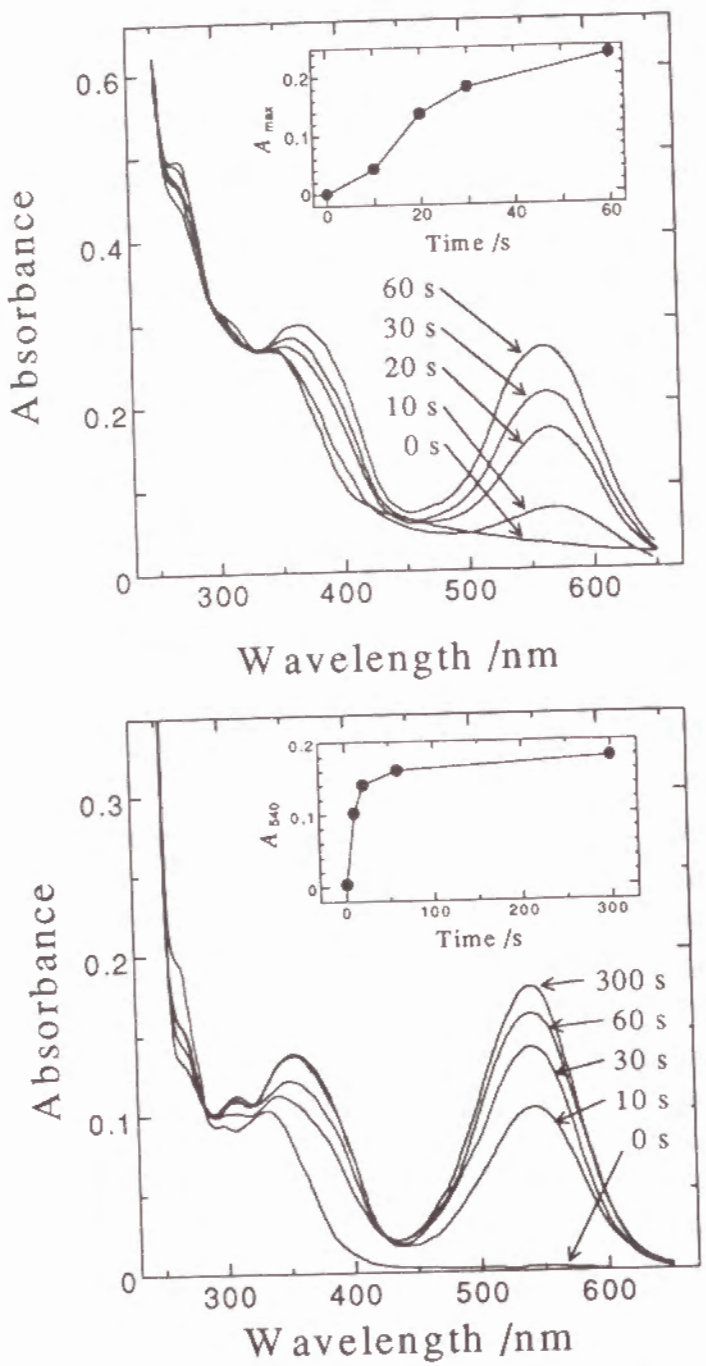

Figure 3. Absorption spectra under UV-light irradiation of M4Sp (a) and M7Sp (b) in the presence of DPPC vesicles. [peptide] = 8.5 μM. [DPPC] = 0.64 mM.

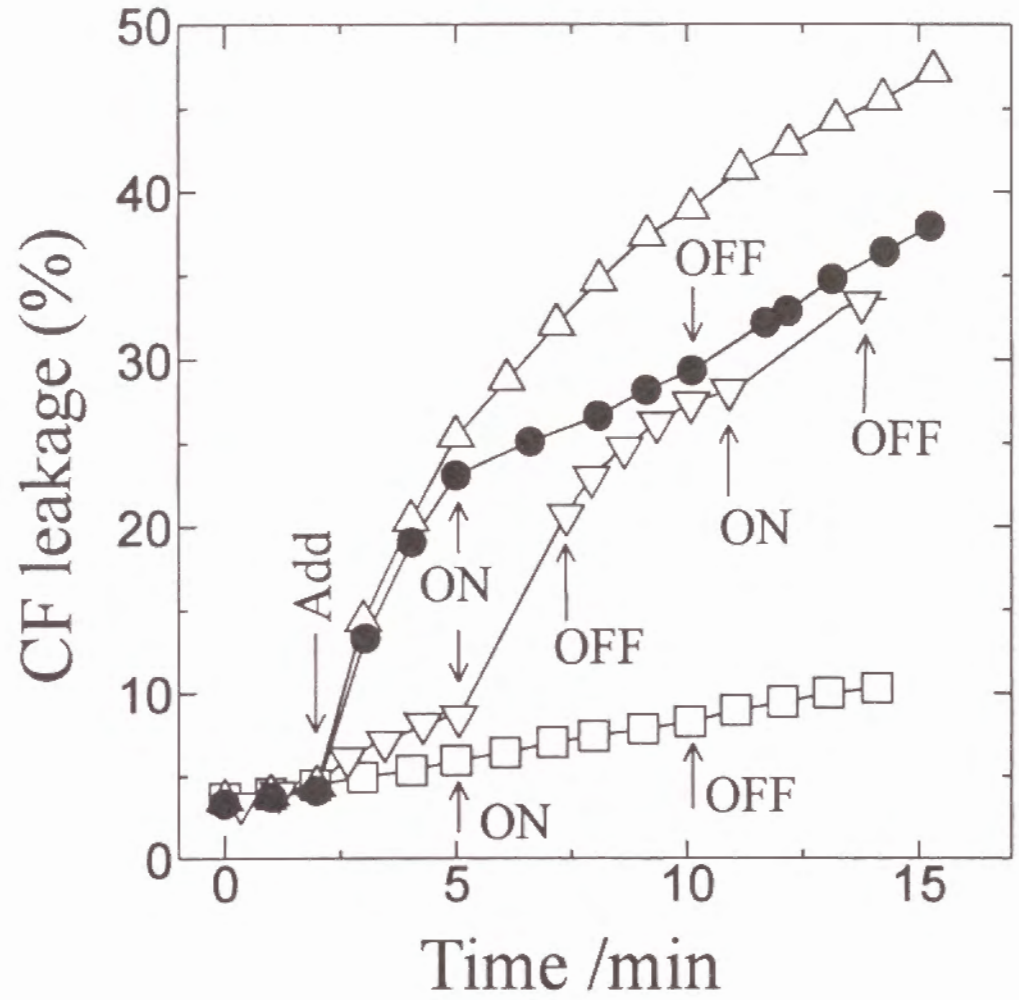

Figure 4. CF leakage from DPPC vesicles induced by the addition of M1Sp (□), M4Sp (▽), and M7Sp (●). Arrows of Add, ON, and OFF represent the addition of the peptide, UV-light irradiation, and visible-light irradiation, respectively. (△) represents the effect of M7Sp addition without UV-light irradiation. [DPPC] = 60 μM. [peptide] = 0.2 μM. Temperature = 25 °C.

Discussion

Melittin 1-7 fragment with Glu(OSp) at the 4th position and a fully protected melittin 4-7 fragment with Glu(OSp) at the N-terminal position were synthesized. It was shown that thermal isomerization from merocyanine to spiropyran form sensitively probes the nature of the microenvironment of the merocyanine group in the lipid membrane. The membrane affinity of M4Sp was higher than M7Sp due to hydrophobic property of the former, but the location of the merocyanine group of M7Sp was close to the core of membrane than that of M4Sp. This observation indicates that melittin 1-7 sequence plays an important role in incorporation of melittin into phospholipid membrane.

Merocyanine is a zwitterionic molecule produced by the ring-opening isomerization of spiropyran, which leads to different interactions of the peptide with phospholipid membrane. Although the charge effect on the interaction cannot be neglected, merocyanine-carrying peptides retain the property of unmodified peptides for lipid membrane as shown in the Results section. Therefore, merocyanine-carrying peptides are very useful for investigation of interactions between peptides and phospholipid membrane.

References

1. D. F. Sargent and R. Schwyzer, *Proc. Natl. Acad. Sci. U.S.A.*, 1986, **83**, 5774.
2. R. Schwyzer, *Biochemistry*, 1986, **25**, 6335.
3. A. Uemura, S. Kimura and Y. Imanishi, *Biochim. Biophys. Acta*, 1983, **729**, 28.
4. A. Chattopadhyay and E. London, *Biochemistry*, 1987, **26**, 39.
5. H.-U. Gremlich, H.-P. Fringeli and R. Schwyzer, *Biochemistry*, 1983, **22**, 4257.
6. F. Macquaire, F. Baleux, E. Giaccobi, T. Huynh-Dinh, J.-M. Neumann and A. Sanson, *Biochemistry*, 1992, **31**, 2576.
7. D. Papahadjopoulos, M. Moscarello, E. H. Eylar and T. Isac, *Biochim. Biophys. Acta*, 1975, **401**, 317.
8. B. Gysin and R. Schwyzer, *Arch. Biochem. Biophys.*, 1983, **225**, 467.
9. R. B. Gennis, *"Biomembranes,"* 1989, Springer Verlag, New York, pp. 166-198.
10. T. Seki and K. Ichimura, *J. Colloid Interface Sci.*, 1989, **129**, 353.
11. E. Habermann, *Science*, 1972, **177**, 314.
12. K. S. Birdi, *J. Colloid Interface Sci.*, 1973, **43**, 545.
13. K. S. Birdi, *J. Colloid Interface Sci.*, 1976, **57**, 228.
14. K. S. Birdi and A. Nikolov, *J. Phys. Chem.*, 1979, **83**, 365.
15. K. S. Birdi, V. S. Grevod, O. S. Ksenzhek, E. H. Stenby and K. L. Rasmussen, *Colloid Polym. Sci.*, 1983, **261**, 767.
16. P. Schoch and D. F. Sargen, *Biochim. Biophys. Acta*, 1980, **60**, 234.
17. M. T. Tosteson and D. C. Tosteson, *Biophys. J.*, 1981, **36**, 109.
18. W. F. Degrado, G. F. Musso, M. Lieber, E. T. Kaiser and F. J. Kezdy, *Biophys. J.*, 1982, **37**, 329.
19. S. Georghious, M. Thompson and A. K. Mukhopadhyay, *Biochim. Biophys. Acta*, 1982, **688**, 441.
20. G. Sessa, J. H. Freer, G. Colacicco and G. Weissman, *J. Biol. Chem.*, 1969, **244**, 3575.
21. J. C. Williams and R. M. Bell, *Biochim. Biophys. Acta*, 1972, **288**, 255.

22. S. P. Verma, D. F. Hoelzl Wallach and I. C. P. Smith, *Biochim. Biophys. Acta*, 1974, **345**, 129.
23. C. Mollay and G. Kreil, *Biochim. Biophys. Acta*, 1973, **316**, 196.
24. C. Mollay and G. Kreil, *FEBS Lett.*, 1974, **46**, 141.
25. J. Schulze, U. Mischeck, S. Wigand and H.-J. Galla, *Biochim. Biophys. Acta*, 1987, **901**, 101.
26. H. Vogel, *Biochemistry*, 1987, **26**, 4562.
27. E. Schroeder, K. Suebke, M. Lehmann and I. Seetz, *Experientia*, 1971, **27**, 764.
28. C. R. Dawson, A. F. Drake, J. Helliwell and R. C. Hilder, *Biochim. Biophys. Acta*, 1978, **510**, 75.
29. E. Habermann and H. Kowallek, *Hoppe-Seyler's Z. Physiol. Chem.*, 1970, **351**, 884.
30. P. H. Vandewyer, J. Hoefnogels and G. Smets, *Tetrahedron*, 1969, **25**, 3251.
31. S. Namba and S. Suzuki, *Bull. Chem. Soc. Jpn.*, 1975, **36**, 563.
32. E. Knoppel, D. Eisenberg and W. Wickner, *Biochemistry*, 1979, **18**, 4177.
33. J. Barbet, P. Machy, A. Truneh and L. D. Leserman, *Biochim. Biophys. Acta*, 1984, **772**, 347.
34. H. Vogel, F. Jahnig, V. Hoffman and J. Stumpel, *Biochim. Biophys. Acta*, 1983, **733**, 201.

Chapter 6

Photoresponsive Melittin Having a Spiropyran Residue in the Hydrophobic Region of the Sequence

Introduction

Many biologically active peptides are amphiphilic in order to help distribution to the phospholipid bilayer membrane [1]. Melittin is composed of 26 amino acid residues. Among them, 6 residues (21-26) of the C-terminal part are hydrophilic, and most of other residues involved in the N-terminal part are hydrophobic [2]. Melittin disturbs the membrane structure due to the primary amphiphilic α-helical structure [3,4]. It has been proposed that the hydrophobic helical part (residues 1-20) penetrates into the lipid bilayer membrane and the cationic C-terminal part (residues 21-26) is anchored to the surface of the bilayer membrane [5]. Consequently, more than four melittin molecules associate together to form a pore in the membrane, through which water and charged molecules are transported, leading to osmotic cell lysis. Therefore, it is believed that the pore formation due to the hydrophobicity of the N-terminal part is the key step in the melittin activity.

In this chapter, a melittin derivative in which a spiropyran group is introduced into the hydrophobic part of the peptide chain was synthesized. The spiropyran group reversibly isomerizes from a nonpolar spiropyran form to a polar merocyanine form by UV-light irradiation and in the opposite direction thermally or by visible-light irradiation. Several compounds having a spiropyran group have been synthesized for a photoresponsive transport system [6] and

photosensitive enzymes [7-9]. These activity changes are principally based on the polarity change of the spiropyran group. It is expected that the melittin derivative carrying spiropyran group is photoresponsive in the interaction with and in the lysis of phospholipid bilayer membrane.

The spiropyran group was connected to the 3rd residue of melittin. Upon UV-light irradiation, the highly polar zwitterionic merocyanine group is produced and forms a hydrophilic cluster with Lys^{7}, Thr^{10}, and Thr^{11} residues. This situation is illustrated by the helical wheel as shown in Figure 1. The secondary amphiphilic helix tends to stay at the membrane surface in contrast to the primary amphiphilic helix before UV-light irradiation [10]. The different orientations of the peptide in the membrane with and without photoirradiation should lead to different activities.

In order to attain photocontrol of the membrane-perturbation activity of the melittin derivative, the spiropyran group was introduced through an amide linkage at the ε-amino group of Orn^{3} residue. [Orn^{3}(Sp), $\varepsilon^{7,21,23}$-amidinated]melittin (MSp) was prepared by a semisynthetic method. The photoisomerization kinetics and irradiation effects on the membrane-disturbing activity of MSp were investigated.

Experimental

Materials

Melittin extracted from a bee venom was obtained from Sigma Chemical Co., USA. Boc-Gly-OSu, Boc-Ile-OSu, and Boc-Orn-OH were obtained from Kokusan Chemical Works, Ltd., Japan. Sephadex G-25 and G-50 gels were purchased from Pharmacia, Co., Sweden. Other chemicals used were of the highest purity available.

Synthesis

The melittin analogue was synthesized by a semisynthetic method. Scheme 1 summarizes the synthetic route of the melittin derivative.

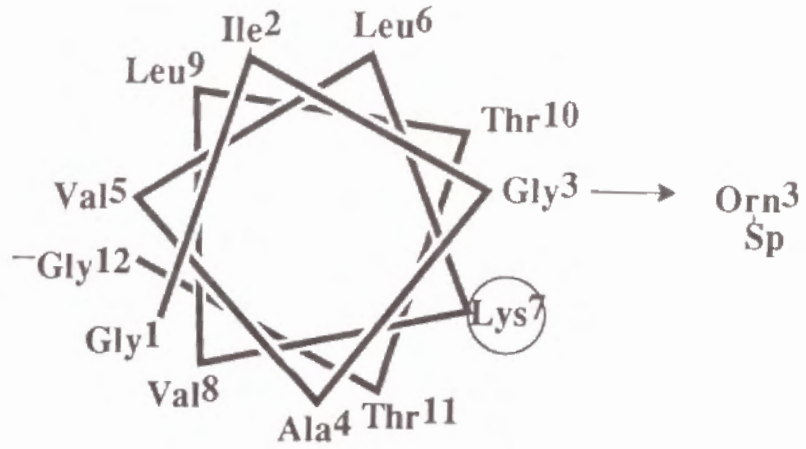

Figure 1. Helical wheel presentation of the N-terminal part of modified melittin. Gly^{3} is replaced by Orn^{3}(Sp). A charged Lys residue is indicated with a circle.

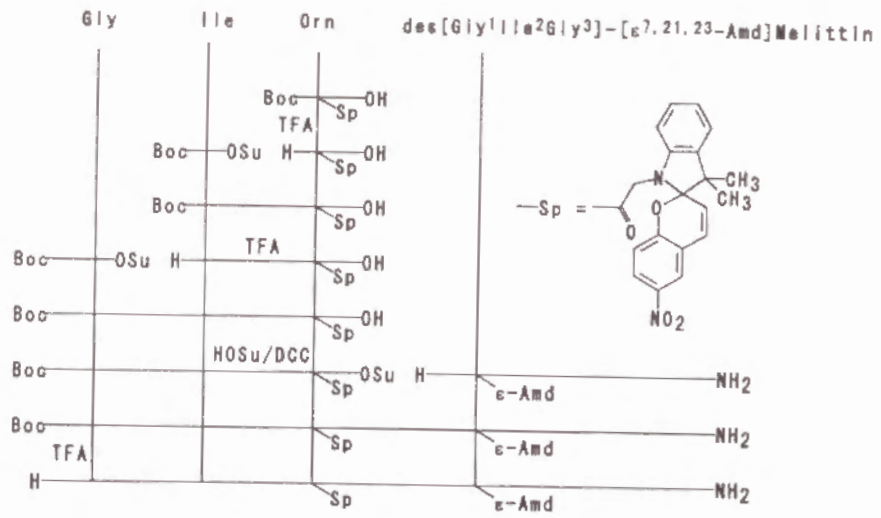

Scheme 1. The semisynthetic method for the preparation of MSp.

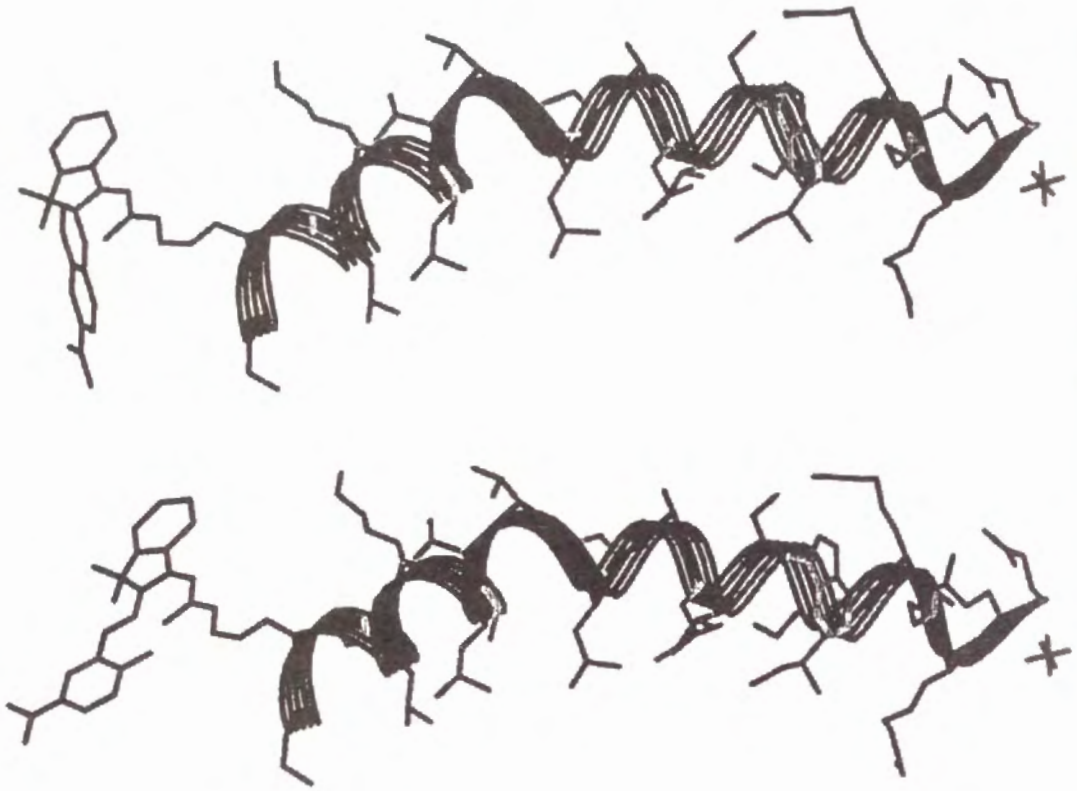

Figure 2. 3D Ribbon drawing of melittin carrying spiropyran in a spiropyran form (top) and in a merocyanine form (bottom). Backbone and side chains are superimposed on the ribbon. Ribbon drawings were created from the X-ray crystallographic data stored in the Protein Data Bank at BNL, USA, by using MAGE Version 2.5.

Boc-Gly-Ile-Orn(Sp)-OH

1-Ethoxycarbonylmethyl-3,3-dimethylindolenium iodide was prepared by the method reported in refs 10 and 11. 2,3,3-Trimethylindolenine (14.8 g) was dissolved in benzene (80 ml) and 2-iodoethyl acetate (20.0 g) was added dropwise. The mixture was refluxed for 3 h at 80 °C. The benzene was

evaporated off under reduced pressure. The obtained oily residue was subjected to a silica gel column (ethyl acetate : methanol = 4:1 as eluent). After the solvent was eliminated by evaporation under reduced pressure, 1-ethoxycarbonyl-3,3-dimethylindolenium iodide was obtained as a red oil, yield 19.27 g (78.3 %). IR (KBr disc); ν_{NH}, 3000 cm^{-1}, $\nu_{C=O}$, 1730 cm^{-1}, $\nu_{C=N}$, 1650 cm^{-1}, $\nu_{C=C}$, 1600 cm^{-1}. NMR (in $CDCl_3$ with tetramethylsilane as the internal standard), δ 1.64 (t, J = 4.32 Hz, 3H, -COO-CH_2-CH_3), 1.72 (s, 6H, 3-CH_3), 1.80 (s, 3H, 2-CH_3), 4.48 (s, 2H, N-CH_2-COO), 4.56 (q, J = 2.88 Hz, 2H, -COO-CH_2-), 7.36 (m, 4H, Ph-H). TLC, R_f = 0.84 (ethyl acetate / methanol = 2:1, v / v), R_f = 0.90 (ethyl acetate / methanol = 4:1, v / v).

1-Ethoxycarbonylmethyl-3,3-dimethyl-6'-nitrospiro[indoline-2,2'-2H-benzopyran] was prepared by the reaction of 1-ethoxycarbonylmethyl-2,3,3-trimethylindolenium iodide (4.52 g) and 5-nitrosalicylaldehyde (2.03 g) dissolved in 2-butanone (27 ml) in the presence of piperidine (1.2 ml) [11,12]. The solution was refluxed for 3 min at 80 °C, followed by standing overnight at room temperature in the dark. The solvent was evaporated off under reduced pressure and the residue was dissolved in small portion of hot methanol. The white precipitate was obtained after gradual cooling of the solution. The precipitate was collected by centrifugation and repeatedly washed with 10 ml of cold methanol. The methanol was removed under reduced pressure and 1-ethoxycarbonylmethyl-3,3-dimethyl-6'-nitrospiro[indoline-2,2'-2H-benzopyran] was obtained as a white solid, yield 1.00 g (21.0 %). NMR (in DMSO-d_6), δ 1.52 (t, J = 4.32 Hz, 3H, -COO-CH_2-CH_3), 1.59 (s, 6H, 3-CH_3), 4.40 (s, 2H, N-CH_2-COO), 4.56 (q, J = 2.88 Hz, 2H, -COO-CH_2-), 6.36 (d, J = 12.96 Hz, 1H,

3'-CH=), 6.96 (d, J = 11.52 Hz, 1H, 4'=CH-), 7.44 (m, 5H, Ph-H), 8.56 (m, 2H, Ph-H). TLC, R_f = 0.81 (chloroform / methanol = 95:5, v / v).

A photochromic compound, 1-hydroxycarbonylmethyl-3,3-dimethyl-6'-nitrospiro[indoline-2,2'-2H-benzopyran] (HOOC-Sp), was prepared by hydrolysis of the ethyl ester with NaOH in dioxane / methanol [11,12]. 1-Ethoxycarbonylmethyl-3,3-dimethyl-6'-nitrospiro[indoline-2,2'-2H-benzopyran] (950 mg) was dissolved in dioxane (8.0 ml) and the same volume of methanol was added slowly. 2 N NaOH solution (2.0 ml) was added dropwise with stirring over a period of 1 h under cooling in water bath. The mixture was transferred on ice. 2.0 N Hydrochloric acid was added slowly with stirring at the temperature below 4 °C and the pH was adjusted to pH 2.0. The solution was poured into ethyl acetate and the precipitate was removed by filtration. The mixture was shaken well and the organic layer was washed with a 10 % aqueous citric acid solution and with concentrated NaCl solution, and dried on anhydrous Na_2SO_4. The solvent was evaporated off and the residue was dried under reduced pressure to obtain a red solid, which was reprecipitated from cold ethyl acetate. The precipitate was recovered by filtration, and dried under reduced pressure, yield 475 mg (54.0 %). NMR (in DMSO-d_6), δ 1.53 (s, 3H, 3-CH$_3$), 1.64 (s, 3H, 3-CH$_3$), 4.25 (s, 2H, N-CH$_2$-COO), 6.31 (d, J = 11.52 Hz, 1H, 3'-CH=), 6.90 (d, J = 7.92 Hz, 1H, 4'-CH=), 7.44 (m, 5H, Ph-H), 8.48 (m, 2H, Ph-H). TLC, R_f = 0.48 (chloroform / methanol / acetic acid = 95:5:1, v / v).

The spiropyran derivative was coupled with HOSu by using DCCD and condensed *in situ* with Boc-Orn-OH to obtain Boc-Orn(Sp)-OH. HOOC-Sp (475 mg, 1.30 mmol) was dissolved in DMF (15 ml), and HOSu (180 mg) and DCCD (322 mg) were added at 0 °C. The reaction mixture was stirred for 24 h. The

precipitated solid was removed by filtration, and the filtrate was mixed with an equimolar solution of Boc-Orn-OH in DMF (20 ml) at the temperature below 4 °C. TEA (236 µl) was added dropwise and stirred for 17 h at 4 °C. The solvent was removed by evaporation under reduced pressure, and the residue was dissolved in ethyl acetate. The solution was washed with 10 % aqueous citric acid solution and with concentrated NaCl solution, and was dried on anhydrous $MgSO_4$. The solution was condensed by evaporation and was purified through a Sephadex LH-20 column using methanol as eluent. After the solvent was evaporated, Boc-Orn(Sp)-OH was obtained as a yellow solid, yield 95.4 mg (12.6 %). NMR (in CD_3OD), δ 1.44 (s, 6H, 3-CH$_3$), 1.60 [s, 9H, -C-(CH$_3$)$_3$], 1.76 (dt, 2H, -NH-CH$_2$-CH$_2$-CH$_2$-), 1.84 (tt, 2H, -NH-CH$_2$-CH$_2$-CH$_2$-), 3.36 (br, 2H, -CO-NH-CH$_2$-CH$_2$-), 3.92 (q, J = 6.48 Hz, 1H, -NH-CH(COOH)-CH$_2$-), 4.24 (s, 2H, N-CH$_2$-COO), 6.16 (d, J = 11.52 Hz, 1H, 3'-CH=), 6.64 (d, J = 8.64 Hz, 1H, 4'-CH=), 7.12 (m, 5H, Ph-H), 8.16 (m, 2H, Ph-H). TLC, R_f = 0.41 (chloroform / methanol / acetic acid = 95:5:1, v / v).

By treatment with TFA (1.0 ml) in the presence of anisole (100 µl) on ice for 30 min, followed by precipitation with diethyl ether, H-Orn(Sp)-OH was obtained as a red solid, yield 60.2 mg (65.3 %).

TEA (0.20 mmol) was added dropwise at 4 °C to a DMF solution containing Boc-Ile-OSu (0.15 mmol) and TFA·H-Orn(Sp)-OH (0.10 mmol), and the solution was stirred for 15 h at room temperature. The product was purified through a Sephadex LH20 column using methanol as eluent, yield 33.8 mg (48.1 %). NMR (in CD_3OD), δ 1.09 (d, 3H, γ'-CH$_3$(Ile)), 1.09 [s, 3H, δ-CH$_3$(Ile)], 1.48 (s, 6H, 3-CH$_3$), 1.63 [s, 9H,

-C-(CH_3)$_3$], 1.84 [m, 8H, -NH-CH_2-CH_2-CH_2-, β-CH_2(Ile), γ-CH_2(Ile)], 3.44 (br, 2H, -CO-NH-CH_2-CH_2-), 3.84 (s, 2H, N-CH_2-COO), 3.92 [q, J = 6.48 Hz, 1H, α-CH(Ile)], 4.48 (q, J = 6.48 Hz, 1H, α-CH(Orn)), 6.16 (d, J = 11.52 Hz, 1H, 3'-CH=), 6.64 (d, J = 8.64 Hz, 1H, 4'-CH=), 7.12 (m, 5H, Ph-H), 8.16 (m, 2H, Ph-H). TLC, R_f = 0.28 (chloroform / methanol / acetic acid = 95:5:1, v / v). The dipeptide was treated with TFA and precipitated by the addition of diethyl ether. TFA·H-Ile-Orn(OSp)-OH was obtained as a red solid, yield, 22.0 mg (63.7 %).

The dipeptide was coupled with Boc-Gly-OSu (0.048 mmol) in the same way as for the coupling of Boc-Ile-OSu with H-Orn(Sp)-OH. Boc-Gly-Ile-Orn(OSp)-OH was obtained as a red solid, yield 16.6 mg (71.2 %). NMR (in CD_3OD), δ 1.09 [d, 3H, γ'-CH_3(Ile)], 1.09 [s, 3H, δ-CH_3(Ile)], 1.48 (s, 6H, 3-CH_3), 1.63 [s, 9H, -C-(CH_3)$_3$], 1.84 [m, 8H, -NH-CH_2-CH_2-CH_2-, β-CH_2(Ile), γ-CH_2(Ile)], 3.44 (br, 2H, -CO-NH-CH_2-CH_2-), 3.84 (s, 2H, N-CH_2-COO), 3.92 [q, J = 6.48 Hz, 1H, α-CH(Ile)], 4.00 [q, J = 6.48 Hz, 2H, α -CH_2(Gly)], 4.48 [q, J = 6.48 Hz, 1H, α -CH(Orn)], 6.16 (d, J = 11.52 Hz, 1H, 3'-CH=), 6.64 (d, J = 8.64 Hz, 1H, 4'-CH=), 7.12 (m, 5H, Ph-H), 8.16 (m, 2H, Ph-H). TLC, R_f = 0.12 (chloroform / methanol / acetic acid = 95:5:1, v / v).

Des[$Gly^1Ile^2Gly^3$]-[$\varepsilon^{7,21,23}$-Amidinated]Melittin

ε-Amino groups of melittin were blocked by the acetimidyl group according to the previously reported method [13]. Melittin was treated with excess amount of methyl acetimidate hydrochloride at pH between 10.1 and 10.5. The reaction mixture was eluted through a Sephadex G-25 column (2.6 x 43 cm) with Tris-HCl buffer (0.1 M, pH 9.4) to remove excess reagents. The pH of the

concentrated solution was adjusted to 6.9 with 1 M hydrochloric acid and the solution was desalted by a Sephadex G-25 column (2.6 x 35 cm). [$\varepsilon^{7,21,23}$-Amidinated]melittin was obtained as a white powder (8.5 mg) after lyophilization. The free amino group of acetimidylmelittin was determined by labelling with TNBS [14]. One amino group remained unblocked, which is assigned to the N-terminal α-amino group.

Acetimidylmelittin was subjected to three cycles of Edman degradation to remove the N-terminal residues Gly^1, Ile^2, and Gly^3 from the peptide chain. The stepwise degradation was checked by the TLC analysis. The degraded peptide was purified with a Sephadex G-50 column. Des[$Gly^1Ile^2Gly^3$]-[$\varepsilon^{7,21,23}$-amidinated]melittin was obtained as a white powder (5.0 mg) after lyophilization.

[Orn^3(Sp)]-[$\varepsilon^{7,21,23}$-Amidinated]Melittin (MSp)

The tripeptide, Boc-Gly-Ile-Orn(Sp)-OH, was reacted with des[$Gly^1Ile^2Gly^3$]-[$\varepsilon^{7,21,23}$-amidinated]melittin (2.0 mg) by using DCCD (1.5 eq. mol) and HOBt (1.5 eq. mol) as coupling reagents. The product was eluted through a Sephadex LH-20 column with DMF (5 cm×100 cm). The Boc group was removed by treatment with TFA, and the product was precipitated with diethyl ether. The solid product was further purified by a reverse-phase HPLC (Cosmosil 5C_{18} column, acetonitrile / water). After lyophilization, [Orn^3(Sp)]-[$\varepsilon^{7,21,23}$-amidinated]melittin was obtained as a red powder, yield 1.2 mg (53.1 %). Figure 2 shows schematic drawings of mutant melittin molecules.

Spectroscopic Measurements

UV- and visible-absorption spectra were recorded on a Jasco Ubest-50 UV / Vis spectrophotometer with a cell of 1-cm optical path length. Circular dichroism spectra were measured on a Jasco J-600 CD spectropolarimeter with a cell of 0.1-cm optical path length. NMR spectra were recorded on Jusco FX-90Q NMR spectrometer.

Thermal Isomerization Kinetics

Thermal decoloration rates were determined by monitoring the decrease of absorbance at the absorption maximum (λ_{max}) of merocyanine group. UV(310 nm < λ < 360 nm)- and visible(500 nm < λ)-light irradiations were performed by using 100-W high-pressure mercury lamp and glass filters.

The decay curves were analyzed by equation (1),

$$\frac{A_t - A_{\inf}}{A_0 - A_{\inf}} = F\exp(-k_{\text{fast}}t) + (1-F)\exp(-k_{\text{slow}}t) \qquad (1)$$

where A_t, A_0, and $A_{\inf}$ are the absorbance at λ_{max} at time t, zero, and infinity, respectively, and F and 1-F are the fractions of k_{fast} and k_{slow} components, respectively.

Vesicle Preparation

DPPC vesicles encapsulating CF were prepared by a sonication method [14]. Hepes buffer (10 mM, pH 7.4, with 100 mM NaCl, 0.67 ml) and an aqueous CF solution (130 mM, 2.0 ml) were added to dry DPPC (25 mg), and the mixture

was sonicated using a bath-type sonicator (40 W) at 50 °C under an N_2 atmosphere. The suspension was centrifuged at 100000 g for 30 min at 45 °C to obtain SUV encapsulating CF in the supernatant. This suspension was subjected to gel filtration on a Sephadex G-50 superfine column (1×25 cm) using Hepes buffer (10 mM, pH 7.4, with 100 mM NaCl) as eluent. The DPPC vesicles without CF were prepared in otherwise the same way as that for the CF-containing DPPC vesicles using Hepes buffer without CF.

CF Leakage

MSp was added to the CF-encapsulated DPPC vesicle at 25 °C and the fluorescence intensity at 515 nm (F) was measured. The excitation wavelength was 470 nm. The fluorescence intensity without MSp (F_0) was determined by the addition of water. Maximal leakage was attained by addition of Triton X-100 (F_{Triton}), which disrupts vesicular structure. The percentage of CF leakage was calculated by equation (2).

$$\text{Leakage}(L\%) = 100 \times \frac{F - F_0}{F_{\text{Triton}} - F_0} \qquad (2)$$

The leakage rates were calculated by 1 / (100 - L) dL / dt from the time course of the leakage. When MSp was irradiated by UV light for 10 min and was added to the CF-containing DPPC vesicles, the curve of the leakage rate was fitted to a two-component exponential function (3), with $G_1 < 0$ and $G_2 > 0$ (see Appendix).

$$\frac{1}{100-L}\frac{\mathrm{d}L}{\mathrm{d}t} = G_1 \exp(-k_{\mathrm{acc}}t) + G_2 \exp(-k_{\mathrm{dec}}t) \quad (3)$$

The notations of k_{acc} and k_{dec} will be described in the text subsequently.

Results

Thermal Decoloration of MSp

MSp exhibited photochromism either in an organic solution or in a lipid membrane. The colorless solution turned blue or violet upon UV-light irradiation, and the colored solution was faded thermally or by visible-light irradiation. The thermal decay of the merocyanine form of MSp was monitored by the absorbance at λ_{max} (λ > 500 nm), and analyzed in terms of the two-exponential process. The rate constants and the fractions of two components are summarized in Table 1. The thermal isomerization rate from merocyanine to spiropyran is strongly dependent on the medium polarity [15]. Two components in the decay were ascribed to two conformers of merocyanine, in which the slow component is stabilized in a polar environment and the fast one in an apolar environment [16]. The higher fraction of the slow component than the fast component suggests that the merocyanine group is located at the polar surface of lipid membrane. This consideration is supported by the fact that the merocyanine group absorbs at a shorter wavelength (533 nm) in the lipid membrane [13].

Table 1. Kinetic constants and preexponential factors of the thermal decay of the merocyanine group of MSp in the presence of DPPC vesicles.

	Slow component		Fast component	
Temp.	Factor	k_{slow}	Factor	k_{fast}
15 °C	0.15 (65 %)	6.6×10^{-4}	0.08 (35 %)	5.4×10^{-3}
25 °C	0.28 (82 %)	3.2×10^{-3}	0.06 (18 %)	2.5×10^{-2}
35 °C	0.61 (97 %)	4.1×10^{-3}	0.02 (3 %)	5.9×10^{-2}

CF Leakage Induced by MSp

The activity of MSp in a membrane was studied by CF leakage from DPPC vesicles. A simple exponential leakage of entrapped CF was observed when MSp was added to the vesicles (Figure 3). In this case, the kinetic constant, k_{obs} = 1 / (L_{inf}-L) dL / dt (L and L_{inf} represent CF leakage at time t and infinity), was nearly constant until 80 % CF-leakage (Figure 3). When UV light was irradiated for 90 s after addition of the melittin derivative, about 8-fold increase of k_{obs} was observed immediately after the irradiation (Figure 3).

To estimate precisely the effect of UV-light irradiation on CF leakage, CF leakage was measured at 15, 25, and 35 °C in the presence of preirradiated (10 min) MSp (Figure 4). If CF leakage is accelerated by MSp in the spiropyran form, accumulation of MSp in the spiropyran form in lipid membrane should cause a simple exponential acceleration of k_{obs}, because the amount of MSp in the membrane increases in an exponential way. On the other hand, if CF leakage is accelerated by the merocyanine form of MSp, k_{obs} should show a two-component

exponential change consisting of acceleration (k_{acc}) and deceleration (k_{dec}), representing binding of the merocyanine-type MSp and its thermal isomerization, respectively. As shown in Figure 4, k_{obs} was initially accelerated and followed by deceleration, indicating that MSp in the merocyanine form disturbs the membrane structure more significantly than MSp in the spiropyran form.

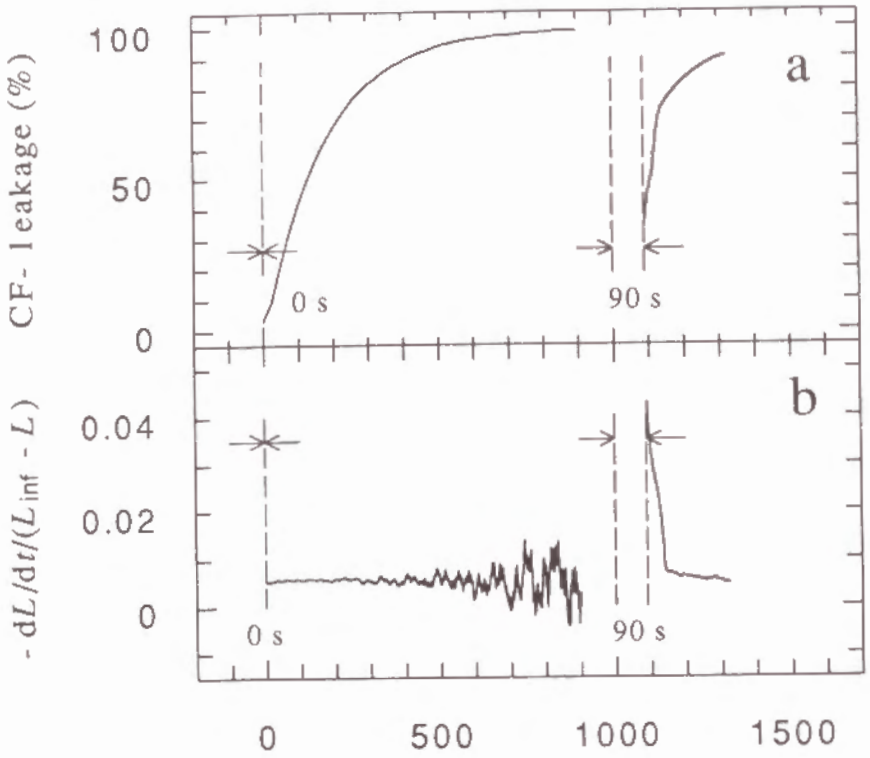

Figure 3. CF leakage from DPPC vesicles induced by MSp at 15 °C. **a**: the percentage of CF leaked from the vesicles. **b**: the rate constant of CF leakage. dL / dt was calculated by numerical differentiation of the experimental data. Left: without UV-light irradiation. Right: UV-light irradiation for 90 s.

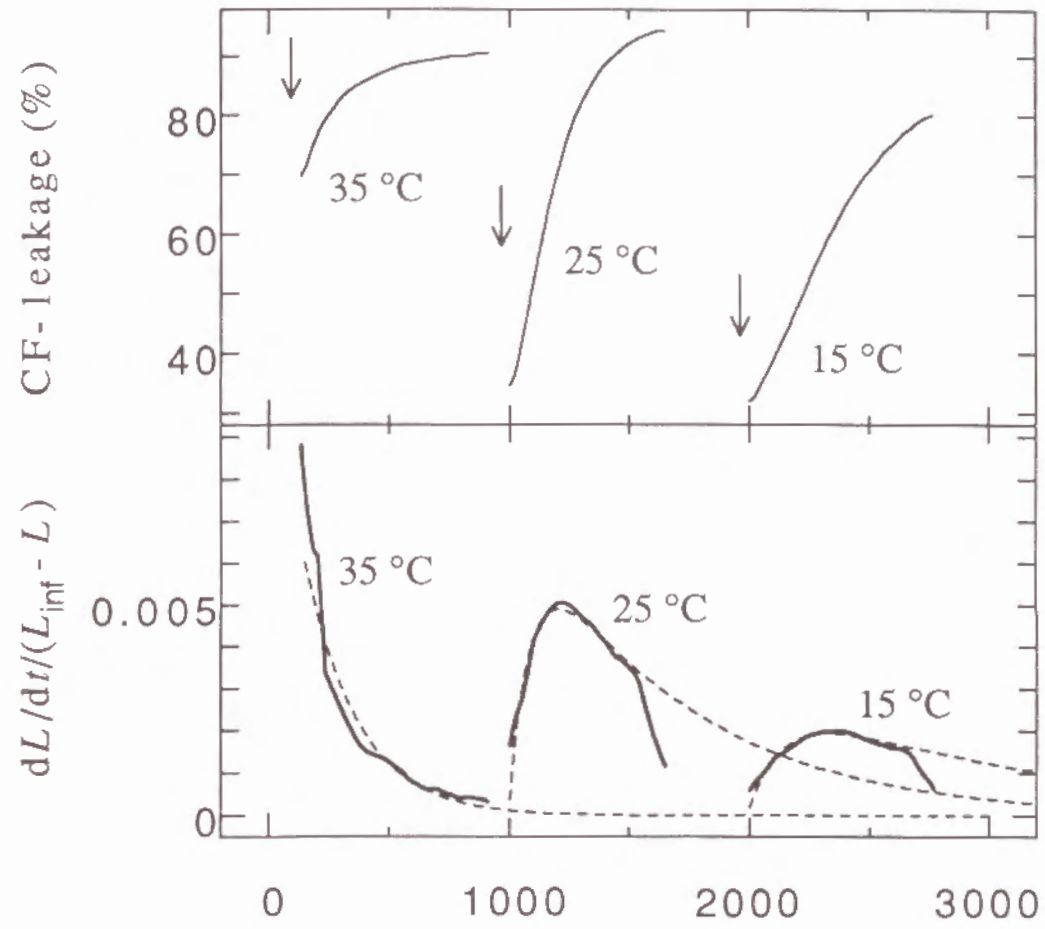

Figure 4. CF leakage from DPPC vesicles induced by adding preirradiated (10 min) MSp. Broken lines were obtained by the bicomponent exponential fitting. Arrows indicate addition of MSp.

The curve of the CF-leakage rate was fitted by a two-component exponential function. The fractions of the acceleration and deceleration processes are nearly the same as shown in Table 2.

Table 2. Kinetic constants and preexponential factors of CF leakage induced by the addition of MSp.

	Acceleration process		Deceleration process	
Temp.	G_1	k_{acc}	G_2	k_{dec}
15 °C	-0.027 (48 %)	7.1×10^{-3}	0.029 (52 %)	8.4×10^{-4}
25 °C	-0.072 (49 %)	1.1×10^{-2}	0.076 (51 %)	1.4×10^{-3}
35 °C	-0.097 (45 %)	4.5×10^{-2}	0.119 (55 %)	4.6×10^{-3}

Discussion

The experimental results above described are explained in terms of the kinetic scheme shown in Figure 5.

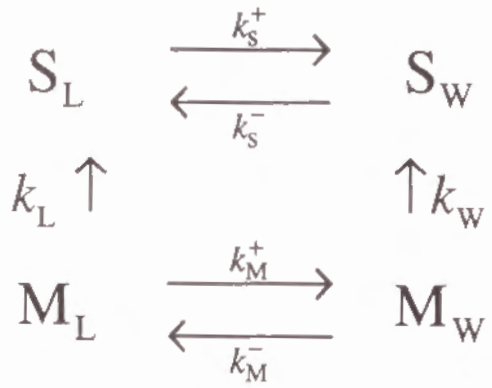

Figure 5. Thermal decoloration pathways of MSp in the presence of vesicles. The subscripts L and W represent the lipid membrane phase and the aqueous phase, respectively. S and M represent MSp in the form of spiropyran and merocyanine, respectively.

The kinetic scheme predicts that the preexponential factor of the acceleration process (binding of M_W to the membrane resulting in an increase of M_L) becomes the same as that of the deceleration process (thermal isomerization of M_L to S_L resulting in a decrease of M_L) under the condition that MSp, taking a merocyanine form in lipid membrane, is the predominant process responsible for the CF leakage. The validity of this belief is confirmed by the agreement of the kinetic constants between the slow component of the thermal decay (Table 1) and the deceleration process of the CF leakage (Table 2) at all temperatures. The result is consistent with the molecular design described in the introduction. The merocyanine-type MSp takes the secondary amphiphilic α-helical structure due to alignment of the hydrophilic residues, Orn^3 (Sp), Lys^7, Thr^{10}, and Thr^{11} residues localized at one surface of the helix peptide, which should disturb the membrane structure severely.

Appendix

A model for the decoloration process of merocyanine to spiropyran can be represented by the scheme below left. Concentrations of spiropyran and merocyanine are expressed by equations (4),

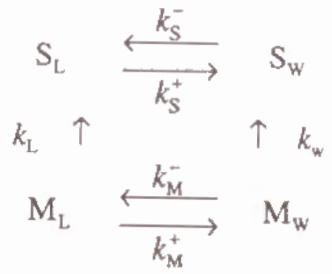

$$V_L \frac{d}{dt} S_L = -k_S^+ S_L + k_S^- S_W + k_L M_L$$
$$V_W \frac{d}{dt} S_W = -k_S^- S_W + k_S^+ S_L + k_W M_W$$
$$V_L \frac{d}{dt} M_L = -(k_L + k_M^+) M_L + k_M^- M_W$$
$$V_W \frac{d}{dt} M_W = -(k_W + k_M^-) M_W + k_M^+ M_L \qquad (4)$$

V_L and V_W are the volume of lipid-membrane phase and water phase, respectively. Since M_L and M_W are independent of S_L and S_W, equation (5) obtains,

$$M_L = \frac{1}{\beta-\alpha}\left\{\left[\left(\beta+\frac{k_L+k_M^+}{V_L}\right)M_L^0-\frac{k_M^-}{V_L}M_W^0\right]e^{\alpha t}+\left[\frac{k_M^-}{V_L}M_W^0-\left(\alpha+\frac{k_L+k_M^+}{V_L}\right)M_L^0\right]e^{\beta t}\right\}$$
$$M_W = \frac{1}{\beta-\alpha}\left\{\left[\left(\beta+\frac{k_W+k_M^-}{V_W}\right)M_W^0-\frac{k_M^+}{V_W}M_L^0\right]e^{\alpha t}+\left[\frac{k_M^+}{V_W}M_L^0-\left(\alpha+\frac{k_W+k_M^-}{V_W}\right)M_W^0\right]e^{\beta t}\right\} \quad (5)$$

where α and β ($\alpha > \beta$) are the solutions of a quadratic equation (6).

$$\lambda^2+\left(\frac{k_L+k_M^+}{V_L}+\frac{k_W+k_M^-}{V_W}\right)\lambda+\left(\frac{k_L+k_M^+}{V_L}\right)\left(\frac{k_W+k_M^-}{V_W}\right)-\frac{k_M^+k_M^-}{V_LV_W}=0 \quad (6)$$

Both α and β are negative, and α is not equal to β, meaning that M_L and M_W are composed of two different components of exponential decay. The total concentration of merocyanine M, is a weighed sum of M_L and M_W, so that it is expressed simply by equation (7).

$$M = \frac{V_LM_L+V_WM_W}{V_L+V_W}$$
$$= \frac{(V_L\alpha+k_L)M_L^0+(V_W\alpha+k_W)M_W^0}{(V_L+V_W)(\alpha-\beta)}e^{\beta t}-\frac{(V_L\beta+k_L)M_L^0+(V_W\beta+k_W)M_W^0}{(V_L+V_W)(\alpha-\beta)}e^{\alpha t} \quad (7)$$

The equation (7) means that the spectroscopically observed decay of merocyanine is expressed as a sum of two exponential decays. Especially in the case that the dye molecule is added after a sufficient irradiation, M_L is 0 at $t = 0$, and equation (8) obtains.

$$M_L = \frac{1}{\beta-\alpha}\frac{k_M^-}{V_L}M_W^0\left(e^{\beta t}-e^{\alpha t}\right)$$
$$M_W = \frac{1}{\beta-\alpha}M_W^0\left[\left(\beta+\frac{k_W+k_M^-}{V_W}\right)e^{\alpha t}-\left(\alpha+\frac{k_W+k_M^-}{V_W}\right)e^{\beta t}\right]$$
$$M = \frac{1}{\beta-\alpha}\frac{V_WM_W^0}{V_L+V_W}\left[\left(\beta+\frac{k_W}{V_W}\right)e^{\alpha t}-\left(\alpha+\frac{k_W}{V_W}\right)e^{\beta t}\right] \quad (8)$$

In these equations, the absolute values of preexponential factor for $e^{\beta t}$ and that for $e^{\alpha t}$ are exactly the same only for M_L, but they are different for others, M_W and M, because α is not equal to β. Under the same condition, concentration of spiropyran species, S_L and S_W, can be represented by equations (9) and (10), respectively, which involve preexponential factors for $e^{\beta t}$ and $e^{\alpha t}$ of different values.

$$S_L = \frac{M_W^0}{(\beta-\alpha)(V_Lk_S^-+V_Wk_S^+)}\left\{\left[\frac{1}{V_L\left(\alpha+\frac{k_S^+}{V_L}+\frac{k_S^-}{V_W}\right)}\left\{k_S^-k_WV_L(V_W\beta+k_W+k_M^-)+k_M^-k_S^+k_LV_W\right\}\right.\right.$$
$$\left.-\frac{k_S^-}{\alpha}\left\{k_WV_W\beta+k_W(k_W+k_M^-)-k_Lk_M^-\right\}\right](1-e^{\alpha t})$$
$$-\left[\frac{1}{V_L\left(\beta+\frac{k_S^+}{V_L}+\frac{k_S^-}{V_W}\right)}\left\{k_S^-k_WV_L(V_W\alpha+k_W+k_M^-)+k_M^-k_S^+k_LV_W\right\}\right.$$
$$\left.\left.-\frac{k_S^-}{\beta}\left\{k_WV_W\alpha+k_W(k_W+k_M^-)-k_Lk_M^-\right\}\right](1-e^{\beta t})\right\} \quad (9)$$

$$S_W = \frac{M_W^0}{(\beta-\alpha)(V_L k_S^- + V_W k_S^+)} \left[\left\{ k_W V_L (V_W \beta + k_W + k_M^-) + \frac{k_S^+}{k_S^-} k_M^- k_L V_W \right\} \frac{1-e^{\alpha}}{\alpha + \frac{k_S^+}{V_L} + \frac{k_S^-}{V_W}} \right.$$

$$\left. - \left\{ \frac{k_S^+}{k_S^-} k_M^- k_L V_W + k_W V_L (V_W \alpha + k_W + k_M^-) \right\} \frac{1-e^{\beta t}}{\beta + \frac{k_S^+}{V_L} + \frac{k_S^-}{V_W}} \right] \quad (10)$$

Taking these results into consideration, it is concluded that when a spectroscopic analysis shows a two-component-type decay with preexponential factors of exactly the same absolute value, the process is controlled by the M_L component, the decay process of merocyanine in a lipid membrane.

References

1. Y. Imanishi and S. Kimura, *Proc. Japan Acad., Ser. B,* 1992, **68**, 121.
2. F. C. Olson, D. Munjal and A. N. Malviya, *Toxicon*, 1974, **12**, 419.
3. S. P. Verma, D. F. Hoelzl Wallach and I. C. P. Smith, *Biochim. Biophys. Acta*, 1974, **345**, 129.
4. C. E. Dempsey, *Biochim. Biophys. Acta*, 1990, **1031**, 143.
5. H. Vogel, and F. Jahnig, *Biophys. J.*, 1986, **50**, 573.
6. J. Sunamoto, K. Iwamoto, Y. Mohri and T. Kominato, *J. Am. Chem. Soc.*, 1982, **104**, 5502.
7. K. Namba and S. Suzuki, *Chem. Lett.*, 1975, 947.
8. I. Karube, Y. Nakamoto, K. Namba and S. Suzuki, *Biochim. Biophys. Acta*, 1976, **429**, 975.
9. I. Karube, Y. Nakamoto and S. Suzuki, *Biochim. Biophys. Acta*, 1976, **445**, 774.
10. R. Schwyzer, *Biochemistry*, 1986, **25**, 6335.
11. P. H. Vandewyer, J. Hoefnogels and G. Smets, *Tetrahedron*, 1969, **25**, 3251.
12. S. Namba and S. Suzuki, *Bull. Chem. Soc. Jpn.*, 1975, **36**, 563.
13. G. Corradin and H. A. Harbury, *Proc. Natl. Acad. Sci. USA*, 1971, **68**, 3036.
14. J. Barbet, P. Machy, A. Truneh and L. D. Leserman, *Biochim. Biophys. Acta*, 1984, **772**, 347.
15. T. Seki and K. Ichimura, *J. Colloid Interface Sci.*, 1989, **129**, 353.
16. T. Ueda, E. Kato, S. Kimura and Y. Imanishi, *Biophys. Chem.*, 1994, **49**, 215

ABSTRACT

PART I IMPROVEMENT AND PHOTOCONTROL OF PROTEIN ACTIVITY BY INCORPORATION OF NONNATURAL AMINO ACIDS

Chapter 1 Biosynthesis of Mutant β-D-Galactosidases Containing Nonnatural Aromatic Amino Acids by *Esherichia coli*

Mutant β-D-galactosidases containing nonnatural aromatic amino acids (napAla, antAla, or pyrAla) were produced by misincorporation during protein overproduction by *E. coli*. It was shown that pyrAla was incorporated into β-D-galactosidase, and that the thermostability of the mutant enzyme increased. The incorporation frequency was not so high in all cases, and there was a difficulty in isolation of the mutant protein. It was, however, notable that such bulky pendant groups can be incorporated into the protein by inducing the protein overproduction state. Improved thermostability of the mutant enzyme indicates potential utility of the misacylation technique to be applicable for fermentation industries.

Chapter 2 Semisynthesis of Mutant Cytochromes *c* Replaced by Nonnatural Aromatic Amino Acid at Phe^{82} and Photoregulation of Reduction Reaction with 2-Mercaptoethanol

Mutant cytochromes *c*, PGL-Cytc and PYR-Cytc, were synthesized by a semisynthetic method. Redox compounds are more accessible to the heme

region of the mutant protein than that of native protein, and the electron transfer reaction of the mutant cytochrome *c* was photosensitive. CD measurements revealed that PGL-Cytc nearly retained the tertiary structure of the native cytochrome *c*, while PYR-Cytc did not. The reduction reaction of PGL-Cytc with 2-mercaptoethanol was retarded compared with that of the native cytochrome *c*. On the other hand, PYR-Cytc was easily reduced with 2-mercaptoethanol, probably due to structural changes around the heme moiety and interaction of the pyrenyl group with the heme. Excitation of the pyrenyl group of PYR-Cytc upon UV irradiation suppressed the reduction reaction strongly. This is ascribed to the occurrence of oxidation reaction from ferrous to ferric heme through photosensitization of the pyrenyl group. This is the first demonstration of photosensitive cytochrome *c*.

Chapter 3 Destabilization of the Heme Region in Mutant Cytochrome *c* by Replacement of Phe^{82} with 3-(1-Pyrenyl)-L-alanine

Using a semisynthetic method, mutant cytochromes *c*, in which pyrAla or pheGly replaced a conserved Phe^{82} residue located near the heme, were produced. The pyrAla residue in the reduced state of the mutant cytochrome *c* was shielded from the access of acrylamide in the aqueous phase, while it was exposed to acrylamide in the oxidized state. The denaturation profile of the mutant protein induced by the addition of GdnHCl was the same as that of the native cytochrome *c*. Therefore, the hydrophobic heme pocket should retain the native structure in terms of accessibility of acrylamide and GdnHCl. However, thermal denaturation of PYR-Cytc showed that the deformation of the heme region occurred at 54 °C, which was lower than 64 °C of the native one.

Thermodynamic analysis revealed that the heme pocket was stabilized by hydrophobic effect of pyrAla. However, the hydrophobic stabilization was overwhelmed by a large entropy change upon denaturation, resulting in destabilization of the heme region. PGL-Cytc, in which the phenyl group is dislocated by one methylene unit from the native cytochrome *c*, was also destabilized in the heme region compared with the native cytochrome *c*, mainly due to decrease of the hydrophobic effect.

PART II PHOTOCONTROL OF PROTEIN ACTIVITY THROUGH STRUCTURAL TRANSITION INDUCED BY PHOTOISOMERIZATION OF NONNATURAL AMINO ACIDS

Chapter 4 Photoregulation of Hydrolysis Activity of Semisynthetic Mutant Phospholipases A_2 Replaced by Nonnatural Aromatic Amino Acids

Trp^3 of PLA_2 was replaced by nonnatural aromatic amino acids, napAla, antAla, and azoPhe, by a semisynthetic method. An AMPA was subjected to three cycles of Edman degradation to obtain des[$Ala^1Leu^2Trp^3$]AMPA (DES3). Subsequently, the tripeptide having a nonnatural amino acid at the third position was connected to DES3 to obtain Nap-AMPA, Ant-AMPA, and AzoF-AMPA. Nap-AMPA and Ant-AMPA partially retained hydrolysis activity for phospholipid membrane, while AzoF-AMPA having a *trans* configuration of the azoPhe residue almost lost the activity. UV-light irradiation during the

hydrolysis reaction reduced the activities of Nap-AMPA and Ant-AMPA. However, AzoF-AMPA taking a *cis* configuration of the azoPhe unit showed hydrolytic activity on UV-light irradiation. The change of enzymatic activity induced by UV-light irradiation is ascribed to conformational change of the mutant proteins.

Chapter 5 Location of Melittin Fragment Carrying Spiropyran in Phospholipid Bilayer Membrane Determined by Thermal Isomerization

Melittin fragments carrying spiropyran were synthesized, and their distribution in phospholipid bilayer membrane was studied by using spiropyran as a probe. Spiropyran was connected to the side chain of a Glu residue (Glu(OSp)), and the residue was replaced for the 4th position of melittin (1-7) fragment (M7Sp). The spiropyran group of M7Sp was converted to a merocyanine group by UV-light irradiation, which reduced the amount of the peptide bound to the membrane to the half of the initial amount. The location of the merocyanine group of M7Sp in the membrane was evaluated by the rate of thermal isomerization from merocyanine to spiropyran, which is sensitive to the microenvironment of merocyanine. A large fraction of the merocyanine group isomerized rapidly back to a spiropyran form, indicating that M7Sp is located in a relatively hydrophobic region of the membrane. Although the interaction of the peptide with phospholipid membrane is affected by photoisomerization of the spiropyran substituent, spiropyran was shown to be a useful tool to evaluate the location of the peptide in the lipid membrane.

Chapter 6 Photoresponsive Melittin Having a Spiropyran Residue in the Hydrophobic Region of the Sequence

A melittin derivative carrying a spiropyran group at the third residue (MSp) was prepared by a semisynthetic method. MSp showed reversible photochromism in a phospholipid bilayer membrane. The kinetics of thermal decoloration and the maximum absorption of MSp in the merocyanine form indicated that the merocyanine moiety is located at the membrane surface. The disturbance of the membrane structure by MSp, as studied by CF leakage, was enhanced by UV-light irradiation. The kinetics of CF leakage indicated that MSp in the merocyanine form disturbs the membrane structure more significantly than that in the spiropyran form.

These results should be a milepost for design and synthesis of artificial proteins with specific functions, which can never be realized by using naturally occurring amino acids only. The methods reported herein enable to incorporate various functional groups in proteins, leading to the production of novel functional materials by exploitation of nonnatural amino acid.

LIST OF PUBLICATIONS

PART I — IMPROVEMENT AND PHOTOCONTROL OF PROTEIN ACTIVITY BY INCORPORATION OF NONNATURAL AMINO ACIDS

Chapter 1 — Biosynthesis of Mutant β-D-Galactosidases Containing Nonnatural Aromatic Amino Acids by *Esherichia coli*
Bull. Chem. Soc. Jpn., 1991, **64**, 1576-1581.

Chapter 2 — Semisynthesis of Mutant Cytochromes *c* Replaced by Nonnatural Aromatic Amino Acid at Phe^{82} and Photoregulation of Reduction Reaction with 2-Mercaptoethanol
J. Chem. Soc. Perkin Trans. 1, 1994, 219-224.

Chapter 3 — Destabilization of the Heme Region in Mutant Cytochrome *c* by Replacement of Phe^{82} with 3-(1-Pyrenyl)-L-alanine
J. Chem. Soc. Perkin Trans. 2, 1995, 359-363.

PART II — PHOTOCONTROL OF PROTEIN ACTIVITY THROUGH STRUCTURAL TRANSITION INDUCED BY PHOTOISOMERIZATION OF NONNATURAL AMINO ACIDS

Chapter 4 — Photoregulation of Hydrolysis Activity of Semisynthetic Mutant Phospholipases A_2 Replaced by Nonnatural Aromatic Amino Acids
J. Chem. Soc. Perkin Trans. 1, 1994, 225-230.

Chapter 5 — Location of Melittin Fragment Carrying Spiropyran in Phospholipid Bilayer Membrane Determined by Thermal Isomerization
Biophys. Chem., 1994, **49**, 215-222.

Chapter 6 — Photoresponsive Melittin Having a Spiropyran Residue in the Hydrophobic Region of the Sequence
J. Chem. Soc. Perkin Trans. 2, 1995, 365-368.

ACKNOWLEDGMENT

This investigation was carried out from 1987 to 1993 at the Department of Polymer Chemistry, Faculty of Engineering, Kyoto University.

The author would like to express his deepest gratitude to Professor Yukio Imanishi for his continuous guidance and encouragement throughout the course of this work, and for detailed criticisms on the manuscript.

The author would like to express his sincere appreciation to Professor Atsuo Tanaka, Department of Synthetic Chemistry and Biological Chemistry, Kyoto University, for his valuable comments and criticisms on this work, especially for molecular genetics investigations.

The author wishes to express his sincere thanks to Professor Masahiko Sisido of Okayama University for his precious suggestions and discussions.

Grateful acknowledgment is due to Dr. Shunsaku Kimura of the Department of Material Chemistry, Kyoto University, for his constant guidance and encouragement.

The author wishes to express his genuine thanks to Dr. Yoshihiro Ito, Kyoto University, for his extensive advices and comments.

The author gratefully acknowledges helpful discussions with Dr. Yoshihito Inai of Nagoya Institute of Technology, Dr. Haruyuki Atomi and Dr. Tatsuo Kurihara of Kyoto University, and Dr. Yuichi Ohya of Kansai University on this work.

The author's special thanks are due to Mr. Koichi Murayama, Mr. Eiichi Kato, Mr. Tadayuki Yamamoto and Mr. Koichi Nagamine of Kyoto University for their persistent experimental works.

Finally, the author wishes to express his thanks to all the collaborators in the Professor Imanishi's laboratory for their kind help in research activities.

March, 1995

Takehiko Ueda